

Manoela Klüppel Riekes

**DESENVOLVIMENTO DE SISTEMAS AMORFOS  
INOVADORES VISANDO AO AUMENTO DA SOLUBILIDADE  
DE FÁRMACOS ADMINISTRADOS EM DOSE FIXA  
COMBINADA**

Tese de doutorado em regime cotutela submetida e apresentada à Universidade Federal de Santa Catarina e à KU Leuven, como requisito parcial para obtenção dos Títulos de Doutora em Farmácia e em *Pharmaceutical Sciences*, respectivamente.

Orientadores: Prof<sup>ª</sup>. Dr<sup>a</sup>. Hellen Karine Stulzer (Brasil) e Prof. Dr. Guy Van den Mooter (Bélgica)

Florianópolis/Leuven  
2017



Manoela Klüppel Riekes

**DEVELOPMENT OF NOVEL AMORPHOUS SYSTEMS  
AIMING TO INCREASE THE SOLUBILITY OF DRUGS  
ADMINISTERED IN FIXED DOSE COMBINATIONS**

Joint PhD Thesis submitted and presented to Universidade Federal de Santa Catarina and KU Leuven, as a partial requisite to obtain the Degree of Doctor in *Farmácia* and in Pharmaceutical Sciences, respectively.

Supervisors: Prof<sup>a</sup>. Dr<sup>a</sup>. Hellen Karine Stulzer (Brazil) e Prof. Dr. Guy Van den Mooter (Belgium)

Florianópolis/Leuven  
2017

Ficha de identificação da obra elaborada pelo autor,  
através do Programa de Geração Automática da Biblioteca Universitária da UFSC.

Kluppel Riekas, Manoela  
DESENVOLVIMENTO DE SISTEMAS AMORFOS INOVADORES  
VISANDO AO AUMENTO DA SOLUBILIDADE DE FÁRMACOS  
ADMINISTRADOS EM DOSE FIXA COMBINADA / Manoela  
Kluppel Riekas ; orientador, Hellen Karina Stulzer  
Koerich, orientador, Guy Van den Mooter, 2017.  
200 p.

Tese (doutorado) - Universidade Federal de Santa  
Catarina, Centro de Ciências da Saúde, Programa de  
Pós-Graduação em Farmácia, Florianópolis, 2017.

Inclui referências.

Trabalho elaborado em regime de co-tutela.

1. Farmácia. 2. Ezetimiba. 3. Lovastatina. 4.  
Amorfo. 5. Dose Fixa Combinada. I. Stulzer Koerich,  
Hellen Karina. II. Van den Mooter, Guy III.  
Universidade Federal de Santa Catarina. Programa de  
Pós-Graduação em Farmácia. IV. Título.





## ACKNOWLEDGEMENTS

To the universe and its amazing energetic power, who some might call God, for guiding me to the right place, at the right moment, with the right people, giving me the opportunity to grow and learn, from pleasant and difficult moments that were presented to me along these 4 years.

To my family, who always supported me and my dreams, no matter how long and how far. Being together does not always mean being present. I love you.

To my dad, who left us so prematurely, to continue his walking at the other side. Thank you for making me so strong.

To Prof. Guy Van den Mooter, who welcomed me at his lab and trusted on me and on my work. Thank you for your kind and so present guidance during all my PhD, for all the opportunities and knowledge shared. It is a honour to me being part of your group. Hartelijk bedankt.

To Prof. Hellen Stulzer, for these almost 10 years working together. You certainly had an influence on the scientist I became.

To the great friends I had the pleasure to encounter, at Drug Delivery and Disposition and Quality Control Lab.

To my beloved Belgian family: Bernard Appeltans, Annick de Troyer, Tim Thijs, Aswin Dereymaker, Yasmin Zorilla, Patrick Rombaut, Annelies Smeets, Anna de Simon, Vicky Barmpatsalou and Matina Vandorou. You are forever in my heart. I miss you.

To my Brazilian friends and half sisters Monika Tagliari and Camila Konell, for everything you mean to me. Thanks for always being there.

To Belgium and its so kind and polite people, who received me so well during my stay. You are a special country.

To my Master students Axel Engelen and Lore Janssens, for the help with the experiments and for sharing with me the passion for science.

To UFSC and KU Leuven, and their respective Doctoral Schools, for the opportunity to develop my PhD project in such renowned institutions.

To CNPq and CAPES, for the scholarships granted in Brazil and in Belgium. I am very grateful for having the opportunity to go abroad and and give my humble contribution to my beloved country and its so tireless and devoted scientific community.





Success is a ladder. You cannot  
climb it with hands in your pockets.

(Arnold Schwarzenegger)



## RESUMO

A baixa solubilidade de fármacos apresenta-se como propriedade desafiadora no desenvolvimento de associações em dose fixa combinada. Visando contornar esta limitação em formulação composta pelos hipolipemiantes ezetimiba (EZE) e lovastatina (LOV), a obtenção de formulação incrementadora da solubilidade e taxa de dissolução foi investigada. Para tanto, sistemas coamorfos e formulações ternárias compostas por gelatina ou polímeros hidrofílicos foram testados para posteriormente compor uma forma farmacêutica final. Evitando a formação prematura do metabólito ativo de LOV, hidróxiácido de lovastatina (LOVh) em ambiente gástrico, uma formulação entericamente revestida preparada por leito fluidizado compôs o objetivo principal deste trabalho. Os sistemas coamorfos foram obtidos por fusão seguida de rápido resfriamento nas taxas molares de 1:1, 1:2, 2:1 e 1:4 (EZE:LOV), enquanto que formulações compostas por dois diferentes tipos de gelatina (com índices de bloom de 75 e 225), em presença ou não de polímeros hidrofílicos, foram preparadas por ativação mecânica em moinho de bolas. Para as dispersões sólidas ternárias, as mesmas foram nebulizadas em *spray dryer* variando-se as proporções fármaco:fármaco (1:1, 1:2 e 1:4, m/m, EZE:LOV), o tipo de polímero (PVP K-30, PVP/VA-64, HPMC e Soluplus®), a quantidade de polímero (50, 75 e 90%) e a adição de surfactantes. As formulações foram caracterizadas através de técnicas em estado sólido e estudos de dissolução *in vitro*. Sistemas coamorfos foram caracterizados como contendo uma única fase amorfa e ligações de hidrogênio entre os compostos foram detectadas. Entretanto, a taxa de dissolução destes fármacos não foi aumentada para nenhuma das formulações. Sistemas ternários com gelatina demonstraram pouco impacto no tipo da gelatina selecionada, especialmente para EZE, e um incremento discreto da taxa de dissolução, de 6 e 12 vezes para EZE e LOV, respectivamente, em comparação à sistema amorfo binário EZE:LOV. Por outro lado, a adição de polímeros demonstrou um aumento significativo na taxa de dissolução de ambos os fármacos, especialmente para as formulações compostas por Soluplus®. Para estas, os melhores resultados foram observados em presença de 90% de polímero, responsáveis pela liberação de 92 e 83% de EZE e LOV, respectivamente, em 5 minutos. Todas as formulações apresentaram-se amorfas com ligações de hidrogênio entre os componentes. Estudos de estabilidade demonstraram estabilidade físico-química a 4°C/0% UR pelo período de 1 ano. Assim sendo, esta formulação foi selecionada para compor a formulação final em dose fixa combinada, preparada em leito

fluidizado. Estudos de formulação investigaram a influência do tipo de polímero entérico (Eudragit L100® e Eudragit L100-55®), do tamanho dos péletes de sacarose (300-415 µm e 710-850 µm) e do tempo de revestimento. Resultados mostraram que os péletes menores tendiam a aglomerar-se e a liberação dos fármacos foi prejudicada em condições ácidas, devido à formação de uma camada de revestimento irregular. O polímero Eudragit L100-55® necessitou de um tempo maior de processamento, mas camadas de revestimento mais finas levaram a uma menor liberação dos fármacos. Ambos os polímeros proporcionaram baixa liberação de EZE e LOV em ambiente gástrico e rápida dissolução em pH 6,8. Medidas *off-line* da espessura da camada de revestimento determinaram um tempo ideal de 15 e 30 min de revestimento entérico para formulações a base de Eudragit L100-55® e Eudragit L100®, respectivamente. Estudos de estabilidade conduzidos por 6 meses demonstraram propriedades físicas e liberação dos fármacos inalterados a temperatura ambiente e 0% UR. Desta forma, é possível concluir que este projeto foi capaz de desenvolver uma formulação final em dose fixa combinada, baseada em sistemas amorfos inovadores, como as dispersões sólidas ternárias, reportadas pela primeira vez em literatura, capazes de aumentar simultaneamente a taxa de dissolução dos fármacos pouco solúveis EZE e LOV. Embora aplicados a estes dois compostos especificamente, os resultados obtidos nesta tese podem servir como base para compor demais sistemas similares compostos por fármacos de baixa solubilidade aquosa.

**Palavras-chave:** *ezetimiba, lovastatina, dispersões sólidas ternárias, coamorfos, gelatina, dose fixa combinada*

## RESUMO EXPANDIDO

### **Introdução**

O desenvolvimento de formulações em dose fixa combinada tem sido estimulada, inclusive por agências regulatórias internacionais, devido às suas vantagens frente à monoterapia. Aumento da adesão ao tratamento, redução de custos para pacientes e instituições, melhor abrangência terapêutica para pacientes com múltiplas enfermidades e a possibilidade de redução de doses e efeitos colaterais são algumas delas. É importante mencionar que a associação de dois ou mais fármacos em uma forma farmacêutica pode ser complexo, e aspectos farmacocinéticos e físico-químicos devem ser levados em consideração. Neste contexto, a solubilidade dos compostos apresenta-se como um fator de elevada importância, principalmente no que concerne formas farmacêuticas sólidas de administração oral.

Atualmente, o percentual de fármacos com baixa solubilidade é preocupante (em torno de 25 a 40% do total de fármacos desenvolvidos), de modo que muitos deles são rejeitados ou subutilizados pela indústria farmacêutica. Ainda, fármacos com baixa solubilidade geralmente requerem maiores doses para apresentar o efeito terapêutico desejado, o que também pode culminar em seu depósito em sítios específicos, formando agregados que aumentam seus efeitos tóxicos.

Dentre as opções atualmente disponíveis visando ao aumento da solubilidade de fármacos, a conversão de sólidos cristalinos em amorfos apresenta-se como promissora e o seu sucesso encontra-se amplamente divulgado em literatura específica. Entretanto, estas estratégias tem sido aplicadas a fármacos administrados em monoterapia, e apenas mais recentemente, os sistemas coamorfos foram introduzidos com vistas à aplicação em associações de dose fixa. Por outro lado, as dispersões sólidas, vastamente investigadas quando compostas apenas por um fármaco lipofílico, nunca foram utilizadas com este propósito. Neste sentido, dispersões sólidas ternárias, compostas por dois fármacos lipofílicos e um polímero hidrofílico, constituem uma proposta inovadora e promissora. Ainda, o biopolímero gelatina, amplamente utilizada com outros propósitos na área farmacêutica é altamente solúvel em água, podendo constituir um promissor sistema carreador para aumentar a solubilidade de fármacos em estado amorfo.

Os hipolipemiantes pouco solúveis ezetimiba (EZE) e lovastatina (LOV) pertencem à Classe II do Sistema de Classificação Biofarmacêutico e sua associação em prática clínica é considerada segura e eficaz. Muito embora, nenhuma formulação em dose fixa combinada composta por estes fármacos encontra-se disponível para comercialização. Ainda, é

importante ressaltar que a associação de EZE e LOV tem sido estimulada devido à ocorrência de importantes efeitos colaterais associados à classe das estatinas, além destas aumentarem o risco de desenvolvimento de diabetes do tipo II em pacientes hipercolesterolêmicos.

## **Objetivos**

Neste contexto, este trabalho propõe a aplicação de estratégias amorfas inovadoras, como sistemas coamorfos, dispersões sólidas ternárias e formulações compostas por gelatina visando aumentar a solubilidade e taxa de dissolução dos fármacos EZE e LOV em uma forma farmacêutica de dose fixa combinada. Devido à instabilidade gástrica de LOV gerando precocemente seu metabólito ativo, este trabalho objetiva o desenvolvimento de uma forma farmacêutica final, baseada em dose fixa combinada e revestida entericamente.

## **Metodologia**

Sistemas coamorfos de EZE e LOV nas proporções molares de 1:1, 1:2, 1:4 e 2:1 (EZE:LOV) foram preparados através de fusão seguida de rápido resfriamento em equipamento de calorimetria exploratória diferencial modulada. Os sistemas ternários compostos por gelatina foram preparados através de moagem de alto impacto, otimizando-se parâmetros experimentais, em diferentes proporções de gelatina e fármaco-fármaco. No que se refere às dispersões sólidas ternárias, as mesmas foram nebulizadas em *spray dryer*, avaliando o impacto de diferentes polímeros hidrofílicos, proporção fármacos:polímero e presença de surfactantes.

Para todos os casos, as proporções fármaco:fármaco foram selecionadas com base nas doses de administração disponíveis para comercialização (10 mg para EZE e 10, 20 e 40 mg para LOV). Todas as formulações foram caracterizadas através de técnicas de estado sólido e avaliadas por estudos de estabilidade e dissolução *in vitro*.

A formulação com a melhor performance *in vitro* e com propriedades físico-químicas apropriadas foi selecionada para compor a forma farmacêutica final em dose fixa combinada, entericamente revestida e preparada em leito fluidizada. Parâmetros de formulação e experimentais foram avaliados visando ao desenvolvimento de uma formulação gastroprotetora e capaz de promover uma liberação rápida e completa de ambos os princípios ativos em ambiente intestinal.

## **Resultados e Discussão**

Os hipolipemiantes EZE e LOV foram escolhidos como fármacos modelo para desenvolvimento de forma farmacêutica em dose fixa combinada

capaz de aumentar a sua solubilidade e taxa de dissolução. Para tanto, estudos de pré-formulação foram realizados, promovendo uma caracterização em estado sólido de ambos os fármacos, a qual foi útil para monitorar as transformações ocorridas por conta do seu processamento. De maneira importante, estudos de solubilidade em equilíbrio demonstraram que EZE e LOV poderiam ser associados em uma forma farmacêutica sem efeitos deletérios à sua solubilidade.

A partir de então, formulações foram desenvolvidas e os sistemas coamorfos foram as primeiras estratégias investigadas. Entretanto, embora completamente amorfos e apresentando ligações de hidrogênio, as quais poderiam beneficiar a sua estabilidade física, estes sistemas não foram capazes de aumentar a dissolução de EZE e LOV. Estes resultados podem ser provavelmente associados à baixa solubilidade em estado amorfo de EZE, a qual refletiu-se nas formulações.

Optou-se então por investigar o potencial da gelatina como carreadora hidrofílica de sistemas ternários com EZE e LOV. Embora o sistema tenha sido otimizado a ponto de gerar sistemas completamente amorfos em muitos casos, o seu potencial *in vitro* não foi confirmado, demonstrando baixo percentual de liberação para a grande maioria dos sistemas desenvolvidos.

Desta forma, a inserção de polímeros foi investigada, almejando aumentar a molhabilidade e área superficial através de seu processamento por meio de *spray drying*. Neste momento, o conceito de dispersões sólidas ternárias foi introduzida pela primeira vez. Diferentes polímeros hidrofílicos foram investigados e os melhores resultados foram observados para formulações constituídas de Soluplus®. Os resultados foram dependentes da concentração de polímero (numa relação diretamente proporcional), e não foram afetadas pelas diferentes proporções de fármaco:fármaco e pela presença de surfactante. A formulação composta por 90% de Soluplus® e numa proporção fármaco:fármaco de 1:1 (m/m) (ELS 1:1 90%) foi capaz de aumentar a eficiência de dissolução em 18 (EZE) e 6 (LOV) vezes em comparação às suas respectivas matérias-primas cristalinas. Ainda, esta mesma formulação foi capaz de liberar mais de 80% de ambos os fármacos em apenas 5 min. É importante mencionar que embora 90% de polímero seja considerada uma alta proporção, a baixa dose de administração de ambos os compostos (10 mg para EZE e 10 a 40 mg para LOV) permite o desenvolvimento de uma forma farmacêutica sólida de administração oral. Desta forma, ELS 1:1 90% foi selecionada como base para compor a forma farmacêutica final em dose fixa combinada.

Entretanto, a instabilidade em ambiente ácido de LOV, gerando precocemente o seu metabólito ativo (cuja concentração hepática deve ser maximizada) requereu o desenvolvimento de uma forma farmacêutica composta por revestimento entérico, a qual também seja capaz de promover rápida liberação de ambos os compostos em ambiente intestinal.

Para tanto, optou-se pelo desenvolvimento de sistema multiparticulado por leito fluidizado utilizando péletes inertes de sucrose. Neste sentido, diferentes polímeros entéricos (Eudragit L100® e Eudragit L100-55®), péletes inertes com variados diâmetros externos (300-415 µm and 710-850 µm) e tempo de revestimento foram investigados. Após extensa avaliação, verificou-se que a formulação composta por péletes de maior diâmetro apresentaram adequadas propriedades de fluidização sem aglomeração, gerando camadas de revestimento homogêneas. O polímero Eudragit L100-55® demonstrou-se mais adequado por permitir em um menor tempo de revestimento (15 min) e com uma camada entérica de 6,5 µm, reduzida liberação em meio gástrico e rápida dissolução de ambos os fármacos em ambiente intestinal.

### **Considerações finais**

Este trabalho reportou pela primeira vez o desenvolvimento de uma forma farmacêutica final em dose fixa combinada baseada em dispersões sólidas ternárias. O sistema utilizou técnicas de preparo de uso corriqueiro pela indústria farmacêutica, como o leito fluidizado, simplificando o seu escalonamento. Ainda, cabe mencionar que embora estes estudos tenham sido realizados com os fármacos EZE e LOV, seu potencial de aplicação estende-se a demais fármacos pouco solúveis e farmacocineticamente compatíveis a serem administrados em uma combinação de doses fixas.

**Palavras-chave:** *ezetimiba, lovastatina, dispersões sólidas ternárias, coamorfos, gelatina, dose fixa combinada*



## ABSTRACT

Low solubility of drugs represents a challenging property on the development of fixed-dose combinations. Aiming to overcome this limitation in formulation composed by the hypolipidemic compounds ezetimibe (EZE) and lovastatin (LOV), the preparation of a system capable of enhancing their dissolution rate was investigated. For this purpose, co-amorphous systems and ternary formulations made up of gelatin or hydrophilic polymers were tested to further compose a final dosage form. In order to avoid the premature formation of the active metabolite of LOV, lovastatin hydroxyacid (LOVh), in gastric environment, an enteric coated formulation prepared by fluid bed coating represented the main goal of this research. Co-amorphous systems were prepared by quench cooling from the melt in molar ratios of 1:1, 1:2, 2:1 and 1:4 (EZE:LOV), whilst formulations composed by two different types of gelatin (bloom 75 and 225), in presence or absence of hydrophilic polymers were obtained through ball milling. Regarding the ternary solid dispersions, they were prepared by spray drying, varying the drug:drug ratio (1:1, 1:2 and 1:4, w/w, EZE:LOV), the type of polymer employed (PVP K-30, PVP/VA-64, HPMC and Soluplus®), the amount of polymer (50, 75 and 90%) and the addition of surfactants. Formulations were characterized by means of solid-state techniques and *in vitro* dissolution studies. Co-amorphous systems were characterized as single amorphous phase and hydrogen bonding between the compounds was detected. However, the dissolution rate of the drugs was not enhanced through any of these co-amorphous systems. Gelatin-based formulations demonstrated low impact regarding the type of gelatin used, especially for EZE. Besides, a slight increase of dissolution rate, of about 6 and 12-fold, for EZE and LOV, respectively, in comparison to a co-spray dried amorphous system of EZE:LOV, was observed. On the other hand, the addition of polymers demonstrated a significant enhancement of dissolution rate for both compounds, especially for Soluplus®-based formulations. For those, the best results were observed in presence of 90% of polymer, releasing 92% and 83% of EZE and LOV, respectively, within 5 minutes. All ternary solid dispersions were amorphous with hydrogen bonding among the components. Stability studies demonstrated physicochemical stability at 4°C/0% RH within 1 year. Based on that, this formulation was selected to compose the final dosage form based on a fixed-dose combination, prepared by fluid bed coating. Formulation studies investigated the influence of enteric polymer (Eudragit L100® and Eudragit L100-55®), sucrose beads size (300-415 µm and 710-850 µm)

and coating time. Results showed that smaller pellets tend to agglomerate and drug release was jeopardized in acidic conditions, due to the formation of an irregular coating layer. Eudragit L100-55® required a longer processing time, although thinner coating layers led to lower drug release. Both polymers provided low drug release in gastric environment and high dissolution in pH 6.8. Off-line measurements of coating thickness determined as 15 and 30 min appeared to be the ideal coating time for Eudragit L100-55® and Eudragit L100®-based formulations, respectively. Stability studies conducted during 6 months demonstrated unaltered physical and release properties of the drugs at room temperature and 0% RH. In this way, it is possible to conclude that this research project was able to develop a final fixed-dose combination, based on novel amorphous systems, such as spray dried ternary solid dispersions, never before reported in literature. This formulation was capable of enhancing simultaneously the dissolution rate of the poorly water-soluble compounds EZE and LOV. Although applied to these two compounds specifically, the results obtained in this thesis can be used as basis to compose other similar systems of poorly water-soluble compounds.

**Keywords:** *ezetimibe, lovastatin, ternary solid dispersions, co-amorphous systems, gelatin, fixed-dose combinations*

## LIST OF FIGURES

<b>Figure 1</b>	Chemical structure of lovastatin (A) and its active $\beta$ -hydroxy acid metabolite (B).....	<b>47</b>
<b>Figure 2</b>	Chemical structure of ezetimibe.....	<b>48</b>
<b>Figure 3</b>	Correlation among solubility, permeability and dose.....	<b>52</b>
<b>Figure 4</b>	Schematic diagram showing changes in enthalpy (H), entropy (S) and volume (V) in liquid, crystalline and glassy state in function of temperature. $T_g$ and $T_f$ represent the glass transition temperature and the temperature of fusion, respectively.....	<b>54</b>
<b>Figure 5</b>	Classification of solid dispersions according to the distribution of drug molecules in the carrier(s).....	<b>59</b>
<b>Figure 6</b>	Monomeric unit of Eudragit L100® (R1 = H <sub>3</sub> C; R2 = H <sub>3</sub> C) and Eudragit L100-55® (R1 = H; R2 = C <sub>2</sub> H <sub>5</sub> ).....	<b>68</b>
<b>Figure 7</b>	Schematic demonstration of drug release from an enteric coated pellet. EC = enteric coating layer, SD= solid dispersion layer.....	<b>68</b>
<b>Figure 8</b>	Different fluid bed coater settings: (a) top spray, (b), bottom spray and (c) Wurster.....	<b>70</b>
<b>Figure 9</b>	XRPD of (A) crystalline raw materials EZE and LOV and (B) quench cooled samples: co-amorphous systems, EZE <sub>qc</sub> and LOV <sub>qc</sub> .....	<b>92</b>
<b>Figure 10</b>	Reversing heat flow curves, experimental glass transition temperatures and heat capacity of co-amorphous systems.....	<b>94</b>
<b>Figure 11</b>	FTIR data of crystalline and quench cooled raw materials.....	<b>95</b>
<b>Figure 12</b>	Calculated versus experimental FTIR data for 1:1, 1:2, 1:4 and 2:1 EZE:LOV (m/m), demonstrating the broadening and shift of hydroxyl and carbonyl bands in all co-amorphous systems.....	<b>97</b>
<b>Figure 13</b>	Intrinsic dissolution profiles of crystalline (A) EZE and (B) LOV raw materials compared to the quench cooled samples and co-amorphous systems.....	<b>98</b>

<b>Figure 14</b>	Diffractograms of (A) EZE <sub>q</sub> c, (B) LOV <sub>q</sub> c, (C) 1:4 and (D) 1:1, 1:2 and 2:1 EZE:LOV (m/m), compared to the diffractograms of SLS, sodium acetate and the XRD patterns of LOV, EZE anhydrate (EZE A) and EZE monohydrate (EZE M), obtained from the Cambridge Structural Database.....	<b>101</b>
<b>Figure 15</b>	X-ray diffractograms of EZE, LOV and gelatin 75 and 225 raw materials.....	<b>110</b>
<b>Figure 16</b>	mDSC thermograms of ELG75 25:25:50 physical mixture. Black, blue and green represent the first, second and third heating cycles, respectively. The three curves up represent the heat flow and the three curves down the reversing heat flow.....	<b>111</b>
<b>Figure 17</b>	X-ray diffractograms regarding samples prepared with (A) different rotation speeds and milling times, (B, C) number and combination of balls and (D) amount of powder.....	<b>112</b>
<b>Figure 18</b>	Diffractograms relative to milled pure raw materials and binary combinations at different ratios.....	<b>115</b>
<b>Figure 19</b>	X-ray diffractograms relative to binary systems composed of EZE:Gelatin and LOV:Gelatin in different ratios.....	<b>116</b>
<b>Figure 20</b>	X-ray diffractograms relative to ternary systems composed of EZE:LOV:Gelatin in different ratios.....	<b>118</b>
<b>Figure 21</b>	X-ray diffractograms relative to ternary systems composed of EZE:LOV in 1:4 ratios in presence of different amounts of gelatin.....	<b>119</b>
<b>Figure 22</b>	X-ray diffractograms regarding E:L:G:Polymer (25:25:25:25 w/w/w/w) milled samples.....	<b>120</b>
<b>Figure 23</b>	mDSC thermograms of (A) ELG75/225 5:20:75, (B) ELG75/225 25:25:50 and (C) ELG75/225 12.5:12.5:75. Black and blue curves represent samples prepared with gelatin 75 and 225, respectively. The two curves up represent the heat flow and the two curves down the reversing heat flow.....	<b>121</b>
<b>Figure 24</b>	<i>In vitro</i> dissolution profiles of ternary ball milled systems ELG75 12.5:12.5:75 (▲), ELG225	

	12.5:12.5:75 (▲), ELG75 25:25:50 (●), ELG225 25:25:50 (●), compared to co-spray dried materials (■) and crystalline raw materials (■).....	123
<b>Figure 25</b>	XRD data regarding spray dried (A) raw materials isolated (EZEsd;LOVsd) and in combination (EZE:LOVsd), and (B) ternary solid dispersions with different hydrophilic polymers.....	135
<b>Figure 26</b>	mDSC data for ternary solid dispersions composed of different hydrophilic polymers. Blue and black curves correspond to the reversing heat flow and its derivative, respectively. The peak temperatures of each glass transition event is shown in °C.....	136
<b>Figure 27</b>	(A) EZE and (B) LOV release profiles from ternary solid dispersions compared to their respective crystalline raw materials.....	137
<b>Figure 28</b>	Dissolution profiles of binary (LS 75% and ES 75%) versus the ternary solid dispersion ELS 1:1 75%.....	139
<b>Figure 29</b>	XRD data relative to ternary solid dispersions composed of Soluplus with (A) 1:1, (B) 1:2 and (C) 1:4 EZE:LOV ratios, and (D) in presence of surfactants.....	139
<b>Figure 30</b>	Experimental and calculated IR data for ternary solid dispersions with Soluplus composed of 1:1 API:API ratio and different polymer concentrations (50, 75 and 90%).....	142
<b>Figure 31</b>	SEM micrographs of (A) EZE:LOVsd (3500x), (B) EZE:LOVsd (10000x), (C) ELS 1:2 50% (5000x) and (D) ELS 1:2 90% (5000x). The arrows in B indicate the presence of crystalline needles on the surface of the spherical EZE:LOVsd particles.....	144
<b>Figure 32</b>	Dissolution profiles of EZE and LOV in the ternary solid dispersion ELS 1:1 90% compared to their respective crystalline raw materials.....	146
<b>Figure 33</b>	‘In vitro’ dissolution data for (A) EZE and (B) LOV regarding ternary solid dispersions composed of surfactants.....	146

<b>Figure 34</b>	XRD data for ELS 1:1 75% at time zero (T0) and after 1 year exposed to different storage conditions.....	<b>148</b>
<b>Figure 35</b>	‘In vitro’ dissolution profiles of ELS 1:1 75% at time zero (T0), after 180 days (180d) and after 1 year (1y) exposed to different stability conditions.....	<b>148</b>
<b>Figure 36</b>	SEM micrographs of enteric-coated smaller beads (300-415 µm) before (A-C) and after (D-F) process optimization. Agglomeration is indicated in A by the arrows. Polymeric nets are shown in B and C after enteric coating. The coating layers relative to the solid dispersion (SD) and enteric coating (EC) are shown in F and their borders are indicated by the arrow.....	<b>162</b>
<b>Figure 37</b>	Influence of coating time on in vitro dissolution of EZE and LOV in acidic conditions (presented as % release), from small (300-415 µm) and large (710-850 µm) beads.....	<b>163</b>
<b>Figure 38</b>	SEM micrographs of pellets coated with the solid dispersion layer (A and D) and enteric-coated with Eudragit L100® (B and E) and Eudragit L100-55® (C and F). Panel B shows an enlarged surface view to provide a better visualization of the pores. The cross-sectioned pellets (D-F) show the core, the solid dispersion (SD) and the enteric coating (EC) layers. Arrows indicate the borders between the SD and the EC layers .....	<b>165</b>
<b>Figure 39</b>	Linear relation between the particle size, in µm, and the coating time of the enteric coating layers composed of Eudragit L100® (●) and Eudragit L100-55® (■).....	<b>166</b>
<b>Figure 40</b>	Diffractograms of (A) crystalline raw materials, (B) formulations with Eudragit L100® and (C) formulations with Eudragit L100-55®, compared to the inert sucrose beads.....	<b>167</b>
<b>Figure 41</b>	Percentage release of EZE and LOV from formulations prepared with (A) Eudragit L100® and (B) Eudragit L100-55®, after 90 min of	

	dissolution studies in HCl 0.1 M + 0.025% of SLS.....	169
<b>Figure 42</b>	<i>In vitro</i> dissolution profiles of enteric-coated formulations composed of (A) Eudragit L100® and (B) Eudragit L100-55®, in phosphate buffer pH 6.8 containing 0.01% of SLS.....	171
<b>Figure 43</b>	Diffractiongrams relative to formulations with Eudragit L100-55®, at time zero (T0) and after 6 months of stability studies.....	173
<b>Figure 44</b>	Dissolution profiles of EZE and LOV from Eudragit L100-55®-based formulation, with 15 min of enteric coating time, at time zero (T0) and after 6 months.....	174
<b>Figure 45</b>	Chromatogram eluted under the following conditions: ACN:H2O (50:50, v/v), 1 mL/min, 25°C, 235 nm, showing peaks of EZE (3.1 min), LOVh (4.2 min) and LOV (8.1 min).....	185
<b>Figure 46</b>	Mean calibration curves of EZE (●) and LOV (■), obtained as a function of the peak areas <i>versus</i> concentration, in µg/mL. Their respective linear equations and correlation coefficients are also depicted.....	186





## **LIST OF SCHEMES**

<b>SCHEME 1</b>	Characteristics of amorphous and crystalline solids.....	<b>53</b>
<b>SCHEME 2</b>	Carriers used in solid dispersions and their main properties.....	<b>62</b>



## LIST OF TABLES

<b>Table 1</b>	Experimental and calculated FTIR data of co-amorphous systems.....	<b>96</b>
<b>Table 2</b>	Intrinsic dissolution data.....	<b>99</b>
<b>Table 3</b>	Composition of spray dried samples.....	<b>130</b>
<b>Table 4</b>	Equilibrium solubility data in acetate buffer pH 4.5 + 0.025% SLS after 48 h.....	<b>138</b>
<b>Table 5</b>	mDSC data of ternary solid dispersions.....	<b>140</b>
<b>Table 6</b>	Experimental and calculated FTIR data of ternary solid dispersions with Soluplus.....	<b>141</b>
<b>Table 7</b>	Percentage of dissolution (% D) at 120 min and dissolution efficiency (DE) data.....	<b>145</b>
<b>Table 8</b>	Data referring to the accuracy of the method.....	<b>186</b>
<b>Table 9</b>	Data referring to the robustness of the method, compared to the parameters of the developed method (ACN:H <sub>2</sub> O (50:50, v/v), 1 mL/min, 25°C, 235 nm).....	<b>187</b>



## LIST OF ABBREVIATIONS

ANVISA: National Health Surveillance Agency (From Portuguese, *Agência Nacional de Vigilância Sanitária*)  
API: active pharmaceutical ingredient  
AUC: area under the curve  
BCS: Biopharmaceutics Classification System  
coSD: co-spray dried  
DCM: dichloromethane  
DE: dissolution efficiency  
DSC: differential scanning calorimetry  
EC: ethyl cellulose  
ELG: ezetimibe:lovastatin:gelatin  
ELS: ezetimibe:lovastatin:Soluplus®  
EZE: ezetimibe  
EZE:LOVsd: co-spray dried of ezetimibe:lovastatin (1:1 m/m)  
EZEqc: quench cooled ezetimibe  
EZESol: ezetimibe:Soluplus®  
FDA: Food and Drug Administration  
FDC: fixed-dose combination  
FTIR: Fourier transform infrared  
GRAS: generally regarded as safe  
HDL: high-density lipoprotein  
HIV: Human Immunodeficiency Virus  
HPC: hydroxypropyl cellulose  
HPLC: high performance liquid chromatography  
HPMC: hydroxypropylmethyl cellulose  
ICH: International Conference on Harmonisation  
IR: infrared  
LDL: low-density lipoprotein  
LOD: limit of detection  
LOQ: limit of quantification  
LOV: lovastatin  
LOVh: lovastatin hydroxyacid  
LOVqc: quench cooled lovastatin  
LOVSol: lovastatin:Soluplus®  
mDSC: modulated differential scanning calorimetry  
MeOH: methanol  
NSAID: non-steroidal anti-inflammatory drug  
PEG: polyethylene glycol  
PTFE: Polytetrafluoroethylene

PVA: polyvinyl acetate  
PVC: polyvinyl caprolactone  
PVP: polyvinylpyrrolidone  
PVP VA: vinylpyrrolidone-vinyl acetate copolymer  
RDC: Resolução de Diretoria Colegiada  
RENAME: Relação Nacional de Medicamentos Essenciais  
RH: relative humidity  
RSD: relative standard deviation  
SD: standard deviation  
SEM: scanning electron microscopy  
SLS: sodium lauryl sulfate  
T0: time zero  
 $T_f$ : temperature of fusion  
 $T_g$ : glass transition temperature  
TPGS: d-alpha tocopheryl polyethylene glycol 1000 succinate  
UR: umidade relativa  
USP: United States Pharmacopoeia  
UV: ultraviolet  
VLDL: very low-density lipoprotein  
WHO: World Health Organization  
XRD: X-ray diffraction



## CONTENT

<b>1</b>	<b>GENERAL INTRODUCTION.....</b>	<b>37</b>
1.1	OBJECTIVES.....	41
1.1.1	Main objective.....	41
1.1.2	Specific objectives.....	41

### CHAPTER I – INTRODUCTION

<b>1</b>	<b>FIXED DOSE COMBINATIONS.....</b>	<b>44</b>
<b>2</b>	<b>EZETIMIBE AND LOVASTATIN.....</b>	<b>46</b>
<b>3</b>	<b>THE AMORPHOUS STATE AND ITS IMPACT ON THE SOLUBILITY OF DRUGS.....</b>	<b>50</b>
<b>4</b>	<b>STRATEGIES IN AMORPHOUS STATE APPLIED TO IMPROVE SOLUBILITY AND DISSOLUTION RATE IN FIXED DOSE COMBINATIONS.....</b>	<b>56</b>
4.1	CO-AMORPHOUS SYSTEMS.....	56
4.2	SOLID DISPERSIONS.....	58
4.3	GELATIN-BASED FORMULATIONS.....	65
<b>5</b>	<b>ENTERIC COATED MUTIPARTICULATE SYSTEMS.....</b>	<b>66</b>
<b>6</b>	<b>REFERENCES.....</b>	<b>71</b>

### CHAPTER II - PREPARATION AND CHARACTERIZATION OF CO-AMORPHOUS SYSTEMS OF EZETIMIBE AND LOVASTATIN MANUFACTURED THROUGH QUENCH COOLING FROM THE MELT

<b>1</b>	<b>INTRODUCTION.....</b>	<b>86</b>
<b>2</b>	<b>EXPERIMENTAL.....</b>	<b>87</b>
2.1	MATERIALS.....	87
2.2	DETERMINATION OF THE EQUILIBRIUM SOLUBILITY.....	87
2.3	PREPARATION OF CO-AMORPHOUS SYSTEMS BY QUENCH COOLING FROM THE MELT.....	88
2.4	X-RAY POWDER DIFFRACTION (XRPD).....	88
2.5	MODULATED DIFFERENTIAL SCANNING CALORIMETRY .....	89
2.6	ATTENUATED TOTAL REFLECTANCE FOURIER TRANSFORM INFRARED (FTIR) SPECTROSCOPY.....	89
2.7	INTRINSIC DISSOLUTION RATE.....	90



<b>3</b>	<b>RESULTS AND DISCUSSION.....</b>	<b>90</b>
3.1	DETERMINATION OF THE EQUILIBRIUM SOLUBILITY .....	91
3.2	SOLID-STATE CHARACTERIZATION OF CO-AMORPHOUS SYSTEMS.....	91
3.3	<i>IN VITRO</i> DISSOLUTION OF CO-AMORPHOUS SYSTEMS.....	98
<b>4</b>	<b>CONCLUSIONS.....</b>	<b>102</b>
<b>5</b>	<b>REFERENCES.....</b>	<b>102</b>

### **CHAPTER III - DEVELOPMENT, CHARACTERIZATION AND *IN VITRO* DISSOLUTION STUDIES OF TERNARY AMORPHOUS SYSTEMS OF EZETIMIBE, LOVASTATIN AND GELATIN PREPARED BY HIGH IMPACT MILLING**

<b>1</b>	<b>INTRODUCTION.....</b>	<b>106</b>
<b>2</b>	<b>EXPERIMENTAL.....</b>	<b>107</b>
2.1	MATERIALS.....	107
2.2	PREPARATION OF BALL-MILLED TERNARY SYSTEMS.....	107
2.3	PREPARATION OF SPRAY DRIED SYSTEMS.....	107
2.4	X-RAY POWDER DIFFRACTION OF MILLED MATERIALS.....	108
2.5	MODULATED DIFFERENTIAL SCANNING CALORIMETRY (mDSC).....	109
2.6	<i>IN VITRO</i> DISSOLUTION STUDIES.....	109
<b>3</b>	<b>RESULTS AND DISCUSSION.....</b>	<b>109</b>
3.1	CHARACTERIZATION OF RAW MATERIALS.....	111
3.2	OPTIMIZATION OF THE MILLING PROCESS.....	114
3.3	X-RAY POWDER DIFFRACTION OF MILLED MATERIALS.....	120
3.4	mDSC ANALYSIS.....	122
3.5	<i>IN VITRO</i> DISSOLUTION STUDIES.....	124
<b>4</b>	<b>CONCLUSIONS.....</b>	<b>125</b>
<b>5</b>	<b>REFERENCES.....</b>	<b>125</b>

### **CHAPTER IV - DEVELOPMENT, CHARACTERIZATION AND *IN VITRO* DISSOLUTION STUDIES OF TERNARY AMORPHOUS SYSTEMS OF EZETIMIBE, LOVASTATIN AND DIFFERENT HYDROPHILIC POLYMERS PREPARED BY SPRAY DRYING**

<b>1</b>	<b>INTRODUCTION.....</b>	<b>128</b>
----------	--------------------------	------------

<b>2</b>	<b>EXPERIMENTAL.....</b>	<b>129</b>
2.1	MATERIALS.....	129
2.2	PREPARATION OF SPRAY DRIED SAMPLES .....	129
2.3	X-RAY POWDER DIFFRACTION (XRPD).....	131
2.4	MODULATED DIFFERENTIAL SCANNING CALORIMETRY .....	131
2.5	ATTENUATED TOTAL REFLECTANCE FOURIER TRANSFORM INFRARED (FTIR) SPECTROSCOPY.....	132
2.6	SCANNING ELECTRON MICROSCOPY (SEM).....	132
2.7	PARTICLE SIZE MEASUREMENT.....	132
2.8	EQUILIBRIUM SOLUBILITY MEASUREMENTS..	132
2.9	<i>IN VITRO</i> DISSOLUTION STUDIES.....	133
2.10	STABILITY STUDIES.....	134
<b>3</b>	<b>RESULTS AND DISCUSSION.....</b>	<b>134</b>
<b>4</b>	<b>CONCLUSIONS.....</b>	<b>150</b>
<b>5</b>	<b>REFERENCES.....</b>	<b>151</b>

## **CHAPTER V - DEVELOPMENT, CHARACTERIZATION AND IN VITRO DISSOLUTION STUDIES OF AN ENTERIC- COATED FIXED-DOSE COMBINATION COMPOSED OF TERNARY SOLID DISPERSIONS OF EZETIMIBE AND LOVASTATIN**

<b>1</b>	<b>INTRODUCTION.....</b>	<b>156</b>
<b>2</b>	<b>EXPERIMENTAL.....</b>	<b>157</b>
2.1	MATERIALS.....	157
2.2	PREPARATION OF THE FLUID BED COATED BEADS .....	158
2.3	X-RAY POWDER DIFFRACTION (XRPD).....	159
2.4	SCANNING ELECTRON MICROSCOPY (SEM).....	159
2.5	PARTICLE SIZE MEASUREMENT.....	159
2.6	<i>IN VITRO</i> RELEASE STUDIES.....	160
<b>3</b>	<b>RESULTS AND DISCUSSION.....</b>	<b>160</b>
3.1	PREPARATION AND CHARACTERIZATION OF THE ENTERIC-COATED FDC.....	160
3.2	IMPACT OF BEAD SIZE.....	161
3.3	IMPACT OF POLYMER TYPE AND COATING TIME.....	164
3.4	STABILITY STUDIES.....	172
<b>4</b>	<b>CONCLUSIONS.....</b>	<b>174</b>
<b>5</b>	<b>REFERENCES.....</b>	<b>175</b>

# APPENDIX - DEVELOPMENT AND VALIDATION OF A HIGH PERFORMANCE LIQUID CHROMATOGRAPHY METHOD FOR SIMULTANEOUS DETECTION OF EZETIMIBE AND LOVASTATIN

<b>1</b>	<b>INTRODUCTION.....</b>	<b>180</b>
<b>2</b>	<b>EXPERIMENTAL.....</b>	<b>181</b>
2.1	MATERIALS.....	181
2.2	METHODS.....	181
2.2.1	Instrumentation and chromatographic conditions.....	181
2.2.2	Preparation of standard solutions.....	181
2.2.3	Method validation.....	182
2.2.3.1	<i>Specificity.....</i>	<b>182</b>
2.2.3.2	<i>Linearity, limits of detection (LOD) and quantification (LOQ).....</i>	<b>182</b>
2.2.3.3	<i>Accuracy.....</i>	<b>183</b>
2.2.3.4	<i>Precision.....</i>	<b>183</b>
2.2.3.5	<i>Robustness.....</i>	<b>183</b>
2.2.3.6	<i>Statistical analysis.....</i>	<b>183</b>
<b>3</b>	<b>RESULTS AND DISCUSSION.....</b>	<b>184</b>
3.1	DEVELOPMENT OF THE ANALYTICAL METHOD BY HPLC.....	<b>184</b>
3.2	ANALYTICAL VALIDATION.....	<b>184</b>
3.2.1	Specificity.....	<b>184</b>
3.2.2	Linearity, limits of detection (LOD) and quantification (LOQ).....	<b>185</b>
3.2.3	Accuracy.....	<b>186</b>
3.2.4	Precision.....	<b>186</b>
3.2.5	Robustness.....	<b>187</b>
<b>4</b>	<b>CONCLUSIONS.....</b>	<b>187</b>
<b>5</b>	<b>REFERENCES.....</b>	<b>188</b>
	<b>GENERAL DISCUSSION.....</b>	<b>189</b>
	<b>RELEVANT REFERENCES.....</b>	<b>198</b>



## 1. GENERAL INTRODUCTION

The development of fixed-dose combinations (FDCs) has been stimulated by international regulatory agencies, due to their advantages compared to the traditional monotherapy. Higher compliance to the treatment, cost reduction for both patients and institutions, better therapeutic approach for patients with multiple pathological conditions and the possibility of reducing dose and side effects, are some of them (SCHWEIN and SCHWEIN, 2014). However, few researches have been focusing on the development of FDCs based on modern formulation technologies (BJERRUM, et al., 2013).

It is important to mention that the association of two or more compounds in a dosage form can be complex, and pharmacokinetic and physicochemical aspects should be considered. In this context, the solubility of the compounds is highly relevant, especially regarding solid oral dosage forms.

The poor aqueous solubility of an active pharmaceutical ingredient (API) is considered one of the most challenging properties regarding the development of successful solid dosage forms. Nowadays, an increasing number of APIs are poorly water-soluble and aiming to overcome this limitation, the conversion of a crystalline material into its amorphous state has been extensively explored (VO et al. 2013; LAITINEN et al., 2012). Different from crystalline materials, amorphous solids lack the three-dimensional long-range order. As a result of this random organization, amorphous materials exhibit high internal energy, greater molecular mobility and enhanced thermodynamic properties compared to crystalline solids. This leads to increased apparent solubility and dissolution rate, but also culminates in their thermodynamic instability. Amorphous solids tend to structurally relax and crystallize during manufacturing, storage or dissolution (JANSSENS and VAN DEN MOOTER, 2009).

In an attempt to prepare more advanced FDCs, formulations based on hot melt co-extrusion (DIERICKX et al., 2014; VYNCKIER et al., 2014), prilling (VERVAECK et al., 2014) and co-amorphous systems (LAITINEN et al., 2013) have been recently reported. In most cases, systems composed of compounds with different solubility and/or intended for a combination of immediate/controlled release are described.

Considered as extremely challenging, the development of immediate-release FDCs composed exclusively of poorly water-soluble compounds has been scarcely investigated. Taupitz and coworkers developed FDCs of pioglitazone/glimepiride and simvastatin/ezetimibe, all BCS class II compounds. Different formulations were prepared and the best results were observed for ternary inclusion complexes composed of hydroxypropyl- $\beta$ -cyclodextrin, Soluplus and one of the APIs. Fast and higher release in comparison to the commercial formulations was observed for both FDCs, prepared through a mixture of ternary complexes of each API (TAUPITZ et al., 2013). Our group recently published the first attempt to prepare spray dried ternary solid dispersions composed of the poorly water-soluble compounds ritonavir, darunavir and one hydrophilic polymer (hydroxypropyl methylcellulose, polyvinylpyrrolidone or polyvinylpyrrolidone-vinyl acetate 64). The main goal was to increase the solubility and dissolution rate of both APIs from a single spray dried formulation. However, the rate and extent of release of both ritonavir and darunavir from ternary spray dried powders were less than the release from binary spray dried formulations, independently of the polymer used. In addition, both APIs had a negative influence on the supersaturation level of each other. In this case, an increased dissolution rate of darunavir and ritonavir was only achieved through complexation with cyclodextrin and the best results were observed for spray dried particles composed of (2-hydroxypropyl)- $\beta$ -cyclodextrin, HPMC and Tween 80 (NGUYEN and VAN DEN MOOTER, 2014).

Co-amorphous systems are recently developed formulations which allow the combination of two poorly water soluble APIs in a stable amorphous system. The major advantage towards well described solid dispersions is the absence of a carrier (polymer) in its composition. This basically means that usual problems in solid dispersions like large bulk volume, hygroscopicity and non-miscibility between the components can be avoided (LAITINEN et al., 2013). The combination of two poorly water-soluble compounds through co-amorphous systems was reported for naproxen:indomethacin (LÖBMANN et al., 2011), simvastatin:glipizide (LÖBMANN et al., 2012) and ritonavir:indomethacin (DENGALÉ et al., 2014). For simvastatin:glipizide and ritonavir:indomethacin binary systems, no intermolecular interactions were observed between the compounds and only one of the APIs presented an increase in the dissolution rate (glipizide and ritonavir, respectively) (DENGALÉ et al., 2014;

LÖBMANN et al., 2012). However, for the naproxen:indomethacin co-amorphous system, intermolecular interactions were assigned by FTIR and both compounds showed an increase of their dissolution rates (LÖBMANN et al., 2011).

The hypolipidemic compounds ezetimibe (EZE) and lovastatin (LOV) belong to Class II of the Biopharmaceutics Classification System (BCS). Presenting synergistic activity on lowering the cholesterol levels, their association in clinical practice is considered safe and efficient (KERZNER et al., 2003). Besides, the use of EZE with statins presents benefits regarding the reduction of statins side effects and low risk on developing type 2 diabetes (CEDERBERG et al., 2015). However, although the promising aspects of this association, no FDC of EZE and LOV is currently marketed.

Due to compatible pharmacokinetic parameters, similar doses and frequency of administration and low aqueous solubility, EZE and LOV were chosen as model compounds for this research. Aiming to overcome the physicochemical limitations of both compounds, as well as maintaining the benefits of their association, different technological approaches were targeted (*e.g.* co-amorphous systems, ternary solid dispersions and gelatin-based formulations) to prepare a final dosage form with possible therapeutic and commercial applications.





## 1.1 OBJECTIVES

### 1.1.1 Main objective

To develop a fixed dose combination solid dosage form based on amorphous systems able to enhance the solubility and dissolution rate of the poorly water-soluble compounds ezetimibe and lovastatin.

### 1.1.2 Specific objectives

To perform the solid-state characterization of ezetimibe and lovastatin through X-ray powder diffraction (XRPD), modulated differential scanning calorimetry (mDSC), infrared spectroscopy (IR) and intrinsic dissolution rate;

To develop and validate a high performance liquid chromatography (HPLC) methodology aiming to quantify simultaneously ezetimibe and lovastatin in the developed formulations and dissolution studies;

To prepare and evaluate, by means of solid-state techniques and *in vitro* dissolution studies, co-amorphous systems composed by ezetimibe and lovastatin, through quench cooling from the melt;

To prepare and evaluate, by means of solid-state techniques and *in vitro* dissolution studies, the impact of adding gelatin or hydrophilic synthetic polymers (PVP K-30, PVP VA-64, HPMC and Soluplus®) to amorphous systems of ezetimibe and lovastatin, prepared by different techniques;

To select the most promising formulation and evaluate its physico-chemical stability during 12 months under different storage conditions (4°C/0% RH, 40°C/0% RH e 40°C/75% RH);

To develop an enteric coated fixed dose combination by fluid bed coating able to avoid the hydrolytic formation of the hydroxyacid derivative of lovastatin in acidic conditions, as well as to promote a fast release of ezetimibe and lovastatin in simulated intestinal conditions.



**CHAPTER I**  
**INTRODUCTION**

---

## 1. FIXED DOSE COMBINATIONS

Fixed-dose combinations (FDCs), defined as a combination of two or more active pharmaceutical ingredients (APIs) in a fixed ratio of doses, are becoming increasingly important from a public health perspective. Nowadays, FDCs have been commonly used for a wide range of conditions, including cardiovascular, metabolic and hormonal-related pathologies, infections, allergies and pain, and have been designed for different routes of administration (EMA, 2015; WHO, 2005).

APIs in association can generate synergism or antagonism, both providing therapeutic benefits. Usually, combined APIs act through different mechanisms of action or target distinct physiological sites, which justifies the synergism. However, when combined, they should not present the same adverse reactions, in order to avoid exacerbation of undesired effects. Besides, their pharmacokinetic parameters should be compatible as to harmonize the route of administration, the interval between doses and the latency, the peak and duration of the therapeutic effect (WANNMACHER and HOEFLER, 2007).

The potential advantages related to a FDC are:

- additive or synergic effect of the associated APIs for each therapeutic indication or;
- improved efficacy of the associated APIs, with no increased risks when compared to monotherapy or;
- same therapeutic efficacy with reduced side effects, when compared to monotherapy or;
- reduced incidence of microbial resistance or;
- simplification of the therapeutic regimen (ANVISA, 2010).

Since the ‘polypharmacotherapy’ and the complexity of the therapeutic regimen have been pointed out as the main reasons for low compliance of patients to the treatment, efforts aiming the simplification of the drug therapy, especially in cases of chronic diseases, are necessary. Recent research has demonstrated that only around 35% of patients submitted to the ‘polypharmacotherapy’ are able to administer their medication correctly and regularly (SCHWEIM and SCHWEIM, 2014).

In this sense, FDCs have been playing an important role, since the risk of non-compliance to the treatment drops 24 to 26% in chronic patients using this kind of medication (BANGALORE et al., 2007).

In Brazil, FDCs are regulated by the RDC (from Portuguese *Resolução da Diretoria Colegiada*) 210, from September 2<sup>nd</sup>, 2004, which requires the proof of the efficacy and safety of new associations. According to this legislation, clinical assays are required for each therapeutic indication, proving the advantage of using the combined drugs in comparison to the monotherapy. A technical report is also requested to justify the rational basis of the association (BRAZIL, 2004). In December 2010, the Brazillian Health Regulatory Agency ANVISA has published two regulatory guidelines concerning the register of new associations (*Guideline to Register New FDCs* and the *Guideline to Register New FDCs intended for Hypertension*). These normatives complement the previous ones and have the purpose of enlightening the regulatory requirements of efficacy and safety necessary to register these medicines (ANVISA, 2010; 2010a). More recently, in 2014, ANVISA published the Technical Note NT 06/2014, that clarifies the relative bioavailability studies required to demonstrate the pharmacokinetic interaction in case of registering FDCs. According to this normative, these studies should be conducted with the reference medication administered isolated and simultaneously, in order to verify the occurrence or not of pharmacokinetic interactions between the compounds (ANVISA, 2014).

Nowadays in Brazil, 40 FDCs are present in the National List of Essencial Medications (RENAME, from Portuguese *Relação Nacional de Medicamentos Essenciais*), updated and revised in June 2015, in different doses, dosage forms and designed to distinct routes of administration (BRAZILIAN HEALTH MINISTRY, 2014). Through the International agency Food and Drug Administration (FDA), more than 100 FDCs have been approved for commercialization. The importance of these associations have been highlighted by FDA through the normative intitled *Guidance for industry: new chemical entity exclusivity determinations for certain fixed-combination drug products*, which stimulates the development of new FDCs, allowing more formulations to be eligible for a longer period of market exclusivity (FDA, 2015).

Different chronic diseases of high social impact are not satisfactorily covered by the currently available monotherapy treatments. Concerning dyslipidemia, although monotherapy with hypolipidemic drugs can provoke multiple changes in the lipidemic profile, the

association of drugs, especially between ezetimibe (EZE) and statins, has been indicated for a broader management of the physiological lipids (V BRAZILIAN GUIDELINE ON DYSLIPIDEMIA AND ATHEROSCLEROSIS, 2013). Besides, this association has been highly recommended due to increased risks of developing type 2 diabetes in hypercholesterolemic patients submitted to monotherapy with statins (CEDERBERG et al., 2015).

The control of physiological lipids, such as triglycerides and cholesterol fractions, is of vital importance due to its relation with the development of atherosclerosis, the main cause of cardiovascular diseases (V BRAZILIAN GUIDELINE ON DYSLIPIDEMIA AND ATHEROSCLEROSIS, 2013). Nowadays, atherosclerosis represents the major cause of death in the world and the World Health Organization (WHO) affirms that levels of total cholesterol above 146 mg/dL ( $> 3.8$  mmol/L) are responsible for 18% of brain vascular diseases and for 56% of heart diseases in global scale (WHO, 2002). Besides, according to the *Atlas of Heart Disease and Stroke*, 17 million people die, every year, in the whole world, due to cardiovascular diseases (WHO, 2004).

In Brazil, the cardiovascular diseases have also been the main cause of death (approximately 30%). They have been responsible for a high frequency of hospitalization, which impacts on high medical and social costs. In November 2009, 91970 hospitalizations occurred due to cardiovascular diseases, resulting in more than R\$ 165 million expenses (VI BRAZILIAN GUIDELINES ON HYPERTENSION, 2010).

## 2. EZETIMIBE AND LOVASTATIN

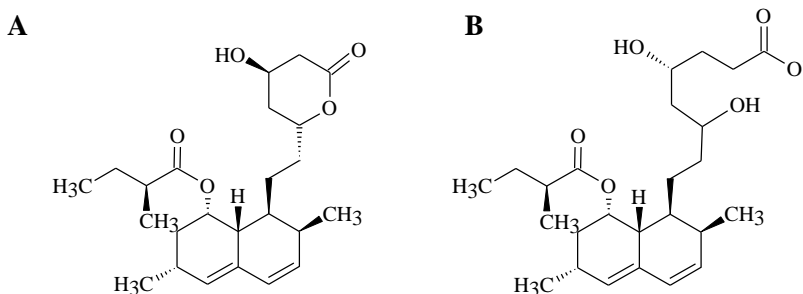
Regarding the treatment of dyslipidemia, the classes of drugs usually used are the statins (which can be administered in association with EZE), cholestiramine, fibrates and nicotinic acid (V BRAZILIAN GUIDELINE ON DYSLIPIDEMIA AND ATHEROSCLEROSIS, 2013).

Statins are considered the first choice drugs to reach the therapeutic target in hypercholesterolemic patients with risk or recurrent manifestation of coronary diseases (ARAÚJO; CASELLA FILHO and CHAGAS, 2005). These drugs inhibit the HMG-CoA reductase, leading to a reduced intracellular synthesis of cholesterol. In consequence, an increase in number of LDL-cholesterol receptors in the hepatocytes is

observed, which in turn, removes more VLDL-cholesterol and LDL-cholesterol from the blood flow. Taken once a day, statins distribute selectively to the liver and are excreted mainly through feces (85%) and urine (10%). Their effect can be verified after 2 weeks of administration, becoming stable from the fourth week. Statins result in decreased levels of total cholesterol (around 30%), LDL-cholesterol (20 to 40%), triglycerides and VLDL-cholesterol (around 20%), associated with increased levels of HDL-cholesterol (up to 10%). Statins reduce cardiovascular mortality and the incidence of acute ischemic coronary events, as well as the need for myocardial revascularization and cerebrovascular accidents (BRAZILIAN CONSENSUS ON DYSLIPIDEMIA, 1996; V BRAZILIAN GUIDELINE ON DYSLIPIDEMIA AND ATHEROSCLEROSIS, 2013).

Among the statins currently available, lovastatin (LOV, Figure 1A), has been widely used in clinical practice, being one of the drugs which compose the RENAME. In Brazil, LOV is commercialized as tablets of 10, 20 and 40 mg (BRAZILIAN MINISTRY OF HEALTH, 2014).

**Figure 1.** Chemical structure of lovastatin (A) and its active  $\beta$ -hydroxy acid metabolite (B)



LOV is a poorly water-soluble pro-drug (Class II in the Biopharmaceutics Classification System (BCS), refer to Topic 3), which is rapidly metabolized to its active  $\beta$ -hydroxy acid metabolite (LOVh, Figure 1B), mainly in the liver. In addition, LOVh can also be formed through chemical hydrolysis of LOV. Importantly, as both LOV and LOVh have the liver as their site of action, their concentration in this

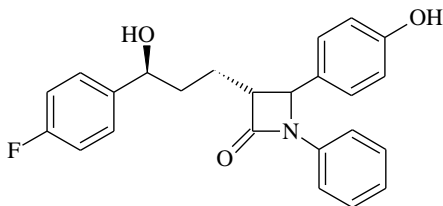
organ should be maximized as much as possible. Studies in animals have demonstrated that LOV presents a better hepatic sequestration than LOVh, which in turn minimizes the systemic side effects (DUGGAN et al., 1988). As the author states that this provides a rational basis for the lactone to be the preferred API for the dosage form, the hydrolytic formation of the active metabolite in gastric conditions should be avoided.

LOV shows high plasma protein binding (95%), fast biotransformation,  $t_{1/2}$  of 1-2 h, less than 5% absorption by oral route and  $t_{max}$  of 2 to 4 h (MARTINDALE, 2009). When administered in 10, 20 and 40 mg, it is capable of reducing LDL-cholesterol levels in 21, 27 and 31%, respectively (HOU and GOLDBERG, 2009).

Concerning its physicochemical properties, LOV ( $C_{24}H_{36}O_5$ ) has a molecular weight of 404.5 g/mol and melting point ranging from 174-176°C. Its pKa is 14.9 and its logP value corresponds to 4.11 (BRITISH PHARMACOPOEIA, 2009). According to previous studies, LOV is considered stable under oxidative and thermal stress conditions, however, it is susceptible to photolysis and hydrolysis (acidic and alkaline). In this last case, its active metabolite LOVh can be generated (CHAUDHARI and UBALE, 2012). Polymorphic forms are not reported.

EZE (Figure 2), is the first member of a new class of compounds, the 2-azetidinones, which selectively inhibit the absorption of biliary and dietary cholesterol from the small intestine by blocking the Niemann-Pick C1 like 1 protein. Its administration results in a reduction of cholesterol absorption from endogenous and exogenous sources (TIWARI and KHOKHAR, 2014).

**Figure 2.** Chemical structure of ezetimibe



Different from LOV, EZE shows pseudopolymorphism (PARTHASARADHI et al., 2003) and can be found as anhydrate (BRÜNING, ALIG and SCHMIDT, 2010) and monohydrate (RAVIKUMAR and SRIDHAR, 2009). It has a melting point around



163°C, molecular weight of 409.4 g/mol ( $C_{24}H_{21}F_2NO_3$ ), pKa of 9.5 and logP value of 4.56 (DE OLIVEIRA, 2007). As LOV, EZE is a poorly water-soluble drug which belongs to Class II in the BCS. EZE is chemically stable under thermal and oxidative stress conditions, although it is susceptible to neutral, acidic and alkaline hydrolysis (SINGH et al., 2006).

EZE is rapidly captured by the intestinal cells after oral ingestion, and glucuronidized to its bioactive metabolite. In this form, it is absorbed and reaches the maximum plasma concentration after 1 h. Its half-life shows age-dependent variability, reaching longer plasma residence time in elderly patients. EZE and its active glucuronide are eliminated mainly through feces (80%) and a small percentage by urine (11%) (ARAÚJO; CASELLA FILHO and CHAGAS, 2005).

EZE is administered once a day and commercialized as 10 mg tablets (ARAÚJO; CASELLA FILHO e CHAGAS, 2005). In monotherapy, it reduces LDL-cholesterol levels up to 20%. It has been more often employed in association with statins, due to a potencialized effect reducing the intracellular cholesterol levels. Reports declare that this association provides 20% extra reduction in LDL-cholesterol levels in comparison to statins in monotherapy (ARAÚJO; CASELLA FILHO and CHAGAS, 2005; SCHULZ, 2006; IV BRAZILIAN GUIDELINE ON DYSLIPIDEMIA AND ATHEROSCLEROSIS, 2007; HOU; GOLDBERG, 2009). Besides, this association promotes an additional reduction of triglycerides in a range of 7 to 13% and an increase of 1 to 5% in HDL-cholesterol levels (HOU and GOLDBERG, 2009). Also, it is important to mention that the association of EZE with statins does not provoke any relevant pharmacokinetic alteration (SCHULZ, 2006).

A clinical study conducted by Kerzner and coworkers in 2003 evaluated the efficacy and safety of the coadministration of EZE (10 mg) and LOV (10, 20 or 40 mg) in 548 patients with primary hypercholesterolemia. Results indicated that the coadministration with EZE led to 10 and 14% reduction of triglycerides and LDL-cholesterol, respectively, besides promoting an increase of 5% of HDL-cholesterol, in comparison to LOV monotherapy. In this way, the therapeutics involving the combined administration of EZE + LOV resulted in an average reduction of 33 to 45% of LDL-cholesterol levels and of 19 to 27% of triglycerides levels. In addition, an increase of 8 to 9% was observed for HDL-cholesterol. These results were dependent on LOV concentration. Besides, the combined administration of 10 mg EZE plus 10 mg LOV

(initial dose) demonstrated similar efficacy to the highest dose of LOV (40 mg) when administered in monotherapy. The coadministration was well tolerated and safe (KERZNER et al., 2003).

In 2005, the coadministration of EZE + LOV was also evaluated by Tadiboyina and coworkers, in an adolescent patient with cholesterol ester storage disease. The administration of increasing doses of LOV during an approximate period of 80 months promoted an average reduction of 15% of LDL-cholesterol levels. However, with the addition of EZE (10 mg) to LOV (40 mg), an additional average decrease of 16% related to the LDL-cholesterol levels was observed. These data demonstrate the efficacy and tolerability of the combined administration of EZE and LOV in patients with this pathology (TADIBOYINA et al., 2005).

Although the association of EZE and LOV can be considered relevant and promising, the low solubility of both compounds makes the development of a FDC more challenging. EZE and LOV are Class II drugs in BCS (WU and BENET, 2005; TAKAGI et al., 2006), which means that they possess low solubility and high permeability. LOV is considered practically insoluble in water, although soluble in acetone and slightly soluble in anhydrous ethanol (BRITISH PHARMACOPOEIA, 2009). Similar solubility is observed for EZE, which is practically insoluble in water, although very soluble in ethanol, methanol and acetone (DE OLIVEIRA, 2007).

In this context, the development of formulations composed by these APIs should involve technological strategies capable of increasing its solubility and dissolution rate. Among the approaches available, such as micronization, solubilization in surfactant systems, formation of complexes soluble in water, utilization of salts, co-crystals and pro-drugs (BIKIARIS, 2011), the conversion of crystalline to amorphous solids is presented as a promising attempt.

### **3. THE AMORPHOUS STATE AND ITS IMPACT ON THE SOLUBILITY OF DRUGS**

Solubility is a thermodynamic parameter defined as the maximum amount of a solid substance which can be dissolved in a certain volume of solvent or solution at constant and specified temperature and pressure (LACHMAN; LIEBERMAN and KANIG, 2001).

According to Florence and Atwood, various are the reasons which justify the vital importance of knowing how drugs dissolve to form a solution and the factors that maintain the solubility or that cause precipitation. Among them, it is well known that drugs should be molecularly dispersed, or in solution, to be absorbed, independent of the dosage form in which they are enclosed. In this sense, it is particularly important to have the knowledge about the solubility of a certain compound in biological fluids, so it can be able to cross the lipoprotein membranes (FLORENCE and ATWOOD, 2003).

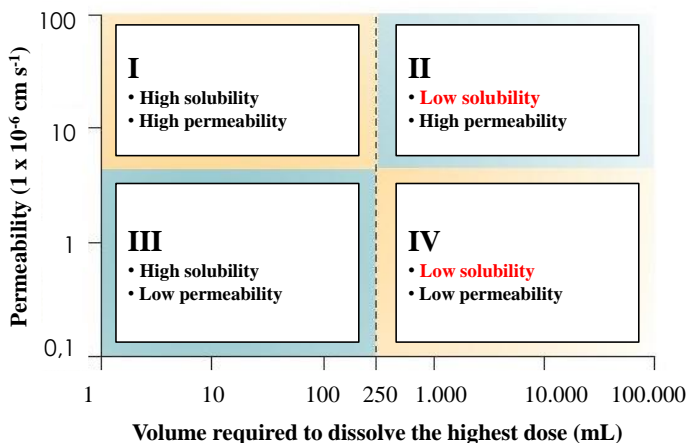
Nowadays, the percentage of APIs showing relevant therapeutic value and low aqueous solubility is estimated at 25 to 40% of the total of developed drugs (BIKIARIS, 2011). Due to their low bioavailability, this percentage of new APIs shows limited therapeutic application, being commonly rejected or subutilized by the pharmaceutical industry (SVENSON, 2009). Besides, drugs with low aqueous solubility can deposit in specific physiological sites, forming aggregates that increase their toxic effects (LIPINSKI, 2002).

The influence of solubility, associated to permeability, on the 'in vivo' performance of a drug, instigated Amidon and coworkers to propose, in 1995, the BCS. In this classification system, drugs are qualified in four distinct classes according to the two parameters previously mentioned (AMIDON et al., 1995).

In this context, the four classes are:

- Class I: high solubility and high permeability;
- Class II: low solubility and high permeability;
- Class III: high solubility and low permeability;
- Class IV: low solubility and low permeability.

In order to be qualified in any of these classes, it is necessary to determine the solubility of the compound based on the dissolution of its highest dose in 250 mL of a buffer solution with pH ranging from 1.2 to 6.8. The compound will be considered highly soluble if its highest dose dissolves in 250 mL of buffer, or less. On the other hand, a pharmaceutical compound is considered highly permeable if the fraction of absorbed dose is at least 85% (BRASIL, 2011) (Figure 3).

**Figure 3.** Correlation among solubility, permeability and dose

Although showing high permeability, BCS Class II drugs present solubility problems in a way that dissolution becomes the limiting factor for its absorption. In this context, technological approaches aiming the optimization of their physicochemical properties (*e.g.* solubility and dissolution rate) are considered as rational options to optimize therapeutics, as they can have a positive impact on the oral bioavailability of these compounds (AMIDON *et al.*, 1995). To contemplate the interests of the pharmaceutical industry, these strategies should be linked to pharmaceutical formulations which present physicochemical stability, financial advantages, easy scale-up, and simple production (LIMA, 2006).

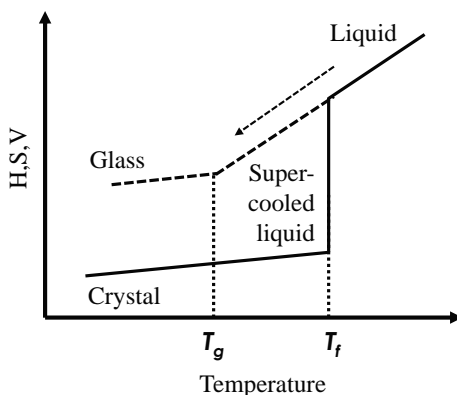
The amorphous materials compose an interesting strategy which aims enhanced solubility of drugs. These materials are considered a distinct class of solids, which do not present the three-dimensional molecular order, characteristic of crystalline solids. On the other hand, molecules in amorphous materials are randomly distributed and their interactions with other molecules, such as hydrogen bonding and electrostatic interaction, are not repeated with any regularity along the whole sample (HANCOCK, 2007). This arrangement provokes important differences in physicochemical properties of amorphous and crystalline solids, in a way that they can be easily differentiated, as described in Scheme 1.

**Scheme 1.** Characteristics of amorphous and crystalline solids. Adapted from Hancock (2007)

Amorphous solids	Crystalline solids
True density of amorphous forms is 5 to 20% lower than the one presented by the crystalline form	True density of pharmaceutical crystals ranges from 1 to 2.5 g/mL
Amorphous particles are not refringent in polarized light microscopes	Crystalline particles exhibit characteristic birefringent patterns when visualized in polarized light microscope
X-rays are randomly diffracted in amorphous samples, resulting in a diffraction pattern composed of a broad halo	X-rays are diffracted in a coherent and ordinated manner in crystalline powders, producing a diffraction pattern with characteristic and well-defined peaks
Amorphous materials usually exhibit a significant increase in water solubility and dissolution rate when compared to crystalline materials	Crystalline samples adsorb water in small quantities unless they form crystalline hydrates
Amorphous materials exhibit a glass transition temperature ( $T_g$ ) which in values, usually correspond to 2/3 of the crystalline melting point	Crystalline materials exhibit defined melting points, which are associated to their enthalpy of fusion

Amorphous solids are characterized by a glass transition temperature. From a thermodynamic point of view, when a crystal melts, it should crystallize when cooled below its melting point. However, at high cooling rates, crystallization is usually suppressed and the material is found in a super-cooled liquid state. As the temperature drops, molecular mobility is reduced and the super-cooled liquid escapes from the liquid state curve. At this point, molecular mobility is insufficient to allow the equilibrium of the system with the timeframe of the cooling process. In this sense, abrupt changes of entropy, enthalpy and volume of the material are observed, characterizing the glass transition. The region below the  $T_g$  is known as glassy state (Figure 4). Due to the high viscosity of this state, molecular mobility is reduced and relaxation processes become slow. In this way, the glassy state has rheological properties of a solid and molecular properties of a liquid (JANSSENS and VAN DEN MOOTER, 2009; BELLANTONE, 2014).

**Figure 4.** Schematic diagram showing changes in enthalpy (H), entropy (S) and volume (V) in liquid, crystalline and glassy state in function of temperature.  $T_g$  and  $T_f$  represent the glass transition temperature and the temperature of fusion, respectively. Adapted from Janssens and Van den Mooter (2009).



Besides the quench cooling from the melt method, amorphous solids can also be prepared by solvent evaporation methods (*e.g.* spray drying and freeze drying), precipitation from a solution, dehydration of hydrates and as consequence of mechanical stress induced by compaction, compression or intense crystal milling (HANCOCK, 2007; JANSSENS and VAN DEN MOOTER, 2009).

To comprehend the relation between the amorphous state and the solubility of a compound, it is necessary to establish a relation between the dissolution process and the energy required for this event. At a certain temperature, the source of heat necessary for dissolution is known as solvation energy. Solvation is a phenomenon in which the solvent molecules “link” to undissolved drug molecules and the kinetic energy from solvent molecules is transferred to a complex drug-solvent. This energy transfer is a function of the attraction energy between drug and solvent and of the number of solvent molecules which effectively transfer energy to the undissolved drug. If this kinetic energy is sufficient to overcome the drug-drug interactions, the drug molecule leaves the undissolved environment and moves to the solvent, where it will be surrounded by more solvent molecules and will make part of the solution.

Once in solution, drug molecules are capable of getting dispersed in the solvent and will comprise the “dispersive region” (BELLANTONE, 2014).

In this context, any modification of the undissolved form that reduces the drug-drug attraction forces will be capable of reducing the energy necessary to make them dissolved. As a consequence of the disordered arrangement of the amorphous state, a larger separation between molecules is observed, as well as a reduction of the intermolecular attraction forces, in comparison to the crystalline state. In this way, the energy required to reach the melting point and the “dispersive region” is lower in amorphous materials than in the crystalline ones. This reduction of the necessary energy in case of amorphous materials culminates in a higher solubility and dissolution rate (BELLANTONE, 2014; HANCOCK, 2007).

Another strategy to reduce the required energy to reach the “dispersive region” occurs through the addition of excipient molecules among drug molecules. In this case, the interactions between drug and excipient are weaker than the drug-drug interactions, and/or the interactions between excipient and water are stronger than the ones happening between drug and water. In the first case, there is a reduction of the necessary energy to displace the drug and reach the “dispersive region”. On the other hand, the second strategy comprehends an increase of the energy obtained from the excipient-water interactions to dissolve the drug molecules. This option is the base of solid dispersions and other polymer-based systems (BELLANTONE, 2014).

However, it is important to mention that amorphous materials are thermodynamically unstable and there is a tendency to crystallize during processing, dissolution and storage (HE, 2009). In this context, the development of stable amorphous systems is a challenge for pharmaceutical researchers.

The stabilization of amorphous drugs have been widely reported by means of solid dispersions and other polymer-based formulations (LEUNER and DRESSMAN, 2000; VASCONCELOS, SARMENTO and COSTA, 2007; VAN DEN MOOTER, 2012), and more recently, also through co-amorphous systems. In all these cases, the physical stabilization of these materials occurs via the increase of the overall  $T_g$ , by the miscibility between drug particles or drug-polymer particles, or through the establishment of intermolecular interactions such as hydrogen bonding (LAITINEN et al., 2013).

## 4. STRATEGIES IN AMORPHOUS STATE APPLIED TO IMPROVE SOLUBILITY AND DISSOLUTION RATE IN FIXED DOSE COMBINATIONS

### 4.1 CO-AMORPHOUS SYSTEMS

Co-amorphous systems have been recently introduced as potential systems involving poorly water-soluble drugs. These type of formulations aim to overcome the commonly reported problems faced with amorphous materials when composing the conventional combinations between drugs and hydrophilic polymers (LÖBMANN et al., 2012).

Co-amorphous systems can be defined as systems which comprise the combination of two or more amorphous solids of low molecular weight, all in a single amorphous phase. These systems are capable of increasing the solubility and dissolution rate of poorly water-soluble drugs, as well as their physical stability, mainly due to solid-state interactions (*e.g.* hydrogen bonding) among the components. Importantly, the co-amorphous systems show advantages even in comparison to the isolated amorphous drugs, demonstrating the efficiency of the combination. So far, co-amorphous systems described in literature have been obtained through solvent evaporation techniques (*e.g.* spray drying or under vacuum conditions), mechanical activation by milling and quench cooling from the melt (ALLESØ et al., 2009; CHIENG et al., 2009; LAITINEN et al., 2012, LÖBMANN et al., 2012, 2012a; SHAYANFAR; JOUYBAN; HAMISHEHKAR, 2012; GAO et al., 2013; LÖBMANN et al., 2013, 2013a; SHIMADA et al., 2013).

As mentioned previously, the major advantage of these systems refers to the replacement of hydrophilic polymers by drugs, since the commonly faced problems in solid dispersions such as their hygroscopic characteristic, miscibility problems and large total bulk volume, are overcome. In co-amorphous systems, the antiplastifying characteristic associated to the hydrophilic polymers in solid dispersions, becomes a property of one of the drugs or other component of the system, usually the one with the highest aqueous solubility (LAITINEN, et al., 2013). Besides, as in solid dispersions, a single and increased  $T_g$  is desired, which is intrinsically correlated to the miscibility of the system and corroborates to its physical stability (ALLESØ et al., 2009; LÖBMANN et al., 2013).



One of the first reports in literature about the combination of two drugs in amorphous state was described by Yamamura and coworkers, through the binary association between cimetidine and the nonsteroidal anti-inflammatory drugs (NSAIDs) naproxen (YAMAMURA et al., 1996), indomethacin (YAMAMURA et al., 2000) and diflunisal (YAMAMURA et al., 2002). Initially, the researchers attributed the formation of the amorphous binary systems to the absence of intermolecular interactions between the imidazolic ring from cimetidine and the carbonyl group of the NSAIDs (YAMAMURA et al., 1996; 2000). However, after a more detailed study with diflunisal, the obtainment of the amorphous systems was then attributed to a salt formation between the molecules, increasing the solubility of the poorly water-soluble drugs (YAMAMURA et al., 2000; 2002).

Later, these studies have been improved and the first co-amorphous systems were reported. In 2009, Chieng and coworkers described the preparation of co-amorphous systems by milling of indomethacin and ranitidine hydrochloride, which comprised a single amorphous phase in 2:1, 1:1 and 1:2 (indomethacin:ranitidine hydrochloride) molar ratios (CHIENG et al., 2009).

In the same year, Alleso and coworkers prepared co-amorphous systems, also by milling, with the BCS Class II compound naproxen and the BCS Class III drug, cimetidine, using the same molar ratios as previously reported. It was observed that the co-amorphous system was able to increase the intrinsic dissolution rate of naproxen and cimetidine up to 4 and 2 times, respectively. The 1:1 molar ratio provided the formation of intermolecular interactions between the compounds, besides being the proportion with the best physical stability (ALLESØ et al., 2009).

Similar reports have been described in 2011 by Löbmann and coworkers, with the preparation of co-amorphous systems of the BCS Class II compounds naproxen and indomethacin, by quench cooling. A 7-fold increase in the dissolution of indomethacin was reported, besides a synchronized dissolution of the compounds, due to the formation of a heterodimer between the APIs (LÖBMANN et al., 2011).

From these promising data, researchers have published the preparation of co-amorphous systems of simvastatin and glipizide (LÖBMANN et al., 2012), atorvastatin calcium and nicotinamide (SHAYANFAR; JOUYBAN; HAMISHEHKAR, 2012), repaglinide and saccharine (GAO et al., 2013), ritonavir and indomethacin (DENGALÉ

et al., 2014), salmeterol xinafoate and mometasone furoate (LIU et al., 2015) and EZE and indapamide (KNAPIK et al., 2015). Recent papers have also demonstrated the potential of using aminoacids to prepare binary and ternary co-amorphous systems (LÖBMANN et al., 2013, 2013a; LAITINEN et al., 2014; JENSEN et al., 2014; LENZ et al., 2015). In cases in which the solubility and/or the dissolution rate were evaluated, the reported co-amorphous systems demonstrated the improvement of both parameters, besides keeping or enhancing the physical stability of the system. In this way, these type of formulation has proven to be a promising alternative for FDCs composed of poorly water-soluble drugs (LÖBMANN et al., 2012a).

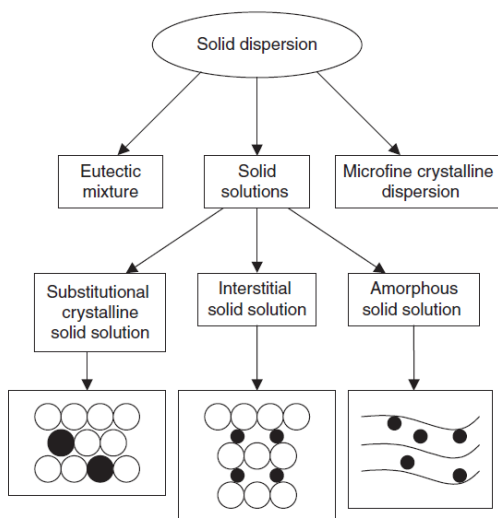
## 4.2 SOLID DISPERSIONS

Solid dispersions can be defined as a system in which a drug, usually lipophilic, is dispersed in one or more hydrophilic and biologically inert carriers. The purpose of this type of formulation is generally to alter the crystallinity of the drug in order to enhance its dissolution rate and to disperse it in material with high solubility in aqueous environment (PADDEN et al., 2011).

The term solid dispersion has been more often associated to glassy solutions, which comprise the dispersion of a poorly water-soluble compound in amorphous carriers. In this case, a single amorphous phase is composed by molecules of drug well mixed with molecules of carrier, generating intimate miscibility which corroborates to the enhancement of the dissolution properties of the drug (VAN DEN MOOTER, 2012). In addition, solid dispersions can also have other different classifications, as depicted in Figure 5, according to their crystallinity degree and how the drug is distributed in the system (HE, 2009).

The improvement of the dissolution rate of a drug by means of solid dispersions can be explained through the reduction of particle size and consequent increase of surface area, better drug wettability by the presence of a hydrophilic polymer, increased porosity of the whole system and especially due to drug amorphization and miscibility between drug and carrier(s) (BLOCK e SPEISER, 1987; CRAIG, 2002; VASCONCELOS; SARMENTO e COSTA, 2007).

**Figure 5.** Classification of solid dispersions according to the distribution of drug molecules in the carrier(s). From HE, 2009



Despite of that, solid dispersions are widely investigated due to their capacity to stabilize amorphous drugs. This occurs mainly via the occurrence of intermolecular interactions among the components, such as hydrogen bonding, and an adequate miscibility of the compounds, usually increasing the overall  $T_g$  of the system. In this last case, the molecular mobility is reduced in conditions of temperature and relative humidity commonly occurrent in storage, delaying the phase separation and crystal growing processes (BHUGRA e PIKAL, 2008; VAN DEN MOOTER, 2012). In general, relatively small amounts of polymer have demonstrated a significant inhibition of crystallization, both in solid-state before administration as well as after the introduction of the solid dispersion in a dissolution medium or gastrointestinal environment (ALONZO et al., 2010).

Sekiguchi and Obi (1961) proposed for the first time the formulation of a eutectic mixture aiming to increase the low solubility of a compound (SEKIGUCHI and OBI, 1961). These researchers have noted that the formation of these systems increased the dissolution rate and the bioavailability of hydrophobic compounds. In this context, many of these mixtures were synthesized with the same purpose, showing satisfactory

results. Many different pharmaceutical carriers were tested, such as urea and saccharose, which are highly water soluble, crystalline excipients.

Nowadays, solid dispersions can be classified as first, second and third generations. Formulations similar to the ones developed by Sekiguchi and Obi are qualified as first generation systems. These ones refer to eutectic mixtures of drugs and highly soluble crystalline carriers (VASCONCELOS; SARMENTO and COSTA, 2007).

Second generation solid dispersions comprise the formulations with amorphous polymers, which present more pronounced solubility and dissolution rate enhancements. The carriers most often employed in this kind of system are divided in two categories, the synthetic and non-synthetic ones. The synthetic polymers include the polyvinyl pyrrolidones (PVP), polyethylene glycol (PEG) and polymethacrylates. The semi-synthetic polymers are mainly derived from cellulose, such as hydroxypropylmethyl cellulose (HPMC), ethyl cellulose (EC), hydroxypropyl cellulose (HPC) or derivatives from starch, like cyclodextrins (VASCONCELOS; SARMENTO and COSTA, 2007).

On the other hand, the third generation of solid dispersions involves the utilization of surfactants, improving even more the low solubility of pharmaceutical compounds. Some examples of surfactants currently used are Soluplus®, Poloxamer 407® and Poloxamer 188® (SERAJUDDIN; SHEEN and AUGUSTINE, 1990; SHEEN et al., 1995).

The choice of a carrier is a crucial point regarding the development of a successful solid dispersion, since it exerts a great influence on the dissolution properties and physical stability of the drug and formulation (BLOCK; SPEISER, 1987).

In this sense, a carrier must accomplish with the following requisites:

- Be highly water-soluble;
- Be non-toxic and pharmacologically inert;
- Be thermostable and present a low melting point, in cases in which the solid dispersions are prepared by melting methods;
- Be soluble in a large variety of solvents, besides being capable of passing through the glassy state when applied to a solid dispersion obtained via a solvent evaporation method;

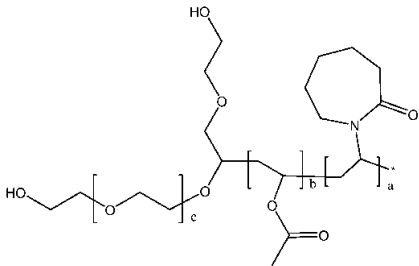
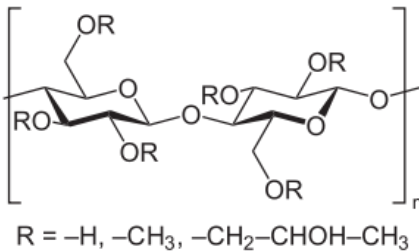
- Be chemically compatible with the drug, not forming too strong and complex chemical bonding with it, which could hamper its release and solubilization (LEUNER e DRESSMAN, 2000; VADNERE, 2007).

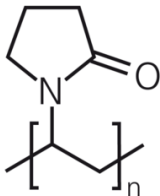
The carriers chosen to compose the solid dispersions in this research are shown in Scheme 2 and their main properties are described.

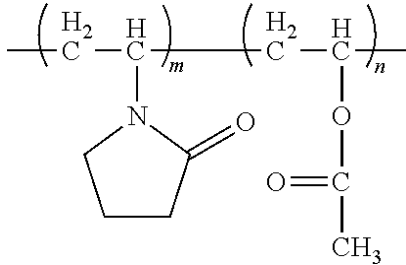
According to their composition, solid dispersions can be classified as binary or ternary. Binary formulations are composed of the drug, usually lipophilic, and a hydrophilic carrier. Ternary solid dispersions most often reported in literature correspond to a drug and a mixture of two carriers. For the first time, this research demonstrates the preparation and investigation of ternary solid dispersions composed of two poorly water-soluble compounds, in order to compose a FDC.

Basically, solid dispersions can be prepared by a fusion method, solvent evaporation method or a combination of both (LEUNER e DRESSMAN, 2000; VAN DEN MOOTER, 2012; VO, PARK e LEE, 2013). More recently, mechanical activation techniques, such as high energy milling, have been also used and have the advantage of being environmentally friendly and easy to scale-up, although more time consuming (RIEKES et al., 2014; NART et al., 2015). Melting methods, such as hot melt extrusion and quench cooling, are more adequate for drugs and carriers which mix in liquid state after the fusion of both. However, it can be more limiting due to the occurrence of sublimation, polymorphic transformation and thermal degradation (GOLDBERG; GIBALDI e KANIG, 1965; LEUNER e DRESSMAN, 2000). Solvent evaporation methods have the disadvantage of using organic solvents, but are especially indicated for thermolabile compounds. In this type of process, drug and carrier are dissolved in the same solvent or mixture of solvents, which are later removed by evaporation, under vacuum conditions, or by spray drying, freeze drying and supercritical fluid technology (BETAGERI and MAKARLA, 1995; LEUNER and DRESSMAN, 2000; SETHIA and SQUILLANTE, 2004; DURET et al., 2012).

**Scheme 2.** Carriers used in solid dispersions and their main properties

Chemical and commercial name	Chemical structure	Observations	Reference
Polyvinyl caprolactone (PVC) - polyvinyl acetate (PVA) – polyethylene glycol (PEG) copolymer  <i>Soluplus®</i>		Amphipillic properties and excelente capacity of forming solid solutions. Due to its wide solubility in organic solvents and low $T_g \sim 70^\circ\text{C}$ , it can be applied to the preparation of solid dispersions by solvent evaporation or melting methods.	LINN et al., 2012; HARDUNG, DJURIC and ALI, 2010.
Hydroxypropilmethyl cellulose (HPMC)  <i>Methocel®</i> , <i>Metolose®</i> , <i>Pharmacoat®</i> , <i>Tylopur®</i> , <i>Tylose MO®</i>	 <p><math>R = -H, -CH_3, -CH_2-CHOH-CH_3</math></p>	Available in various grades, which vary according to its viscosity and substitution grade. Its molecular weight ranges from 10,000 to 1,500,000 g/mol. It is soluble in cold water, forming a viscous colloidal solution, practically insoluble in hot water, chloroform, ethanol (95%) and ether, but soluble in mixtures of ethanol:dichloromethane,	ROGERS, 2009; WANG et al., 2015.

		methanol:dichloromethane and water:ethanol. Presents a high $T_g$ (~ 170-180°C).	
<p>Polyvinyl pyrrolidone (PVP)</p> <p><i>Plasdone</i>®, <i>Kollidon</i>®, <i>Povipharm</i>®</p>		<p>Synthetic linear polymer with different degrees of polymerization, resulting in materials with distinct molecular weights. It is characterized by its viscosity in aqueous solutions, which are expressed in <math>K</math> values, ranging from 10 to 120. It is easily soluble in acids, chloroform, ethanol (95%), ketones, methanol and water; practically insoluble in ether, hydrocarbonates and mineral oil. Presents a <math>T_g</math> value around 150°C.</p>	KIBBE, 2009

<p>Polyvinyl pyrrolidone- polyvinyl acetate copolymer (PVP/VA)</p> <p><i>Kollidon VA 64®</i>, <i>Luviskol VA®</i>, <i>Plasdone S-630®</i></p>		<p>Composed of a copolymer of 1-vinyl-2-pyrrolidone and vinyl acetate, in a mass ratio of 3:2. The association of these two monomers implies to this polymer surfactant and stabilizer properties. It shows a <i>K</i> value varying from 25.4 to 34.2, which is associated to its viscosity in aqueous solutions. It shows solubility higher than 10% in 1,4 butanediol, glycerol, butanol, chloroform, dichloromethane, ethanol (95%), methanol, polyethyleneglycol 400, 2-propanol, propanol, propileneglycol and water. It is soluble in less than 1% of cyclohexane, diethylether, liquid parafine and pentane and has a <i>T<sub>g</sub></i> value of 106 °C.</p>	<p>ABUBAKER, 2009; GOUVEIA, 2011</p>
---	---	---	--



### 4.3 GELATIN-BASED FORMULATIONS

Gelatin is widely known as a natural, biocompatible, biodegradable and multifunctional highly water-soluble biopolymer. Obtained through partial hydrolysis of animal-source collagen, mainly from cattle bones, cattle hides, and porkskins, it can be qualified as Type A and Type B, if derived from acid or alkali-treated processes, respectively (GMIA, 2012; FOOX and ZILBERMAN, 2015).

Extraction processes applied to prepare Type A and Type B gelatin involve some important parameters such as pH, time, temperature and number of extractions, which vary according to the product needs, type of equipment employed, timing and costs. Usually, the number of extraction ranges from 3 to 6 and temperature varies from 50 to 60 °C, at a first stage, being subsequently increased in steps from 5 to 10°C, close to the boiling point, in later stages. Initial extraction provides superior quality material, with higher molecular weights, viscosity, gel strength and lighter color, in comparison to later stages. Type A process usually applies hydrochloric acid or sulfuric acid, whilst alkali-treated process uses mainly lime (GMIA, 2012).

Composed by a heterogeneous mixture of water-soluble proteins of high average molecular weight (15,000 to 400,000 Da), the final composition of gelatin depends mainly on its source and extraction process, generating a wide variety of aminoacids, after hydrolysis. The three more abundant aminoacids found in gelatin are glycine, proline and hydroxyproline. In terms of basic elements, gelatin is composed of 50.5% carbon, 6.8% hydrogen, 17% nitrogen and 25.2% oxygen (KALLINTERI and ANTIMISIARIS, 2001; GMIA, 2012; FOOX and ZILBERMAN, 2015).

In comparison to other materials, gelatin offers the advantages of being cheap, readily available, biocompatible and biodegradable (ELZOGHBY, 2013). Besides, although mainly derived from animal sources, the digestive process confers gelatin very low antigenicity, with the formation of harmless metabolic products upon degradation (SANTORO, TATARA and MIKOS, 2014). Being recognized as a Generally Regarded as Safe (GRAS) material by FDA, gelatin is widely employed due to its unique properties in food, pharmaceutical, cosmetic and medical applications (FOOX and ZILBERMAN, 2015).

Having a long history of safe use in pharmaceuticals, especially in the composition of hard capsules, more recently, gelatin has been also used in the development of modern drug delivery systems. Its application has been reported in controlled drug delivery formulations, as an absorption enhancer or improving the dissolution of poorly water-soluble compounds (FOOX and ZILBERMAN, 2015). Regarding this last case, literature described gelatin-based formulations able to enhance the dissolution rate of nitrofurantoin, chlorothiazide, phenobarbital, prednisolone, griseofulvin, diazepam and piroxicam, as reported by Kallinteri and Antimisiaris (2001). These researchers stated that there is a tendency for larger gelatin-induced increases in solubility as drug lipophilicity increases. In the same context, gelatin-based systems were able to improve the dissolution rate of the poorly soluble drugs pranlukast (CHONO et al., 2008), ibuprofen (LI et al., 2008) and fenofibrate (YOUSAF et al., 2015).

However, although gelatin has a high ability to absorb water, leading usually to a very fast release profile, this biopolymer is also quite unstable in certain exposure conditions, which can have a negative impact on drug dissolution. Its exposure to environmental factors, such as humidity, heat and light, and/or chemical catalysts, results in the formation of a swollen, very thin, tough, rubbery, water-insoluble membrane, also known as pellicle. This membrane acts as a barrier and can restrict the release of a drug from a gelatin-based formulation. Not disrupted by gentle agitation, this membrane formation can be the reason of failure of some gelatin-based formulations or even of formulations comprised in gelatin capsules. Although some stabilizers have been identified and added in formulation fills or films to avoid this matter, more effort has to be done to optimize the use of such promising biopolymer for pharmaceutical applications (SINGH and PAKHALE, 2007).

## **5. ENTERIC COATED MUTIPARTICULATE SYSTEMS**

Basically, oral dosage forms are classified according to its release behavior in immediate and modified release systems. In the first case, the dosage form is developed to disintegrate and release its active compound without controlling the dissolution rate through polymeric coating, for example. On the other hand, modified release dosage forms can comprise the extended or delayed types. In extended release, the dosage form is

developed to release the active compound in a controlled way, under predetermined conditions of rate, duration and location, to reach and keep optimal therapeutic levels for a longer period of time (8-12 hours). For delayed release dosage forms, the drug is not immediately released when administered, but after a certain period of time, as observed in enteric coated formulations (ANSEL, POPOVICH and ALLEN JR, 2011; COLLETT and MORETON, 2001).

Enteric coated dosage forms use polymers insoluble in gastric environment which avoid or delay the release of the drug in the stomach. These polymers are known to dissolve in a pH range from 4.8 to 7.2. The reasons which justify the enteric coating include:

- Dosage forms composed by drugs unstable in gastric environment;
- Dosage forms composed by drugs which irritate the gastric mucosa and cause undesired side effects, such as nausea and vomiting;
- Dosage forms composed by drugs in which a delayed release with a lag time of 3 to 4 hours is indicated;
- Dosage forms composed by drugs with a specific absorption site (absorption window) in the intestine (SINGH and KIM, 2002; ANSEL, POPOVICH and ALLEN JR, 2011a).

Among the different enteric polymers available, the polymethacrylates Eudragit L100® and Eudragit L100-55® (Figure 6) have been often applied to protect APIs from the gastric environment (NGUYEN et al., 2016; TAYEL et al., 2016; BESENHARD et al., 2014; SAUER et al., 2009). Eudragit L100® is a pH dependent anionic polymer based on methacrylic acid and methyl methacrylate, in which the ratio of free carboxyl to ester groups is approximately 1:1. It starts to dissolve at pH 6.0. Eudragit L100-55® is also an anionic polymer, but it starts to dissolve at a slightly lower pH, 5.5. Its chemical structure consists of a copolymer of methacrylic acid and ethyl acrylate, and the ratio of free carboxyl to ester groups is approximately 1:1 (VAKA et al., 2014; NOLLENBERGER and ALBERS, 2013; CHANG et al., 2009).

The enteric coating can be applied to single unit dosage forms, such as tablets, or multiparticulate systems, like pellets. Figure 7 depicts an enteric coated pellet and the release process of drugs (*e.g.* EZE and LOV) under gastrointestinal conditions. The figure shows the enteric

coating layer (*e.g.* Eudragit L100<sup>®</sup> or Eudragit L100-55<sup>®</sup>), the intermediate layer composed by a highly water-soluble solid dispersion and the inert core composed by sucrose. In gastric conditions, the enteric coating layer remains intact, avoiding drug release in stomach. At a certain pH (5.5 for Eudragit L100-55<sup>®</sup> and 6.0 for Eudragit L100<sup>®</sup>), the enteric coating layer starts to dissolve and the compounds are rapidly released due to the improved dissolution properties of the solid dispersion.

**Figure 6.** Monomeric unit of Eudragit L100<sup>®</sup> (R1 = H<sub>3</sub>C; R2 = H<sub>3</sub>C) and Eudragit L100-55<sup>®</sup> (R1 = H; R2 = C<sub>2</sub>H<sub>5</sub>)

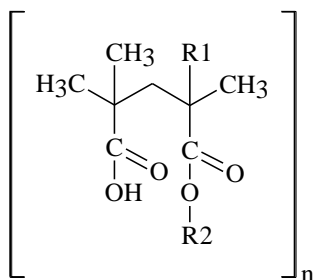
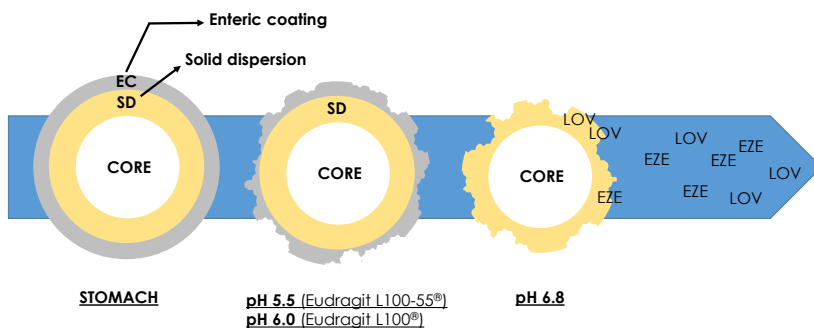


**Figure 7.** Drug release from an enteric coated pellet. EC = enteric coating layer, SD = solid dispersion layer



Pellets are one of the main representatives of multiparticulate systems, along with granules and mini tablets. As the name suggests,

these systems comprise more than one dosage unit in a pharmaceutical dosage form. In case of pellets, they are conditioned inside of hard gelatin capsules, according to their doses of administration (COLLETT and MORETON, 2001).

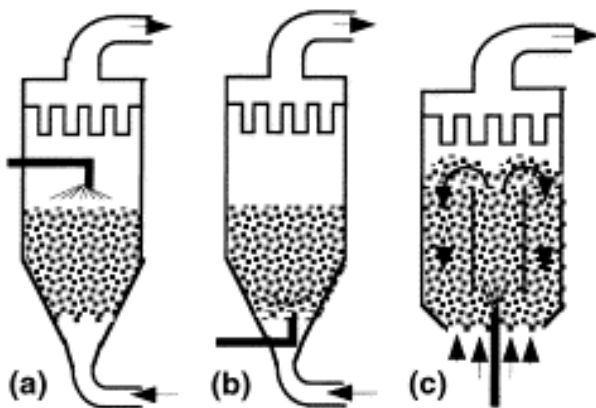
Preparation of multiparticulate systems instead of the conventional single unit dosage forms, offers the advantage of presenting a more predictable gastric transit time, better distribution and absorption, facilitated disintegration, less frequent dose dumping issues and reduced risks of systemic toxicity and local irritation (ASGHAR and CHANDRAN, 2006). In theory, multiparticulate systems can also be an interesting choice to compose a FDC, since they allow the combination of more than one API, obtaining various release profiles from a single dosage form.

Fluid bed coating is one of the most used coating processes, and the term ‘fluidized bed’ is used because the powder bed or pellet bed acts as if it is a fluid (DIXIT and PUTHLI, 2009). Basically, every coating process consists of subjecting particles to continuous coating and drying cycles in order to accumulate coating layers. In a fluid bed coating operation, the three phases involved, solid (particles), liquid (coating solution) and gas (fluidizing air) are continuously interacting throughout the process. In a first step, the solid particles are loaded into the processor and submitted to the fluidizing air. Subsequently, the coating material is pumped through a nozzle and sprayed as droplets onto the particles, generating a homogeneous layering of the coating material. The non-stop drying, provided by the drying air set at a temperature able to promote solvent evaporation, allows the occurrence of the continuous layering. The success of the coating process depends on the ability of the droplet to be homogeneously spread on the particle surface, avoiding particle agglomeration (SAUER et al., 2013; DIXIT and PUTHLI, 2009).

Fluid bed coaters can be found in different settings as shown in Figure 8. The first type developed, known as top spray (Figure 8a), presents a nebulization system located at the superior part of the chamber. The efficiency, in terms of material deposited and coating quality, is low, generating materials with poor controlled release properties. From that, a bottom spray fluid bed coater was developed (Figure 8b), in which the coating solution is nebulized from the inferior part of the equipment. This kind of system increases considerably the collision among particles and droplets of coating solution, resulting in a higher coating efficiency. However, due to the high concentration of humid particles, the

agglomeration risk is high. Despite of the different configurations of fluid bed coaters, the bottom spray mode with a Würster insert (Figure 8c) is especially interesting to coat small particles, as pellets, since it diminishes the risk of agglomeration, typical of the standard bottom spray mode. This type of fluid bed coater presents a higher drying rate and reduction of the potential of agglomeration, generating particles with a more homogeneous coating layer (FUKUMORI and ICHIKAWA, 2002; TEUNOU and PONCELET, 2002).

**Figure 8.** Different fluid bed coater settings: (a) top spray, (b), bottom spray and (c) Wurster. Adapted from TEUNOU e PONCELET, 2002.



## 6. REFERENCES

- ABUBAKER, O. Copovidone. In: ROWE, R. C.; SHESKEY, P. J.; QUINN, M. E. **Handbook of pharmaceutical excipients**. 6 ed. London: Pharmaceutical Press, 2009, p. 196-198.
- ALLESØ, M.; CHIENG, N.; REHDER, S.; RANTANEN, J.; RADES, T.; AALTONEN, J. Enhanced dissolution rate and synchronized release of drugs in binary systems through formulation: Amorphous naproxen-cimetidine mixtures prepared by mechanical activation. **Journal of Controlled Release**, v. 136, p. 45-53, 2009.
- ALONZO, D. E.; ZHANG, G. G. Z.; ZHOU, D.; GAO, Y.; TAYLOR, L. S. Understanding behavior of amorphous pharmaceutical systems during dissolution. **Pharmaceutical Research**, v. 27, p. 608–618, 2010.
- AMIDON, G. L.; LENNERNÄS, H.; SHAH, V. P.; CRISON, J.R. A theoretical basis for a biopharmaceutic drug classification: the correlation of in vitro drug product dissolution and in vivo bioavailability. **Pharmaceutical Research**. v.12, p.413-420, 1995.
- ANSEL, H.C.; POPOVICH, N.G.; ALLEN JR, L.V. Solid oral modified-release dosage forms and drug delivery systems. In: **Ansel's Pharmaceutical Dosage Forms and Drug Delivery Systems**. 9<sup>a</sup> ed. Philadelphia: Lippincott Williams & Wilkins, 2011, p. 257-271.
- ANSEL, H.C.; POPOVICH, N.G.; ALLEN JR, L.V. Tablets. In: **Ansel's Pharmaceutical Dosage Forms and Drug Delivery Systems**. 9<sup>a</sup> ed. Philadelphia: Lippincott Williams & Wilkins, 2011a, p. 225-256.
- ANVISA, National Health Surveillance Agency, **Guideline to Register FDCs Intended for Hypertension**, Brasília, 2010a.
- ANVISA, National Health Surveillance Agency. **Guideline to Register New FDCs**, Brasília, 2010.
- ANVISA, National Health Surveillance Agency. **Technical Note 06/2014**. Clarification about relative bioavailability studies to demonstrate the pharmacokinetic interaction aiming the register of FDCs, Brasília, 2014.
- ARAÚJO, R. G.; CASELLA FILHO, A.; CHAGAS, A. C. P. **Ezetimiba – farmacocinética e terapêutica**, Arquivo Brasileiro de Cardiologia, v. 85, p. 20-24, 2005.

ASGHAR, L.F.A. and CHANDRAN, S., 2006. Multiparticulate formulation approach to colon specific drug delivery: Current perspectives. **Journal of Pharmaceutical Sciences**, v. 9, p. 327-338, 2006.

BANGALORE, S.; KAMALAKKANNAN, G.; PARKAR, S.; MESSERLI, F. H. Fixed-dose combinations improve medication compliance: A meta analysis. **The American Journal of Medicine**, v. 120, p. 713-719, 2007.

BELLANTONE, R.A. Fundamentals of amorphous systems: Thermodynamic Aspects. **In: Amorphous Solid Dispersions: Theory and Practice**. Nova Iorque: Springer, p. 3-34, 2014.

BESENHARD, M.O.; THURNBERGER, A.; HOHL, R.; FAULHAMMER, E.; RATTENBERGER, J.; KHINAST, J.G. Continuous API-crystal coating via coacervation in a tubular reactor. *International Journal of Pharmaceutics*, v. 475, p. 198-207, 2014.

BETAGERI, G. V.; MAKARLA, K. R. Enhancement of dissolution of glyburide by solid dispersion and lyophilization techniques. **International Journal of Pharmaceutics**, v. 126, p. 155-160, 1995.

BHUGRA, C.; PIKAL, M. J. Role of thermodynamic, molecular and kinetic factors in crystallization from the amorphous state. **Journal of Pharmaceutical Sciences**, v. 97, p.1329–1349, 2008.

BIKIARIS, D.N. Solid dispersions, part II: new strategies in manufacturing methods for dissolution rate enhancement of poorly water-soluble drugs. **Expert Opinion on Drug Delivery**, v. 8, p. 1663-1680, 2011.

BJERRUM, O.J.; GAUTAM, Y.; BJERRUM, E.J.; SCHMIEGELOW, M. BOONEN, H.C.M. Medicines combinations options and regulatory hurdles. **European Journal of Pharmaceutical Sciences**, v. 49, p. 659-663, 2013.

BLOCK, D. W; SPEISER, P.P. Solid Dispersions – Fundamental and Examples. **Pharmaceutica Acta Helvetiae**. v. 62, p. 23-27, 1987.

BRAZIL, **Resolution nº 210, from September 02<sup>nd</sup>, 2004**. Official State Journal, , Brasilia, DF, 2004.

BRAZIL. Resolution nº 37, from August 03<sup>rd</sup>, 2011a. **Refers to the Guideline for exemption and replacement of relative bioavailability/bioequivalence studies and provides other statements.**



Official State Journal, Brasilia, DF, 2011. Available in: <[http://bvsms.saude.gov.br/bvs/saudelegis/anvisa/2011/res0037\\_03\\_08\\_2011.html](http://bvsms.saude.gov.br/bvs/saudelegis/anvisa/2011/res0037_03_08_2011.html)>. Accessed at em: 20 set. 2015.

BRAZILIAN CONSENSUS ON DYSLIPIDEMIA, **Arquivo Brasileiro de Cardiologia**, v. 67, p. 113-128, 1996.

BRAZILIAN MINISTRY OF HEALTH, **National List of Essential Medications**, updated at September 27<sup>th</sup>, 2014, , Brasilia, 2014.

BRITISH PHARMACOPOEIA, The Department of Health. London, 2009.

BRÜNING, J.; ALIG, E.; SCHMIDT, M.U. Ezetimibe anhydrate, determined from laboratory powder diffraction data. **Acta Crystallographic C**, v. 66, p. o341-o344, 2010.

CEDERBERG, H.; STANCÁKOVÁ, A.; YALURI, N.; MODI, S.; KUUSISTO, J.; LAAKSO, M. Increased risk of diabetes with statin treatment is associated with impaired insulin sensitivity and insulin secretion: a 6 year follow-up study of the METSIM cohort. **Diabetologia**, v. 58, p. 1109-1117, 2015.

CHANG, R.K.; PENG, Y.; TRIVEDI, N.; SHUKLA, A.J. Polymethacrylates. In: ROWE, R. C.; SHESKEY, P. J.; QUINN, M. E (ed). **Handbook of pharmaceutical excipients**. 6 ed. London: Pharmaceutical Press, 2009, p. 525-533.

CHAUDARI, V.; UBALE, M. A Validated stability-indicating HPLC assay method for lovastatin in bulk drug. **Research Journal of Pharmaceutical, Biological and Chemical Sciences**, v. 3, p. 261-270, 2012.

CHIENG, N; AALTONEN, J.; SAVILLE, D.; RADES, T. Physical characterization and stability of amorphous indomethacin and ranitidine hydrochloride binary systems prepared by mechanical activation. **European Journal of Pharmaceutics and Biopharmaceutics**, v. 71, p. 47-54, 2009.

CHONO, S.; TAKEDA, E.; SEKI, T.; MORIMOTO, K. Enhancement of the dissolution rate and gastrointestinal absorption of pranlukast as a model poorly water-soluble drug by grinding with gelatin. **International Journal of Pharmaceutics**, v. 347, p. 71-78, 2008.

COLLETT, J.; MORETON, C. Modified-release peroral dosage form. In: AULTON, M. E (ed). **Pharmaceutics: The science of dosage form**

**design**. 2 ed. London: Churchill Livingstone Publishers, 2001, p. 289-306.

CRAIG, D.Q.M. The mechanisms of drug release from solid dispersions in water-soluble polymers. **International Journal of Pharmaceutics**, v. 231, p.131-144, 2002.

DE OLIVEIRA, P. R. **Desenvolvimento e validação de metodologias para avaliação de ezetimiba por cromatografia líquida e espectrometria de massas**. 2007. 82 f. Master Thesis (UFSM), Santa Maria, 2007.

DENGAL, S.J.; RANJAN, O.P.; HUSSEN, S.S.; KRISHNA, B.S.; MUSMADE, P.B.; GAUTHAM SHENOY, G.; BHAT, K. Preparation and characterization of co-amorphous Ritonavir-Indomethacin systems by solvent evaporation technique: improved dissolution behavior and physical stability without evidence of intermolecular interactions. **European Journal of Pharmaceutical Sciences**, v. 62, p. 57-64, 2014.

DIERICKX L.; VAN SNICK B.; MONTEYNE T.; DE BEER T.; REMON J.P.; VERVAET C. Co-extruded solid solutions as immediate release fixed-dose combinations. **European Journal of Pharmaceutics and Biopharmaceutics**, v. 88, p. 502-509, 2014.

DIXIT, R. and PUTHLI, S. Fluidization technologies: Aerodynamic principles and process engineering. **Journal of Pharmaceutical Sciences**, v. 98, p. 3933-3960, 2009.

DUGGAN, D.E.; CHEN, I.W.; BAYNE, W.F.; HALPIN, R.A.; DUNCAN, C.A.; SCHWARTZ, M.S.; STUBBS, R.J.; VICKERS, S. The physiological disposition of lovastatin. **Drug Metabolism and Disposition**. v. 17, p. 166-173, 1989.

DURET, C.; WAUTHOZ, N.; SEBTI, T.; VANDERBIST, F.; AMIGHI, K. Solid dispersions of itraconazole for inhalation with enhanced dissolution, solubility and dispersion properties. **International Journal of Pharmaceutics**, v. 428, p. 103-113, 2012.

ELZOGHBY, A.O. Gelatin-based nanoparticles as drug and gene delivery systems: Reviewing three decades of research. **Journal of Controlled Release**, v. 172, p. 1075-1091, 2013.

EUROPEAN MEDICINES AGENCY (EMA), 2015. Guideline on clinical development of fixed combination medicinal products. Available at:

[http://www.ema.europa.eu/docs/en\\_GB/document\\_library/Scientific\\_guideline/2015/05/WC500186840.pdf](http://www.ema.europa.eu/docs/en_GB/document_library/Scientific_guideline/2015/05/WC500186840.pdf) (accessed 11.07.2016).

FERRAZ, H. G. Novas ferramentas farmacotécnicas para modular a biodisponibilidade de medicamentos. In: STORPIRTIS, S.; GONÇALVES, J. E.; CHIANN, C.; GAI, M. N. **Ciências Farmacêuticas: Biofarmacotécnica**. 1 ed. Rio de Janeiro: Guanabara Koogan, 2009, p. 66-71.

FLORENCE, A. T; ATTWOOD, D. **Princípios físico-químicos em farmácia**. 3 ed. São Paulo: Editora da Universidade de São Paulo, 2003, p. 29-65.

FOOD AND DRUG ADMINISTRATION. Guidance for industry: new chemical entity exclusivity determinations for certain fixed-combination drug products. Disponível em <http://www.fda.gov/downloads/drugs/guidancecomplianceregulatoryinformation/guidances/ucm386685.pdf>. Acesso em 23 de julho de 2015.

FOOX, M. and ZILBERMAN, M. Drug delivery from gelatin-based systems. **Expert Opinion on Drug Delivery**, v. 12, p. 1.-17, 2015.

FUKUMORI, Y.; ICHIKAWA, H. Fluid bed processes for forming functional particles. In: SWARBRICK, J (ed). **Encyclopedia of Pharmaceutical Technology**. 2 ed. New York: Marcel Dekker, Inc., 2002. p. 1773-1778.

GAO, Y.; LIAO, J.; QI, X.; ZHANG, J. Coamorphous repaglinice-saccharin with enhanced dissolution. **International Journal of Pharmaceutics**, v. 450, p. 290-295, 2013.

GELATIN MANUFACTURERS INSTITUTE OF AMERICA (GMIA). **Gelatin Handbook**. 26 p., 2012.

GOLDBERG, A.H.; GIBALDI, M.; KANIG, J.L. Increasing dissolution rates and gastrointestinal absorption of drugs via solid solution and eutetic mixture I. Theoretical consideration and discussion of the literature. **Journal of Pharmaceutical Sciences**, v. 54, p.1145-1148, 1965.

GOUVEIA, M. A. **Obtenção e caracterização de dispersões sólidas de nimesulida**. 2011. 123 f. Dissertação (Mestrado em Ciências Farmacêuticas) Faculdade de Ciências Farmacêuticas, Universidade de São Paulo, Ribeirão Preto, 2011.

HANCOCK, B. C. Amorphous pharmaceutical systems. In: SWARBRICK, J. **Encyclopedia of Pharmaceutical Technology**. 3 ed. New York: Marcel Dekker, Inc., 2007, p. 83-91.

HARDUNG, H.; DJURIC, D.; ALI, S. Combining HME e solubilization: Soluplus® - The solid solution. **Drug Delivery Technology**, v. 10, 2010.

HE, X. Integration of physical, chemical, mechanical, and biopharmaceutical properties in solid oral dosage form development. In: QIU, Y.; CHEN, Y.; ZHANG, G. G. Z.; LIU, L.; PORTER, W. R. **Developing solid oral dosage forms**. 1 ed. Burlington: Academic Press, 2009, p. 410-441.

HOU, R.; GOLDBERG, A. C. Lowering Low-Density Lipoprotein Cholesterol: Statins, Ezetimibe, Bile Acid Sequestrants, and Combinations: Comparative Efficacy and Safety. **Endocrinology and Metabolism Clinic of North America**, v. 38, p. 79-97, 2009.

JANSSENS, S.; VAN DEN MOOTER, G. Review: Physical chemistry of solid dispersions. **Journal of Pharmacy and Pharmacology**, v. 61, p. 1571-1586, 2009.

JENSEN, K.T.; LÖBMANN, K.; RADES, T.; GROHGANZ, H. Improving co-amorphous drug formulations by the addition of the highly water soluble amino acid, proline. **Pharmaceutics**, v. 6, p. 416-435, 2014.

KALLINTERI, P.; ANTIMISIARIS, S.G. Solubility of drugs in presence of gelatin: effect of drug lipophilicity and degree of ionization. **International Journal of Pharmaceutics**, v. 221, p. 219-216, 2001.

KERZNER, B.; CORBELLI, J.; SHARP, S.; LIPKA, L.; MELANI, L.; LEBEAUT, A., et al. Efficacy and safety of ezetimibe coadministered with lovastatin in primary hypercholesterolemia. **The American Journal of Cardiology**, v. 91, p. 418-424, 2003.

KIBBE, A. H. Povidone. In: ROWE, R. C.; SHESKEY, P. J.; QUINN, M. E (ed). **Handbook of pharmaceutical excipients**. 6 ed. London: Pharmaceutical Press, 2009, p. 581-585.

KOROKOLVAS, A. Lovastatina. In: **Dicionário Terapêutico Guanabara**. Edition 2005/2006. Rio de Janeiro: Guanabara Koogan, p. 13.10, 2005.

LACHMAN, L.; LIEBERMAN, H.A.; KANING, J.L. **Teoria e Prática na Indústria Farmacêutica**. Lisboa: Fundação Calouste, 2001, p. 295-339.

LAITINEN, R.; LÖBMANN, K.; GROHGANZ, H.; STRACHAN, C.; RADES, T. Amino acids as co-amorphous excipients for simvastatin and glibenclamide: Physical properties and stability. **Molecular Pharmaceutics**, v. 11, p. 2381-2389, 2014.

LAITINEN, R.; LÖBMANN, K.; STRACHAN, C. J.; GROHGANZ, H.; RADES, T. Emerging trends in the stabilization of amorphous drugs. **International Journal of Pharmaceutics**, v. 453, p. 65-79, 2013.

LARSSON, A.; ABRAHMSÉN-ALAMI, S.; JUPPO, A. Oral extended-release formulations. In: GAD, S.C. (ed). **Pharmaceutical Manufacturing Handbook: Production and processes**. New Jersey: Wiley Interscience, 2008, p. 1191-1222.

LENZ, E.; JENSEN, K.T.; BLAABJERG, L.I.; KNOP, K.; GROHGANZ, H.; LÖBMANN, K.; RADES, T.; KLEINEBUDDE, P. Solid-state properties and dissolution behaviour of tablets containing co-amorphous indomethacin-arginine. **European Journal of Pharmaceutics and Biopharmaceutics**, v. 96, p. 44-52, 2015.

LEUNER, C.; DRESSMAN, J. Improving drug solubility for oral delivery using solid dispersions. **European Journal of Pharmaceutics and Biopharmaceutics**, v. 50, p. 47-60, 2000.

LI, D.X.; OH, Y.-K.; LIM, S.-J.; KIM, J.O.; YANG, H.J.; SUNG, J.H.; YONG, C.S.; CHOI, H.-G. Novel gelatin microcapsule with bioavailability enhancement of ibuprofen using spray-drying technique. **International Journal of Pharmaceutics**, v. 355, p. 277-284, 2008.

LIMA, A. C. **Obtenção e caracterização de dispersões sólidas de praziquantel**. 2006. 83 p. Master Thesis (Master in Pharmaceutical Sciences), Universidade Estadual Paulista, Araraquara, 2006.

LINN, M.; COLLNOT, E.M.; DJURIC, D.; HEMPEL, K.; FABIAN, E.; KOLTER, K.; LEHR, C.M. Soluplus® as an effective absorption enhancer of poorly soluble drugs in vitro and in vivo. **European Journal of Pharmaceutical Sciences**, v. 45, p. 336-343, 2012.

LIPINSKI, C. Poor aqueous solubility – An industry wide problem in drug discovery. **American Pharmaceutical Review**, v. 5, p. 82-85, 2002.

LIU, S.; WATTS, A.B.; DU, J.; BUI, A.; HENGSAWAS, S.; PETERS, J.I.; WILLIAMS, R.O. Formulation of a novel fixed dose combination of salmeterol xinafoate and mometasone furoate for inhaled drug delivery.

**European Journal of Pharmaceutics and Biopharmaceutics**, v. 96, p. 132-142, 2015.

LÖBMANN, K.; LAITINEN, R.; STRACHAN, C.; RADES, T.; GROHGANZ, H. Amino acids as co-amorphous stabilizers for poorly water-soluble drugs - Part 2: molecular interactions. **European Journal of Pharmaceutics and Biopharmaceutics**, v. 85, p. 882-888, 2013a.

LÖBMANN, K.; GROHGANZ, H.; LAITINEN, R.; STRACHAN, C.; RADES, T. Amino acids as co-amorphous stabilizers for poorly water soluble drugs - Part 1: preparation, stability and dissolution enhancement. **European Journal of Pharmaceutics and Biopharmaceutics**, v. 85, p. 873-881, 2013.

LÖBMANN, K.; LAITINEN, R.; GROHGANZ, H.; GORDON, K.C.; STRACHAN, C.; RADES, T. Coamorphous drug systems: enhanced physical stability and dissolution rate of indomethacin and naproxen. **Molecular Pharmaceutics**, v. 8, p. 1919-1928, 2011.

LÖBMANN, K.; LAITINEN, R.; GROHGANZ, H.; STRACHAN, C.; RADES, T.; GORDON, K.C. A theoretical and spectroscopic study of co-amorphous naproxen and indomethacin. **International Journal of Pharmaceutics**, v. 453, p. 80-87, 2012a.

LÖBMANN, K.; STRACHAN, C.; GROHGANZ, H.; RADES, T.; KORHONEN, O.; LAITINEN, R. Co-amorphous simvastatin and glipizide combinations show improved physical stability without evidence of intermolecular interactions. **European Journal of Pharmaceutics and Biopharmaceutics**, v. 81, p. 159-169, 2012.

NART, V.; FRANÇA, M.T.; ANZILAGGO, D.; RIEKES, M.K.; KRATZ, J.M.; CAMPOS, C.E.M.; SIMÕES, C.M.O.; STULZER, H.K. Ball-milled solid dispersions of BCS Class IV drugs: Impact on the dissolution rate and intestinal permeability of acyclovir. **Materials Science and Engineering: C**, v. 53, p. 229-238, 2015.

NGUYEN D.N. and VAN DEN MOOTER G. The fate of ritonavir in the presence of darunavir. **International Journal of Pharmaceutics**, v. 475, p. 214-226, 2014.

NGUYEN, D.N.; PALANGETIC, L.; CLASEN, C.; VAN DEN MOOTER, G. One-step production of darunavir solid dispersion nanoparticles coated with enteric polymers using electrospraying. **Journal of Pharmacy and Pharmacology**, v. 68, p. 625-633, 2016.

- NOLLENBERGER, K. and ALBERS, J. Poly(meth)acrylate-based coatings. **International Journal of Pharmaceutics**. 457, 461-469, 2013.
- PADDEN, B. E.; MILL, J. M.; ROBBINS, T.; ZOCHARSKI, P. D.; PRASAD, L.; SPENCE, J. K.; LA FOUNTAINE, J. Amorphous solid dispersions as enabling formulations for discovery and early development. **American Pharmaceutical Reviews**, v. 1, p.66-73, 2011.
- PARTHASARADHI, B. R.; RATHNAKAR, K. R.; RAJI, R. R.; SUBASH, K. C. R. **Ezetimibe polymorphs**, Patente WO 2005/009955 A1, publicada em 03 de fevereiro de 2005.
- PAUDEL, A.; WORKU, Z.A.; MEEUS, J.; GUNS, S.; VAN DEN MOOTER, G. Manufacturing of solid dispersions of poorly water soluble drugs by spray drying: formulation and process considerations. **International Journal of Pharmaceutics**, v. 453, p. 253-284, 2013.
- PEZZINI, B. R.; SILVA, M., A. S.; FERRAZ, H. G. Formas farmacêuticas sólidas orais de liberação prolongada: sistemas monolíticos e multiparticulados. **Revista Brasileira de Ciências Farmacêuticas**, v.43,p. 491-502, 2007.
- RAVIKUMAR, K.; SRIDHAR, B. Ezetimibe monohydrate. **Acta Crystallographic E**, v. 61, p.o2907-o2909, 2005.
- RIEKES, M.K.; KUMINEK, G.; RAUBER, G.S.; CAMPOS, C.E.M.; BORTOLUZZI, A.J.; STULZER, H.K. HPMC as a potential enhancer of nimodipine biopharmaceutical properties via ball-milled solid dispersions. **Carbohydrate Polymers**, v. 99, p.474-482, 2014.
- ROGERS, T. L. Hypromellose. In: ROWE, R. C.; SHESKEY, P. J.; QUINN, M. E. **Handbook of pharmaceutical excipients**. 6 ed. London: Pharmaceutical Press, 2009, p. 326-329.
- ROY, P.; SHAHIWALA, A. Multiparticulate formulation approach to pulsatile drug delivery: Current perspectives. **Journal of Controlled Release**, v. 134, p. 74-80, 2009.
- SANTORO, M., TATARA, A.M., MIKOS, A.G. Gelatin carriers for drug and cell delivery in tissue engineering. **Journal of Controlled Release**, v. 28, p. 210-218, 2014.
- SAUER, D.; WATTS, A.B.; COOTS, L.B.; ZHENG, W.C.; MCGINITY, J.W. Influence of polymeric subcoats on the drug release properties of tablets powder-coated with pre-plasticized Eudragit® L 100-55. **International Journal of Pharmaceutics**, v. 367, p. 20-28, 2009.

SCHULZ, I. Tratamento das dislipidemias: Como e quando indicar a combinação de medicamentos hipolipemiantes. **Arquivos Brasileiros de Endocrinologia e Metabolismo**, v. 50, p. 344-359, 2006.

SCHWEIM, J.K. e SCHWEIM, H.G. Status quo and future developments of combinations of medicinal products. **Synergy**, v. 1, p. 70-75, 2014.

SEKIGUCHI, K.; OBI, N. Studies on absorption of eutectic mixture. A comparison of the behavior of eutectic mixture of sulfathiazole and that of ordinary sulfathiazole in man. **Chemical and Pharmaceutical Bulletin**, v. 9, p. 866-872, 1961.

SERAJUDDIN, A.T. Solid dispersion of poorly water-soluble drugs: early promises, subsequent problems, and recent breakthroughs. **Journal of Pharmaceutical Sciences**, v. 88, p. 1058-66, 1999.

SERAJUDDIN, A.T.M.; SHEEN, P.C.; AUGUSTINE, M.A. Improved dissolution of a poorly water-soluble drug from solid dispersions in polyethylene glycol: polysorbate 80 mixtures. **Journal of Pharmaceutical Sciences**, v.79, p.463-464, 1990.

SETHIA, S.; SQUILLANTE, E. Solid dispersions of carbamazepine in PVP K 30 by conventional solvent evaporation and supercritical methods. **International Journal of Pharmaceutics**, v. 19, p. 1-10, 2004.

SETHIA, S.; SQUILLANTE, E. Solid dispersions: revival with greater possibilities and applications in oral drug delivery. **Critical Review on Therapy and Drug Carrier Systems**, v.20, p. 215-247, 2003.

SHAYANFAR, A.; JOUYBAN, A.; HAMISHEHKAR, H. Coamorphous drug system to improve physicochemical properties of atorvastatin calcium. **Research in Pharmaceutical Sciences**, v. 7, p. S978, 2012.

SHEEN, P. C.; KHETARPAL, V. K.; CARIOLA, C. M.; ROWLINGS, C. E. Formulation studies of a poorly soluble drug in solid dispersion to improve bioavailability. **International Journal of Pharmaceutics**, v. 118, p. 221-227, 1995.

SHIMADA, Y.; GOTO, S.; UCHIRO, H.; HIROTA, K.; TERADA, H. Characteristics of amorphous complex formed between indomethacin and lidocaine hydrochloride. **Colloids and Surfaces B: Biointerfaces**, v. 105, p. 98-105, 2013.

SINGH, B.N.; KIM, K.H. Drug delivery: Oral route. In: SWARBRICK, J (ed). **Encyclopedia of Pharmaceutical Technology**. 2 ed. New York: Marcel Dekker, Inc., 2002. p. 1242-1265.



SINGH, S. and PAKHALE, S.P. Gelatin-containing formulations: Changes in Dissolution Characteristics. In: SWARBRICK, J. **Encyclopedia of Pharmaceutical Technology**. 2 ed. New York: Marcel Dekker, Inc., 2007. p. 1861-1874.

SINGH, S.; SINGH, B.; BAHUGUNA, R.; WADHWA, L.; SAXENA, R. Stress degradation studies on ezetimibe and development of a validated stability-indicating HPLC assay. **Journal of Pharmaceutical and Biomedical Analysis**, v. 41, p. 1037-1040, 2006.

SVENSON, S. Dendrimers as versatile platform in drug delivery applications. **European Journal of Pharmaceutics and Biopharmaceutics**, v. 71, p. 445-462, 2009.

SWEETMAN, S. C. Lovastatin. In: **Martindale: The complete drug reference**. 36 ed. London: Pharmaceutical Press, 2009, p. 1328-1329.

TADIBOYINA, V. T.; LIU, D. M.; MISKIE, B. A.; WANG, J.; HEGELE, R. A. Treatment of dyslipidemia with lovastatin and ezetimibe in an adolescent with cholesterol ester storage disease. **Lipids and Health Diseases**, v. 4, p. 26-32, 2005.

TAKAGI, T.; RAMACHANDRAN, C.; BERMEJO, M.; YAMASHITA, S.; YU, L. X.; AMIDON, G. L. A provisional biopharmaceutical classification of the top 200 oral drug products in the United States, Great Britain, Spain and Japan, **Molecular Pharmaceutics**, v. 3, p. 631-643, 2006.

TAYEL, S.A.; EL-NABARAWI, M.A.; TADROS, M.I.; ABD-ELSALAM, W.H. Duodenum-triggered delivery of pravastatin sodium: II. Design, appraisal and pharmacokinetic assessments of enteric surface-decorated nanocubosomal. **Drug Delivery**, v. 19, p. 1-13, 2016.

TEUNOU, E.; PONCELET, D. Batch and continuous fluid bed coating: Review and state of the art. **Journal of Food Engineering**, v. 53, p. 325-340, 2002.

TIWARI, V.; KHOKHAR, M. Mechanism of action of anti-hypercholesterolemia drugs and their resistance. **European Journal of Pharmacology**, v. 741, p. 156-170, 2014.

V BRAZILIAN GUIDELINE ON DYSLIPIDEMIA AND ATHEROSCLEROSIS , **Arquivo Brasileiro de Cardiologia**, v. 88, p. 1-19, 2013.

VADNERE, M. K. Coprecipitates and melts. In: SWARBRICK, J. **Encyclopedia of Pharmaceutical Technology**. 2 ed. New York: Marcel Dekker, Inc., 2002. p. 774-781.

VAKA, S.R.K.; BOMMANA, M.M.; DESAI, D.; DJORDJEVIC, J.; PHUAPRADIT, W.; SHAH, N. Excipients for amorphous solid dispersions, in: Shah, N.; SANDHU, H.; CHOI, D.S.; CHOKSHI, H.; MALICK, W.; MALICK, A.W. (Eds.), **Amorphous solid dispersions: Theory and practice**. Springer, New York, pp. 123-164, 2014.

VAN DEN MOOTER, G. The use of amorphous solid dispersions: A formulation strategy to overcome poor solubility and dissolution rate. **Drug Discovery Today: Technologies**, v. 9, p. e79-e85, 2011.

VASCONCELOS, T.; SARMENTO, B.; COSTA, P. Solid dispersions as strategy to improve oral bioavailability of poor water soluble drugs. **Drug Discovery Today**, v. 12, p. 1068-1075, 2007.

VERVAECK A.; MONTEYNE T.; SAERENS L.; DE BEER T.; REMON J.P.; VERVAET C. Prilling as manufacturing technique for multiparticulate lipid/PEG fixed-dose combinations. **European Journal of Pharmaceutics and Biopharmaceutics**, v.88, p. 472-482, 2014.

VI GUIDELINES ON HYPERTENSION, **Revista Brasileira de Hipertensão**, v. 17, p. 9-69, 2010.

VO, C.L.; PARK, C.; LEE, B.J. Current trends and future perspectives of solid dispersions containing poorly water-soluble drugs. **European Journal of Pharmaceutics and Biopharmaceutics**, v. 85, p. 799-813, 2013.

VYNCKIER A.K.; DIERICKX L.; SAERENS L.; VOORSPOELS J.; GONNISSEN Y.; DE BEER T.; VERVAET C.; REMON J.P. Hot-melt co-extrusion for the production of fixed-dose combination products with a controlled release ethylcellulose matrix core. **International Journal of Pharmaceutics**, v. 464, p. 65-74, 2014.

WANG, S.; LI, J.; LIN, X.; FENG, Y.; KOU, X.; BABU, S.; PANICUCCI, R. Novel compressed excipients composed of lactose, HPMC, and PVPP for tableting and its application. **International Journal of Pharmaceutics**, v. 436, p. 370-379, 2015.

WANNMACHER, L.; HOEFLER, R. Combinações em doses fixas: comentários farmacológicos, clínicos e comerciais. **Organização Pan-Americana de Saúde**, v. 4, p. 1-6, 2007.

WISER, L.; GAO, X.; JASTI, B.; LI, X. Solubility of pharmaceutical solids. In: HU, M e LI, X (Eds). **Oral bioavailability: Basic principles, advanced concepts, and applications**. New Jersey: John Wiley & Sons, Inc., 2011, p. 21-38.

WORLD HEALTH ORGANIZATION (WHO), 2005. **Annex 5: Guidelines for registration of fixed-dose combination medicinal products**. Available at: <http://apps.who.int/medicinedocs/documents/s19979en/s19979en.pdf> (access 11.07.2016).

WORLD HEALTH ORGANIZATION (WHO), **Atlas de Doenças Cardíacas e Derrames**. Genebra, 2004.

WORLD HEALTH ORGANIZATION (WHO), **The World Health Report: reducing risks, promoting healthy life**. Genebra, 2002.

WU, C.; BENET, L. Z. Predicting drug disposition via application of BCS: transport/absorption/elimination interplay and development of a biopharmaceutics drug disposition classification system. **Pharmaceutical Research**, v. 22, p. 11-23, 2005.

YAMAMURA, S.; GOTOH, H.; SAKAMOTO, Y.; MOMOSE, Y. Physicochemical properties of amorphous salt of cimetidine and diflunisal system. **International Journal of Pharmaceutics**, v. 241, p. 213-221, 2002.

YAMAMURA, S.; GOTOH, H.; SAKAMOTO, Y.; MOMOSE, Y. Physicochemical properties of amorphous precipitates of cimetidine-indomethacin binary system. **European Journal of Pharmaceutics and Biopharmaceutics**, v. 49, p. 259-265, 2000.

YAMAMURA, S.; MOMOSE, M.; TAKAHASHI, K.; NAGATANI, S. Solid-state interaction between cimetidine and naproxen. **Drug Stability**, v. 50, p. 173-178, 1996.

YOUSAF, A.M.; KIM, D.W.; KIM, J.K.; KIM, J.O.; YONG, C.S.; CHOI, H.-G. Novel fenofibrate-loaded gelatin microcapsules with enhanced solubility and excellent flowability: Preparation and physicochemical characterization. **Powder Technology**, v. 275, p. 257-262, 2015.



## **CHAPTER II**

### **PREPARATION AND CHARACTERIZATION OF CO-AMORPHOUS SYSTEMS OF EZETIMIBE AND LOVASTATIN MANUFACTURED THROUGH QUENCH COOLING FROM THE MELT**

---

## 1. INTRODUCTION

Co-amorphous systems have been recently introduced with the purpose of increasing the solubility and dissolution rate of drugs in therapeutic relevant combinations. These systems usually comprise amorphous binary mixtures of two small organic molecules, in a single phase, like drugs or amino acids (LAITINEN et al., 2013; LÖBMANN et al., 2013a, 2013b). More often, they are obtained in 1:1, 1:2 or 2:1 molar ratios through quench cooling from the melt, milling or solvent evaporation methods. The increase in the dissolution rate due to the conversion of the crystalline APIs to their amorphous state is reported in most cases (LAITINEN et al., 2013; DENGALÉ et al., 2014; LENZ et al., 2015).

In addition, co-amorphous systems also stabilize the amorphous drug by the same mechanism described for the well-known solid dispersions. Increasing the overall glass transition temperature ( $T_g$ ) of the system and ensuring the miscibility between APIs and the occurrence of intermolecular interactions like hydrogen bonding, are some possible ways to reach this purpose through co-amorphous systems (JANSSENS and VAN DEN MOOTER, 2009; LAITINEN et al., 2013).

However, different from solid dispersions, co-amorphous systems are not composed by hydrophilic polymers. This basically means that usual problems in solid dispersions like large bulk volume, hygroscopicity and non-miscibility between the components can be avoided (LAITINEN et al., 2013).

In order to enhance the solubility and dissolution rate of ezetimibe (EZE) and lovastatin (LOV), the preparation of co-amorphous systems was the first approach investigated. These compounds were chosen as model drugs as they both are poorly water-soluble compounds, qualified in Class 2 of the Biopharmaceutics Classification System (BCS), besides representing a relevant therapeutic combination to alternatively treat hypercholesterolemia. In addition, they present similar molecular weights (409,4 g/mol for EZE and 404,54 g/mol for LOV), low and similar doses of administration (10 mg for EZE and 10, 20 or 40 mg for LOV, once a day) and their chemical structures show specific groups which are potential sites of hydrogen bonding.

Based on that, the purpose of this chapter was to investigate co-amorphous systems as an approach to improve the solubility and dissolution rate of EZE and LOV.

## 2 EXPERIMENTAL

### 2.1 MATERIALS

EZE (anhydrous, 409.41 g/mol) and LOV (404.54 g/mol) were purchased from Pharma Nostra (Rio de Janeiro, Brazil) with batch numbers FM017H13 and 130312, respectively. In all experiments de-ionized water (Maxima Ultra Pure Water, Elga Ltd., Wycombe, England) was used and the organic solvents were of pharmaceutical grade.

### 2.2 DETERMINATION OF THE EQUILIBRIUM SOLUBILITY

The equilibrium solubility of EZE, LOV, and the binary physical mixtures of EZE:LOV (1:1, w/w) were determined in acetate buffer pH 4.5 + 0.025% of sodium lauryl sulfate (SLS). In glass test tubes, an excessive amount of pure EZE, LOV and the binary mixtures were added into 5 ml of the above media and the samples were kept for 48 hours in a rotary mixer (L26 Labinco BV, Breda, The Netherlands). After that, 1 ml of the supernatant was filtered through a Polytetrafluoroethylene (PTFE) membrane with 0.45  $\mu\text{m}$  pore size (Grace Davison Discovery Science, Illinois, USA).

The content of EZE and LOV dissolved in the filtrate was determined via isocratic HPLC analysis (Merk-Hitachi LaChrom system). The experiments were conducted on a reversed-phase Chromolith® Performance C18 column (100 x 4.6 mm i.d., 5  $\mu\text{m}$  pore size). The mobile phase was composed of acetonitrile:water (50:50 v/v), with a flow rate of 1.0 ml/min, at room temperature. The UV detection was performed at 235 nm. 20  $\mu\text{l}$  of samples was injected and the data acquisition was performed using Merck LaChrom D-7000 System Manager software. A standard calibration curve (peak area vs. known concentration) was developed by using standard solutions (0.0125–50

µg/ml) prepared by diluting the stock standard solution (200 µg/mL of EZE and LOV in acetonitrile) with the mobile phase. The statistical analysis of the data was conducted in GraphPad Prism 6 software through one-way ANOVA followed by Tukey test. Results were considered statistically significantly different if  $p < 0.05$ .

### 2.3 PREPARATION OF CO-AMORPHOUS SYSTEMS BY QUENCH COOLING FROM THE MELT

Co-amorphous systems of EZE and LOV in 1:1, 1:2, 1:4 and 2:1 molar ratios (EZE:LOV) were prepared through quench cooling from the melt using a modulated differential scanning calorimetry (mDSC) equipment (Q2000 DSC, TA Instruments, Leatherhead, UK). The samples were placed in DSC sample holders, heated at 2°C/min to 180°C, kept isothermal for 5 min and quench cooled to -10°C. The experiments were performed in triplicate and the obtained samples were stored in a desiccator before analysis.

The theoretical  $T_g$  of the binary systems was calculated through the Gordon Taylor equation (eq. 1):

$$T_{g \text{ mix}} = (W1 \cdot T_{g1} + K \cdot W2 \cdot T_{g2}) / (W1 + K \cdot W2) \quad (\text{Equation 1}),$$

where  $T_{g \text{ mix}}$  is the theoretical  $T_g$  of the mixture,  $K$  is a constant,  $W1$  and  $W2$  correspond to the mass fraction of compounds 1 and 2, respectively and  $T_{g1}$  and  $T_{g2}$  refer to the experimental  $T_g$  of compounds 1 and 2, respectively.  $T_{g1}$  denotes the compound with the lowest  $T_g$ . The constant  $K$  is calculated as follows:

$$K \cong (\rho_1 \cdot T_{g1}) / (\rho_2 \cdot T_{g2}) \quad (\text{Equation 2}),$$

where  $\rho_1$  and  $\rho_2$  represent the amorphous density of compounds 1 and 2, respectively. Unit cell (crystalline) densities of 1.34 g cm<sup>-3</sup> and 1.17 g cm<sup>-3</sup> for EZE anhydrate and LOV, respectively, were obtained from the calculation of density (density = [1.66 x molecular weight x number of



molecules per assymetrical unit]/unit cell volume), based on data reported in literature for the single crystal elucidation of these crystalline forms (SATO et al., 1984; BRÜNING, ALIG and SCHMIDT, 2010). Values corresponding to a decrease of 5% of the crystalline density were used as density values for the amorphous components. This approximation of densities is valid for small drug molecules such as those used in this study and has been already described for the estimation of the theoretical glass transition temperature of naproxen-cimetidine binary mixtures (ALLESO, et al., 2009).

In order to obtain the pure amorphous APIs, EZE and LOV were submitted to the same experimental conditions described above and were denoted as EZE<sub>qc</sub> and LOV<sub>qc</sub>.

## 2.4 X-RAY POWDER DIFFRACTION (XRPD)

XRPD experiments were carried out at room temperature using an automated X'pert PRO diffractometer (PANalytical, Almelo, The Netherlands) with a Cu tube ( $K\alpha \lambda = 1.5418 \text{ \AA}$ ) and the generator was set at 45 kV and 40 mA. EZE and LOV raw materials were applied on spinning zero background sample holders. Measurements were performed in a continuous scan mode from 4° to 40° with 0.0167° step size and 200 s per step counting time.

Co-amorphous samples were analyzed in the same conditions but using regular sample holders. The samples were prepared and analyzed in DSC sample holders in a continuous scan mode from 4° to 35°.

## 2.5 MODULATED DIFFERENTIAL SCANNING CALORIMETRY (mDSC)

mDSC analyses were performed on a Q2000 DSC (TA instruments, Leatherhead, UK), equipped with a refrigerated cooling system (RCS90) accessory) under a dry nitrogen purge at a flow rate of 50 ml/min. Indium standard was used for routine calibration (temperature, enthalpy), sapphire disks were used for heat capacity calibration. Approximately 5 mg samples were weighed using an analytical balance into aluminium pans with aluminium lids. The samples were scanned at

2°C/min from -10°C to 190°C (isothermal for 5 min) with an amplitude of 0.636°C and a period of 40 s. DSC thermograms were acquired and analyzed using Universal Analysis software (version 4.4, TA instruments, Leatherhead, UK). All samples were analyzed in duplicate.

## 2.6 ATTENUATED TOTAL REFLECTANCE FOURIER TRANSFORM INFRARED (FTIR) SPECTROSCOPY

FTIR spectra were acquired on a Vertex 70 spectrometer (Bruker, Billerica, USA), at room temperature, from 4000 to 400  $\text{cm}^{-1}$ , with the collection of 32 scans. Samples were analyzed as such.

## 2.7 INTRINSIC DISSOLUTION RATE

For the determination of the intrinsic dissolution rate of co-amorphous systems, a stationary disk apparatus was used and the paddles were rotated at 100 rpm. The dissolution medium was 900 ml of acetate buffer pH 4.5 with 0.5% of SLS, kept at 37°C. Samples were taken at different time intervals, filtered using a PTFE filter (pore size 0.45  $\mu\text{m}$ ) and immediately replaced with the same volume of fresh dissolution medium. Crystalline powders were firstly compressed using a hydraulic press at 460 kPa for 10 s, in a die of 6.5 mm diameter (surface area of 0.33  $\text{cm}^2$ ). Co-amorphous samples were quench cooled from the melt in the same dies. The drug concentration was calculated using HPLC (section 2.2 of this chapter).

The intrinsic dissolution profile was determined by plotting the cumulative amount of drug dissolved (mg) against time (min). The intrinsic dissolution rate was expressed as the amount of API dissolved per unit of time and normalized for the area ( $\text{mg} \cdot \text{cm}^{-2} \cdot \text{min}^{-1}$ ). After 3 hours of dissolution, the co-amorphous systems and quench cooled samples were immediately analyzed as such, by XRD, in order to verify the possibility of a solution-mediated crystallization.

Acetate buffer pH 4.5 was chosen as the dissolution medium due to the chemical stability of EZE and LOV in this solution. Preliminary tests performed in pH 1.2 and 7.0 indicated the instability of LOV under these conditions, demonstrated by the appearance of degradation peaks in

HPLC (see appendix). In addition, as both compounds are essentially non-ionized over the physiological pH range, the dissolution profiles should be similar in solutions with different pH values. Besides, acetate buffer pH 4.5 is the recommended dissolution medium for EZE tablets according to Food and Drug Administration (FDA) (FDA, 2015). Also, as LOV must be administered with food, since its absorption can be decreased in fasted state (SWEETMAN, 2009), this pH is within the pH range of the gastric fed condition (JANTRATID et al., 2008).

*In vitro* profiles were compared applying one-way ANOVA followed by Tukey test. Results were considered statistically significantly different if  $p < 0.05$ .

### 3. RESULTS AND DISCUSSION

#### 3.1 DETERMINATION OF THE EQUILIBRIUM SOLUBILITY

Firstly, in order to verify the feasibility of a fixed dose combination (FDC) based on EZE and LOV, equilibrium solubility experiments were carried out with pure APIs and a combination of both (1:1 w/w). After 48 hours, the solubility of EZE and LOV was  $0.9 \pm 0.1$   $\mu\text{g/ml}$  and  $3.8 \pm 0.4$   $\mu\text{g/ml}$ , respectively, when isolated, and  $0.8 \pm 0.1$   $\mu\text{g/ml}$  (EZE) and  $4.3 \pm 0.1$   $\mu\text{g/ml}$  (LOV) in combination. The equilibrium solubility values for both APIs separately and in combination were considered similar ( $p \leq 0.05$ ), indicating that their solubility in presence of each other is not influenced. Hence, EZE and LOV are promising candidates to be co-formulated in a FDC.

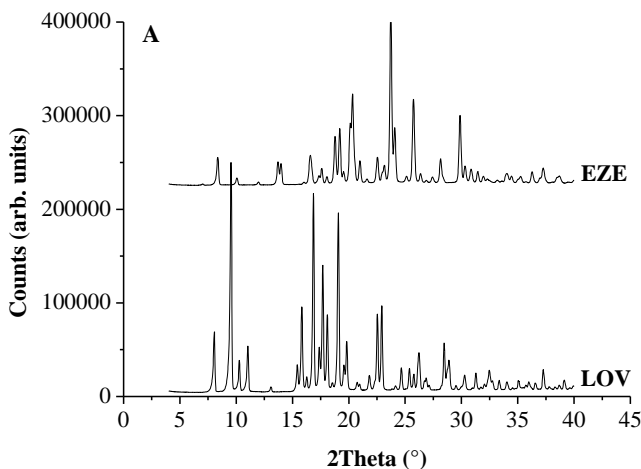
#### 3.2 SOLID-STATE CHARACTERIZATION OF CO-AMORPHOUS SYSTEMS

As a first attempt to obtain a FDC, co-amorphous systems of EZE and LOV were prepared in different molar ratios. Different preparation techniques such as spray drying, cryomilling and quench cooling from the melt were attempted but only the latter was successful. Remaining crystallinity or more than one amorphous phase were observed in the other cases (data not shown).

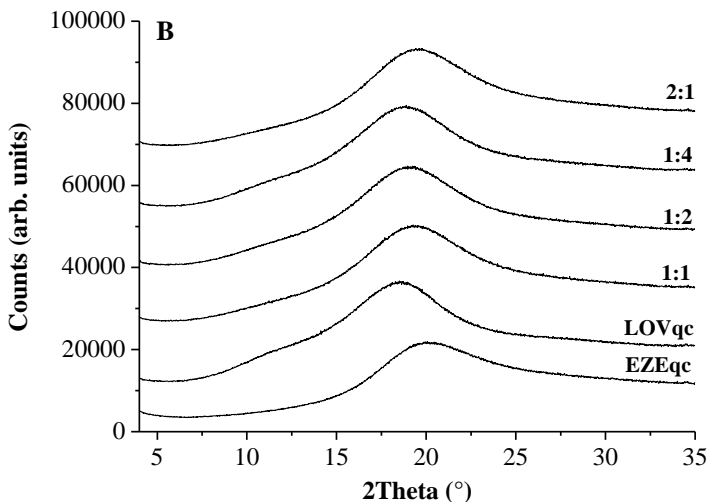
Based on that, co-amorphous systems were prepared through quench cooling from the melt and the corresponding XRD data are shown in Figure 9. Both raw materials are crystalline, as indicated by the

presence of characteristic Bragg peaks (Fig. 9A). According to literature, EZE can exist as an anhydrate or monohydrate form, which can be differentiated at low  $2\theta$  angles in XRD data. The peaks at  $7.02^\circ$ ,  $8.36^\circ$  and  $10.04^\circ$  belong exclusively to the anhydrate, while the characteristic peaks of the monohydrate form are found at  $7.98^\circ$ ,  $9.84^\circ$  and  $13.23^\circ$  (BRÜNING, ALIG and SCHMIDT, 2010; RAVIKUMAR and SRIDHAR, 2005). It can be concluded that, the crystalline form of the EZE raw material used in this study corresponds to the anhydrate. No polymorphs are reported in literature for LOV and its main Bragg peaks are observed at  $2\theta$   $8.05^\circ$ ,  $9.54^\circ$ ,  $11.03^\circ$ ,  $15.83^\circ$ ,  $16.86^\circ$ ,  $17.68^\circ$  and  $19.07^\circ$ , in agreement with previous reported data (YOSHIDA et al., 2011). After quench cooling from the melt, both APIs present an amorphous halo without crystalline peaks. Similar results are observed for all the co-amorphous samples, indicating complete X-ray amorphization.

**Figure 9.** XRPD of (A) crystalline raw materials EZE and LOV and (B) quench cooled samples: co-amorphous systems, EZE<sub>qc</sub> and LOV<sub>qc</sub>



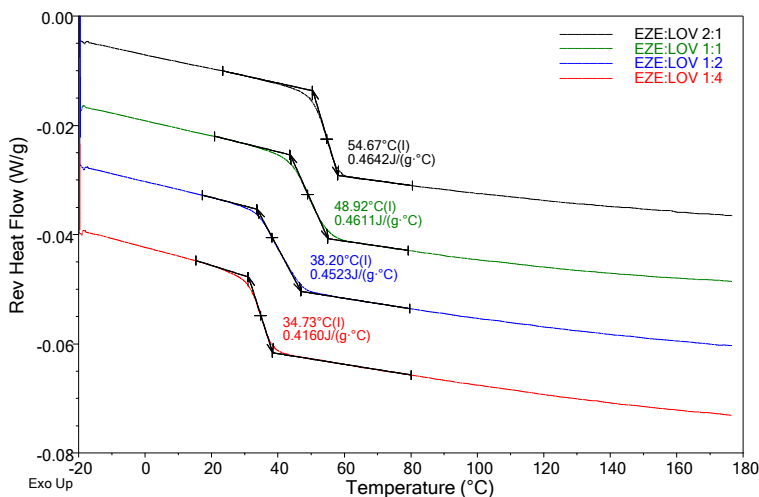
(to be continued)



The amorphous state of the quench cooled samples was confirmed through mDSC analysis. Regarding EZEqc, after the first heat/cooling cycle, the melting peak of EZE at 163°C disappears and a glass transition event is observed at 64°C. For LOVqc, the first heating cycle shows an endothermic event at 172°C and after cooling, at the second heating cycle, its amorphous state is confirmed by a glass transition temperature ( $T_g$ ) at 25°C, followed by a heat-mediated crystallization around 80°C and a melting event at 171°C, in agreement with previous reports in literature.

For the co-amorphous systems, single  $T_g$  values and the absence of melting events confirm the amorphous and single phase characteristics of these samples (Figure 10). Taking into account the Gordon Taylor equation (Equation 1) and the composition of the four different co-amorphous systems, the theoretical  $T_g$  values were calculated. All the calculated values (41.6, 35.7, 31.5 and 28.8°C for 2:1, 1:1, 1:2 and 1:4, respectively) were lower in comparison to the experimental ones: 54.7°C (2:1), 48.9°C (1:1), 38.2°C (1:2) and 34.7°C (1:4).

**Figure 10.** Reverse heat flow curves, experimental glass transition temperatures and heat capacity of co-amorphous systems



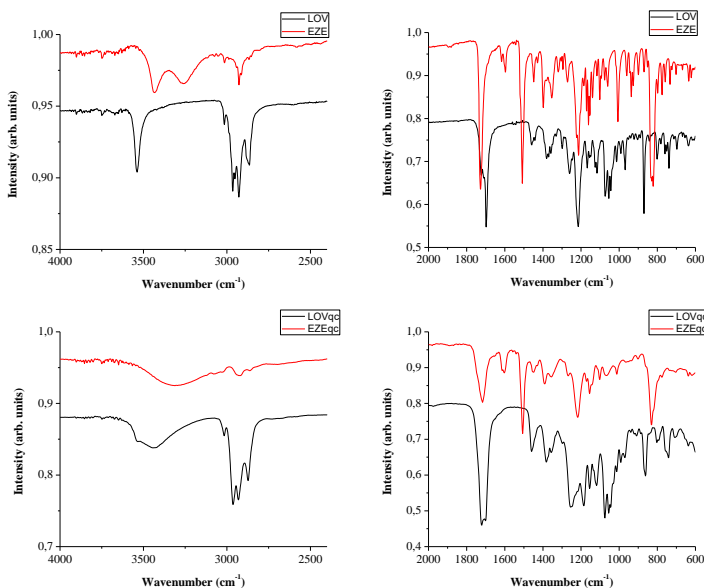
According to the Gordon-Taylor equation, deviations between these values indicate differences in the strengths of the intermolecular interactions between the components. If positive, it indicates that the amount and strength of bonding between the components of the mixture is stronger than the interactions occurring individually in each compound. On the other hand, if negative, this deviation can be attributed to an overall loss in the number and strength of hydrogen bonding in the mixture or to an increase in the free volume due to the mixing (LÖBMANN et al., 2011; 2012). Based on that, these results suggest a possible intermolecular interaction between EZE and LOV in all co-amorphous systems. In addition, it is important to note that higher  $T_g$  values of the samples are directly related to an increased amount of EZE. This is due to the fact that EZE has a higher  $T_g$  value than LOV (64°C and 25°C, respectively).

FTIR analyses were performed to investigate potential interactions between the compounds in co-amorphous systems, as suggested by the deviations of the experimental  $T_g$  values. Both compounds present donor and acceptor H-bonding groups, which favour the occurrence of these interactions. Based on that, the most important

changes are observed concerning the broadening of the O-H band and shifts relative to O-H and C=O bands.

EZE main bands appear at 3428 and 3252  $\text{cm}^{-1}$  (O-H stretch), 1725  $\text{cm}^{-1}$  (C=O of lactam), 1508  $\text{cm}^{-1}$  (ring C=C stretch), 1448 and 1429  $\text{cm}^{-1}$  (C-N stretch), 1214  $\text{cm}^{-1}$  (C-F stretch), 1063  $\text{cm}^{-1}$  (C-O stretch of secondary alcohol) and 821  $\text{cm}^{-1}$  (ring vibration due to paradisubstituted benzene). EZE<sub>qc</sub> showed a similar spectrum, but with considerable changes regarding the broadening of the band at 3312  $\text{cm}^{-1}$  and a shift of the C=O band from 1725 to 1717  $\text{cm}^{-1}$ . For LOV, characteristic bands are observed at 3538  $\text{cm}^{-1}$  (O-H stretch), 2965, 2929 and 2868  $\text{cm}^{-1}$  (methyl and methylene C-H stretch), 1722 and 1697  $\text{cm}^{-1}$  (lactone and ester carbonyl stretch), 1459  $\text{cm}^{-1}$  (C-C stretch in the aromatic ring), 1260, 1214, 1073 and 1055  $\text{cm}^{-1}$  (lactone and ester C-O-C bending vibration) and 969  $\text{cm}^{-1}$  (C-OH stretch). Changes regarding the LOV<sub>qc</sub> spectrum are observed especially for the broader shifted band at 3443  $\text{cm}^{-1}$ , the inversion of the intensity between the bands at 1721 and 1701  $\text{cm}^{-1}$ , and the broadening and decreasing of the intensity respective to the band at 1255  $\text{cm}^{-1}$  (Figure 11).

**Figure 11.** FTIR data of crystalline and quench cooled raw materials



The broadening of the O-H band for both EZE<sub>q</sub>c and LOV<sub>q</sub>c can be due to distinct chemical environments and establishment of different intramolecular interactions favoured by the high mobility and loss of order of amorphous materials (MARTÍNEZ et al., 2014). Shifts in the C=O bands result from the interaction of the lone pairs on the oxygen with a hydrogen donor group. This promotes an increase in the electronic polarization of the double bond, resulting in the weakening of the carbonyl bond. In an FTIR spectrum, this chemical arrangement is verified through shifts of the carbonyl stretch to lower wavenumbers (VOGT, ROBERTS-SKILTON and KENNEDY-GABB, 2013).

The analysis of FTIR data of co-amorphous systems was done through the comparison between calculated and experimental spectra. The calculation was based on data of the pure amorphous APIs, taking into account the four different molar ratios used to prepare the co-amorphous systems and assuming simple signal additivity of the compounds.

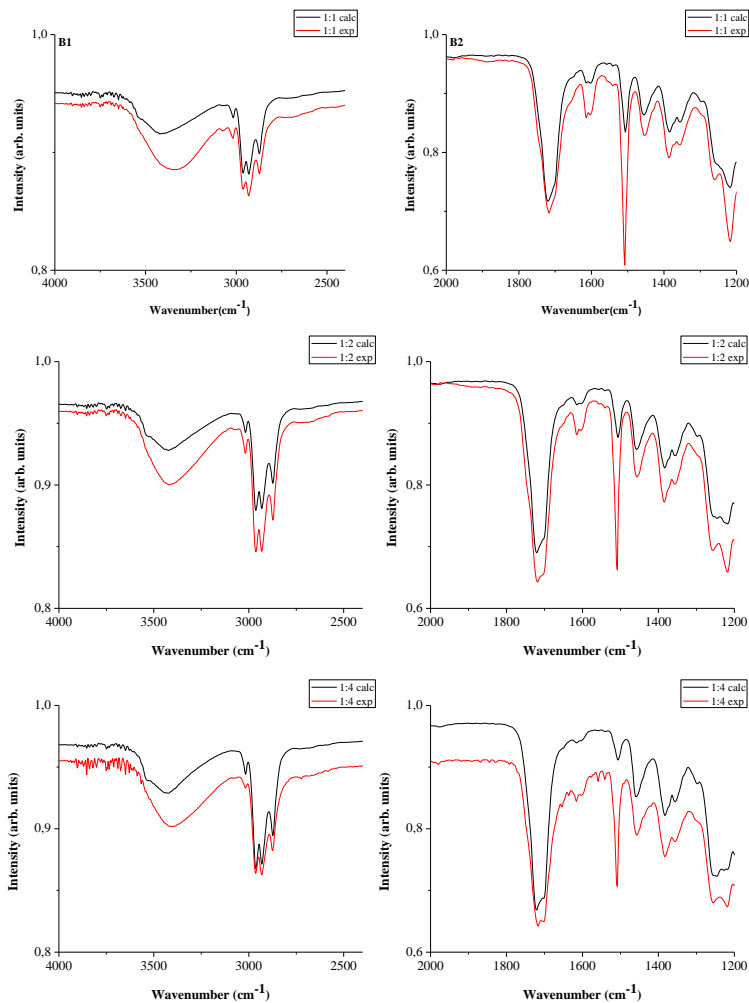
FTIR spectra of the co-amorphous systems show that all the samples presented differences when compared to the calculated amorphous physical mixtures (Table 1 and Figure 12). Shifts are observed concerning the O-H and C=O bands, as well as the appearance of a small shoulder in the region of 1749 cm<sup>-1</sup>. These data confirm the occurrence of hydrogen bonding between EZE and LOV in co-amorphous systems.

**Table 1.** Experimental and calculated FTIR data of co-amorphous systems

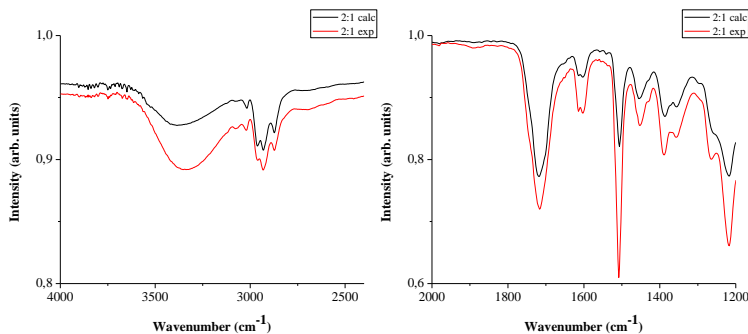
Sample	O-H band (cm <sup>-1</sup> )		C=O band (cm <sup>-1</sup> )	
	Calculated	Experimental	Calculated	Experimental
EZE:LOV 1:1	3403	3350	1720	1715
EZE:LOV 1:2	3430	3414	1721	1717
EZE:LOV 1:4	3432	3404	1721	1717
EZE:LOV 2:1	3383	3343	1719	1715



**Figure 12.** Calculated versus experimental FTIR data for 1:1, 1:2, 1:4 and 2:1 EZE:LOV (m/m), demonstrating the broadening and shift of hydroxyl and carbonyl bands in all co-amorphous systems



(to be continued)

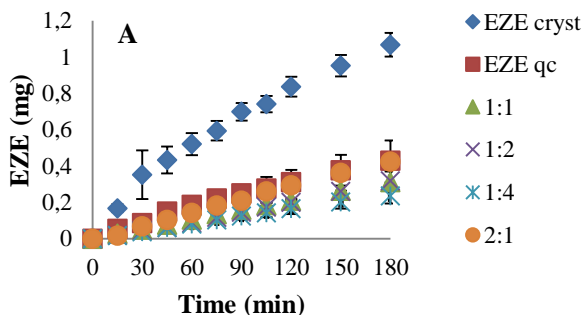


Almost all co-amorphous systems reported present intermolecular interactions (LAITINEN et al., 2013), which favour their physical stability. However, binary systems composed of ritonavir:indomethacin (DENGALÉ et al., 2014) and simvastatin:glipizide (LÖBMANN et al., 2012) showed no interactions between the compounds and their physical stability was not affected, being justified by the molecular level miscibility between the APIs.

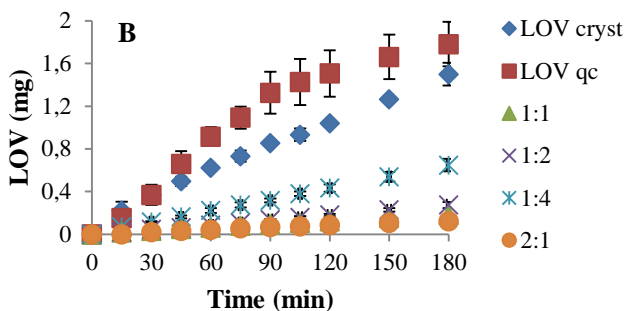
### 3.3 *IN VITRO* DISSOLUTION OF CO-AMORPHOUS SYSTEMS

Figure 13 shows the intrinsic dissolution profiles of the co-amorphous systems and the quench cooled raw materials compared to those of the crystalline forms of EZE and LOV. The intrinsic dissolution data are presented in Table 2.

**Figure 13.** Intrinsic dissolution profiles of crystalline (A) EZE and (B) LOV raw materials compared to the quench cooled samples and co-amorphous systems



(to be continued)



**Table 2.** Intrinsic dissolution data

Sample	Equation ( $y = ax + b$ )	Correlation coefficient (r)	Intrinsic dissolution rate ( $\text{mg} \cdot \text{cm}^{-2} \cdot \text{min}^{-1}$ ) $\pm$ SD
<b>EZE</b>			
RM*	$y = 9 \times 10^{-5}x + 0,1304$	0.98102	$1.8 \times 10^{-2}$
EZEqc	$y = 4 \times 10^{-5}x + 0,0258$	0.99378	$7.2 \times 10^{-3}$
1:1	$y = 3 \times 10^{-5}x + 0,0002$	0.99970	$4.8 \times 10^{-3}$ $\pm 1.0 \times 10^{-3}$
1:2	$y = 3 \times 10^{-5}x - 0,0116$	0.99805	$5.4 \times 10^{-3}$
1:4	$y = 2 \times 10^{-5}x + 0,0004$	0.99915	$4.2 \times 10^{-3}$ $\pm 1.0 \times 10^{-3}$
2:1	$y = 4 \times 10^{-5}x - 0,0056$	0.99865	$8.4 \times 10^{-3}$ $\pm 2.0 \times 10^{-3}$
<b>LOV</b>			
RM*	$y = 1 \times 10^{-4}x + 0,1041$	0.99529	$2.4 \times 10^{-2}$ $\pm 3.4 \times 10^{-3}$
LOVqc	$y = 2 \times 10^{-5}x - 0,0198$	0.99564	$4.2 \times 10^{-2}$ $\pm 3.4 \times 10^{-3}$
1:1	$y = 2 \times 10^{-5}x + 0,0014$	0.99965	$3.0 \times 10^{-3}$ $\pm 3.5 \times 10^{-4}$
1:2	$y = 3 \times 10^{-5}x - 0,002$	0.99950	$4.8 \times 10^{-3}$ $\pm 3.5 \times 10^{-4}$
1:4	$y = 6 \times 10^{-5}x + 0,0069$	0.99965	$1.0 \times 10^{-2}$ $\pm 3.5 \times 10^{-4}$
2:1	$y = 1 \times 10^{-5}x - 0,0014$	0.99529	$2.4 \times 10^{-3}$ $\pm 3.7 \times 10^{-4}$

\* RM: raw material

Linear dissolution profiles were observed for the samples along the assay. In case of LOV, LOVqc presented the highest dissolution rate ( $4.2 \times 10^{-2} \pm 3.4 \times 10^{-3} \text{ mg.cm}^{-2}.\text{min}^{-1}$ ), although not significantly different ( $p \leq 0.05$ ) from the raw material ( $2.4 \times 10^{-2} \pm 3.4 \times 10^{-3} \text{ mg.cm}^{-2}.\text{min}^{-1}$ ). The dissolution profile of LOVqc showed a change in its slope after 90 min, which was attributed to a solvent mediated crystallization (Figure 14A). This data can be explained by the low  $T_g$  of the amorphous form of LOV (at 25°C), below the temperature of the dissolution medium ( $37 \pm 0.5^\circ\text{C}$ ).

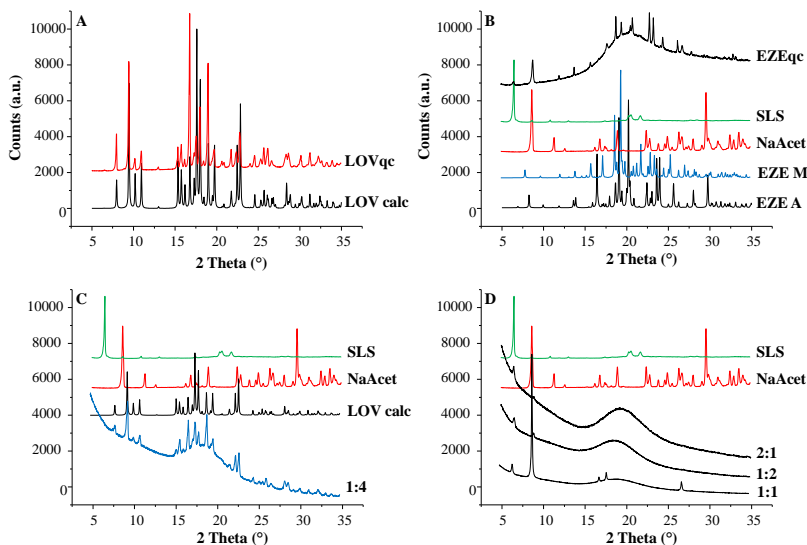
Unexpectedly, none of the co-amorphous systems increased the dissolution rate of the API and their dissolution rates are significantly different of LOVqc and raw material ( $p \leq 0.05$ ). The co-amorphous systems 1:1, 1:2 and 2:1 were considered similar, but significantly different from 1:4 ( $p \leq 0.05$ ). Solution-mediated crystallization was ruled out by XRD analyses for the samples 1:1, 1:2 and 2:1 (EZE:LOV m/m) (Figure 14D), indicating that EZE plays an important role on the stabilization of LOV, probably due to the increase in the  $T_g$  values. However, for 1:4 (EZE:LOV, m/m), which presents a  $T_g$  of  $34.7^\circ\text{C}$ , a solution-mediated crystallization was observed and all the crystalline peaks were attributed to LOV (Figure 14C).

For EZE, the crystalline raw material showed the highest dissolution rate ( $1.8 \times 10^{-2}$  *versus*  $7.2 \times 10^{-3} \text{ mg.cm}^{-2}.\text{min}^{-1}$  for EZEqc). In case of EZEqc, after 3 hours of dissolution, crystalline peaks corresponding to its anhydrate and monohydrate forms were observed (as well as crystalline peaks respective to the components of the dissolution medium), superimposed with the amorphous halo (Figure 14B). This partial transition to the monohydrate form has a negative effect on the dissolution of EZE, since its monohydrate form presents a lower aqueous solubility ( $8 \mu\text{g ml}^{-1}$ ) than its anhydrous form ( $12 \mu\text{g ml}^{-1}$ ). However, a complete crystallization of EZE did not occur until the end of the assay (evidenced by the amorphous halo observed by XRD), and its dissolution rate is still lower than the starting crystalline raw material.

For all the co-amorphous samples, none of them were able to increase the dissolution rate of EZE. A solution-mediated crystallization was ruled out by XRD analyses after 3 hours of dissolution (Figure 14C and 14D), indicating that the amorphous form of EZE has a lower dissolution rate than its crystalline counterpart. Statistical analyses show that the raw material is significantly different from EZEqc and co-

amorphous samples. All co-amorphous systems are considered similar ( $p \leq 0.05$ ).

**Figure 14.** Diffractograms of (A) LOV, (B) EZE, (C) 1:4 and (D) 1:1, 1:2 and 2:1 EZE:LOV (m/m), compared to the diffractograms of SLS, sodium acetate and the XRD patterns of LOV, EZE anhydrate (EZE A) and EZE monohydrate (EZE M), obtained from the Cambridge Structural Database



Amorphous materials generally increase the solubility and dissolution rate in comparison to the crystalline ones, but exceptions are reported. The example concerns the anti-HIV drug darunavir, where the crystalline darunavir ethanolate shows a higher dissolution than its amorphous form. This is due to the fact that darunavir ethanolate is a channel solvate that can exchange ethanol and water freely with one another, which facilitates wetting and dissolution, while its amorphous form shows only limited wettability (VAN GYSEGHEM et al., 2009). The amorphous form of carvedilol also presented a lower dissolution rate at 37°C, compared to its crystalline form. This finding was attributed to the formation of cohesive supercooled liquid state, supported by enthalpy relaxation studies, which indicated increase in enthalpy recovery and structural relaxation of amorphous form towards the supercooled liquid

region (POKHARKAR et al., 2006). However, for EZE, the reasons for a lower dissolution rate observed for its amorphous state remain unclear.

#### 4. CONCLUSIONS

Co-amorphous systems of EZE and LOV composing a single amorphous phase were successfully obtained by quench cooling from the melt. Occurrence of intermolecular hydrogen bonding was suggested through the comparison of theoretical and experimental  $T_g$  values and confirmed by FTIR. However, unexpectedly, amorphous EZE showed a lower dissolution rate in comparison to its crystalline form and this result was also observed for all co-amorphous formulations, which were also not able to increase the dissolution rate of LOV. As this type of formulation was not able to increase the dissolution rate of EZE and LOV, other strategies were further investigated, such as the addition of gelatin and hydrophilic polymers.

#### 5. REFERENCES

ALLESO, M.; CHIENG, N.; REHDER, S.; RANTANEN, J.; RADES, T.; AALTONEN, J. Enhanced dissolution rate and synchronized release of drugs in binary systems through formulation: Amorphous naproxen-cimetidine mixtures prepared by mechanical activation. **Journal of Controlled Release**, v. 136, p. 45-53, 2009.

BRÜNING, J.; ALIG, E.; SCHMIDT, M.U. Ezetimibe anhydrate, determined from laboratory powder diffraction data. **Acta Crystallographic C**, v. 66, p. o341-o344, 2010.

DENGALÉ, S.J.; RANJAN, O.P.; HUSSEN, S.S.; KRISHNA, B.S.; MUSMADE, P.B.; GAUTHAM SHENOY, G.; BHAT, K. Preparation and characterization of co-amorphous Ritonavir-Indomethacin systems by solvent evaporation technique: improved dissolution behavior and physical stability without evidence of intermolecular interactions. **European Journal of Pharmaceutical Sciences**, v. 62, p. 57-64, 2014.

US FOOD AND DRUG ADMINISTRATION. Guidance for industry: new chemical entity exclusivity determinations for certain fixed-combination drug products. Disponível em:

<http://www.fda.gov/downloads/drugs/guidancecomplianceregulatoryinformation/guidances/ucm386685.pdf>. Acesso em 25 de julho de 2015.

JANSSENS, S.; VAN DEN MOOTER, G. Review: Physical chemistry of solid dispersions. **Journal of Pharmacy and Pharmacology**, v. 61, p. 1571-1586, 2009.

JANTRATID, E.; JANSSEN, N.; REPPAS, C.; DRESSMAN, J. Dissolution media simulating conditions in the proximal human gastrointestinal tract: An update. **Pharmaceutical Research**, v. 25, p. 1663-1676, 2008.

LAITINEN, R.; LÖBMANN, K.; STRACHAN, C. J.; GROHGANZ, H.; RADES, T. Emerging trends in the stabilization of amorphous drugs. **International Journal of Pharmaceutics**, v. 453, p. 65-79, 2013.

LENZ, E.; JENSEN, K.T.; BLAABJERG, L.I.; KNOP, K.; GROHGANZ, H.; LÖBMANN, K.; RADES, T.; KLEINEBUDDE, P. Solid-state properties and dissolution behaviour of tablets containing co-amorphous indomethacin-arginine. **European Journal of Pharmaceutics and Biopharmaceutics**, v. 96, p. 44-52, 2015.

LÖBMANN, K.; STRACHAN, C.; GROHGANZ, H.; RADES, T.; KORHONEN, O.; LAITINEN, R. Co-amorphous simvastatin and glipizide combinations show improved physical stability without evidence of intermolecular interactions. **European Journal of Pharmaceutics and Biopharmaceutics**, v. 81, p. 159-169, 2012.

LÖBMANN, K. LAITINEN, R.; STRACHAN, C.; RADES, T.; GROHGANZ, H. Amino acids as co-amorphous stabilizers for poorly water-soluble drugs - Part 2: molecular interactions. **European Journal of Pharmaceutics and Biopharmaceutics**, v. 85, p. 882-888, 2013a.

LÖBMANN, K.; GROHGANZ, H.; LAITINEN, R.; STRACHAN, C.; RADES, T. Amino acids as co-amorphous stabilizers for poorly water soluble drugs - Part 1: preparation, stability and dissolution enhancement. **European Journal of Pharmaceutics and Biopharmaceutics**, v. 85, p. 873-881, 2013.

LÖBMANN, K.; LAITINEN, R.; GROHGANZ, H.; GORDON, K.C.; STRACHAN, C.; RADES, T. Coamorphous drug systems: enhanced physical stability and dissolution rate of indomethacin and naproxen. **Molecular Pharmaceutics**, v. 8, p. 1919-1928, 2011.

MARTÍNEZ, L.M.; VIDEA, M.; LÓPEZ-SILVA, G.A.; DE LOS REYES, C.A.; CRUZ-ANGELES, J.; GONZÁLEZ, N. Stabilization of amorphous paracetamol based systems using traditional and novel strategies. **International Journal of Pharmaceutics**, v. 477, p. 294-305, 2014.

POKHARKAR, V.B.; MANDPE, L.P.; PADAMWAR, M.N.; AMBIKE, A.A.; MAHADIK, K.R.; PARADKAR, A. Development, characterization and stabilization of amorphous form of a low Tg drug. *Powder Tech.* 2006;167:20-25.

RAVIKUMAR, K.; SRIDHAR, B. Ezetimibe monohydrate. **Acta Crystallographic E**, v. 61, p.o2907-o2909, 2005.

SATO, S.; HATA, T.; TSUJITA, Y.; TERAHARA, A.; TAMURA, C. The structure of monacolin K,  $C_{24}H_{36}O_5$ . **Acta Crystallographica**, v. C40, p.195-198, 1984.

SWEETMAN, S. C. Lovastatin. In: **Martindale: The complete drug reference**. 36 ed. London: Pharmaceutical Press, 2009, p. 1328-1329.

VAN GYSEGHEM, E.; STOKBROEKX, S.; DE ARMAS, H.N.; DICKENS, J.; VANSTOCKEM,M.; BAERT, L.; ROSIER, J.; SCHUELLER, L.; VAN DEN MOOTER, G. Solid state characterization of the anti-HIV drug TMC114: interconversion of amorphous TMC114, TMC114 ethanolate and hydrate. **European Journal of Pharmaceutical Sciences**, v. 38, p. 489-497, 2009.

VOGT,F.G.; ROBERTS-SKILTON, K.; KENNEDY-GABB, S.A. A solid-state NMR study of amorphous ezetimibe dispersions in mesoporous silica. **Pharmaceutical Research**, v. 30, p.2315-2331, 2013.

YOSHIDA, M.I.; OLIVEIRA, M.A.; GOMES, E.C.L.; MUSSEL, W.N.; CASTRO, W.V.; SOARES, C.D.V. Thermal characterization of lovastatin in pharmaceutical formulations. **Journal of Thermal Analysis and Calorimetry**, v. 106, p. 657-664, 2011.



### **CHAPTER III**

#### **DEVELOPMENT, CHARACTERIZATION AND *IN VITRO* DISSOLUTION STUDIES OF TERNARY AMORPHOUS SYSTEMS OF EZETIMIBE, LOVASTATIN AND GELATIN PREPARED BY HIGH IMPACT MILLING**

---

## 1. INTRODUCTION

Gelatin is a water-soluble natural biopolymer derived from acidic or alkaline hydrolysis of collagen. Its composition varies according to the raw material used but it is mainly proteins (85-92%), mineral salts and water (DUCONSEILLE et al., 2015). In comparison to other materials, gelatin offers the advantages of being cheap, readily available, biocompatible and biodegradable (ELZOGHBY, 2013). Having a long history of safe use in pharmaceuticals, especially in the composition of hard capsules, more recently, gelatin has been also used in the development of modern drug delivery systems composed of poorly water-soluble APIs.

Kallinteri and Antimisiaris (2001) reported the increase of the solubility of seven drugs (nitrofurantoin, chlorothiazide, phenobarbital, prednisolone, griseofulvin, diazepam and piroxicam) in presence of gelatin and they stated that there is a tendency for larger gelatin-induced increases in solubility as drug lipophilicity increases. In the same context, gelatin-based systems were able to improve the dissolution rate of the poorly soluble APIs pranlukast (CHONO et al., 2008), ibuprofen (LI et al., 2008) and fenofibrate (YOUSAF et al., 2015).

The previous chapter has demonstrated that the obtainment of a binary co-amorphous system between ezetimibe (EZE) and lovastatin (LOV) was not enough to enhance their dissolution rate, in comparison to amorphous and crystalline raw materials. In this context, the addition of a ternary compound to this amorphous system seems like a promising approach.

In this context, this chapter proposed the preparation of ternary amorphous systems composed of gelatin, EZE and LOV, in order to investigate the potential of this biopolymer to enhance the dissolution rate of the respective compounds. As an environmentally friendly, relatively simple process and of easy scaling up (BARZEGAR-JALALI et al., 2010), the high impact milling was chosen as the preparation method. The obtained samples were characterized by means of X-ray powder diffraction and modulated scanning calorimetry and evaluated through in vitro dissolution studies.

## 2. EXPERIMENTAL

### 2.1 MATERIALS

Porcine gelatins type A bloom 75 (batch number 1408053) and bloom 225 (batch number 1386268), both mesh 100, were kindly supplied by Rousselot NV (Gent, Belgium). EZE and LOV were purchased from Pharma Nostra (Rio de Janeiro, Brazil), with batch numbers FM017H13 and 130312, respectively. Soluplus® (batch number 23597787V0), Kollidon® VA64 (batch number 28569368E0) and Kollidon® 30 (batch number 72888756P0) were obtained from BASF® ChemTrade GmbH (Ludwigshafen, Germany) and HPMC E5 derived from Federa (Rotterdam, Netherlands).

### 2.2 PREPARATION OF BALL-MILLED TERNARY SYSTEMS

Different ratios of APIs, gelatin and polymers (when applicable) were accurately weighed comprising a final mass of 30 mg. The ratios between the APIs varied from 1:1 to 1:4 (EZE:LOV w/w) according to their therapeutic doses and the percentages of gelatin ranged from 25 to 75 %. The formulations were named as ELG (EZE:LOV:Gelatin) 75 or 225 (according to the type of gelatin tested), followed by the percentage of each compound in the final composition. When polymers were added, they were identified as S, K30, VA64 and H for Soluplus®, Kollidon® 30, Kollidon® VA64 and HPMC E5, respectively.

Samples were kept in 2 mL eppendorf tubes and milled in a Retsch PM 400 MA ball mill (Haan, Germany) for 8 hours, at 400 rpm. High wear resistant zirconia beads (TOSOH Corporation, Tokyo, Japan) of 1, 3 and 5 mm external diameter were used as grinding media. Milling was performed at room temperature and no significant heating of the samples was noted at the end of the process. All samples were stored in desiccators containing  $P_2O_5$  at room temperature prior to analysis.

### 2.3 PREPARATION OF SPRAY DRIED SYSTEMS

Co-spray dried (coSD) samples composed of EZE:LOV 1:1 (w/w) were prepared in order to compare with amorphous formulations in presence of gelatin. The spray drying method was chosen since it was not possible to obtain binary amorphous samples through milling. Spray dried powders were prepared using a Buchi mini spray dryer B191 (Buchi, Flawil, Switzerland). Briefly, an accurate amount of the drugs was dissolved in dichloromethane and methanol in a volumetric ratio of 50:50, comprising a final solid content of 2% (w/v). The operational conditions were: inlet temperature 65 °C, drying air flow rate 28 L/min, atomizing air flow 15 L/min and 6 mL/min feed rate using a peristaltic pump. The spray dried samples were prepared in duplicate and were kept in a vacuum oven at room temperature for 3 days to remove residual solvent. All samples were stored over phosphorous pentoxide in desiccators at room temperature prior to analysis.

## 2.4 X-RAY POWDER DIFFRACTION (XRPD)

XRPD experiments were carried out at room temperature using an automated X'pert PRO diffractometer (PANalytical, Almelo, Netherlands) with a Cu tube ( $K\alpha$   $\lambda = 1.5418$  Å) and the generator set at 45 kV and 40 mA. Ball milled samples were applied on spinning zero background sample holders. Measurements were performed in a continuous scan mode from 4° to 40° (2 $\theta$ ) with 0.0167° step size and 200 s counting time.

## 2.5 MODULATED DIFFERENTIAL SCANNING CALORIMETRY (mDSC)

mDSC was performed on a Q2000 DSC (TA Instruments, Leatherhead, UK), equipped with the refrigerated cooling system (RCS90) accessory under a dry nitrogen purge at a flow rate of 50 ml/min. Indium standard was used for routine calibration (temperature, enthalpy), sapphire disk was used for heat capacity calibration. Approximately 5 mg samples were weighed using an analytical balance into aluminum pans. The samples were then scanned at 2 °C/min from -10 to 230 °C with the following modulation parameters: amplitude of 0.636 °C every 40 s. DSC thermograms

were acquired and analyzed by using Universal Analysis software (version 4.4, TA Instruments, Leatherhead, UK).

## 2.6 *IN VITRO* DISSOLUTION STUDIES

Dissolution profiles of the crystalline EZE and LOV materials, as well as ball milled samples, were evaluated using USP II Dissolution Apparatus. In brief, accurately weighted samples equivalent to 10 mg EZE and 10 mg LOV were added into 500 mL acetate buffer pH 4.5 + 0.025% SLS, in a dissolution vessel at 37 °C. The solution was stirred at a speed of 100 rpm for 120 minutes. Drug release was calculated from the drug concentration at different time intervals (5, 15, 30, 45, 60, 90 and 120) and determined by HPLC (acetonitrile:water 50:50 v/v, 1 mL/min,  $\lambda$  = 235 nm, see appendix).

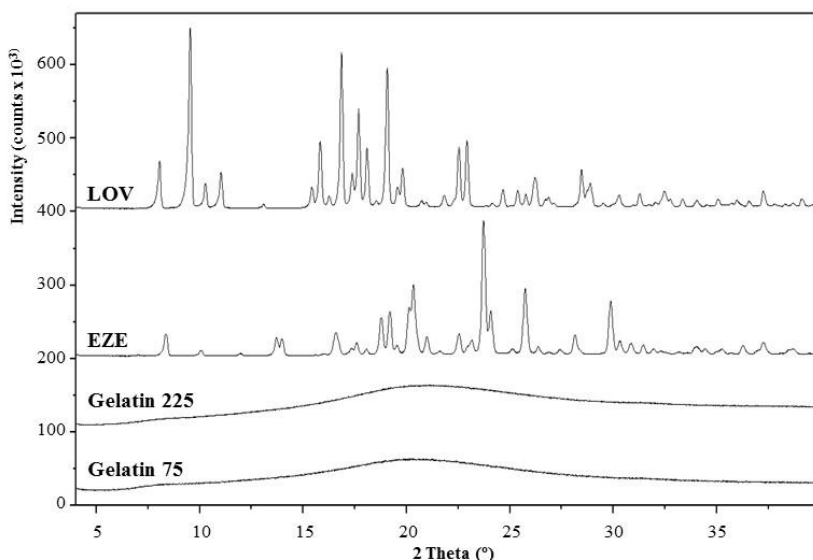
## 3. RESULTS AND DISCUSSION

### 3.1 CHARACTERIZATION OF RAW MATERIALS

Prior to milling, drugs and gelatins were characterized by means of solid-state techniques in order to compare with the processed materials. X-ray diffractograms are shown in Figures 15.

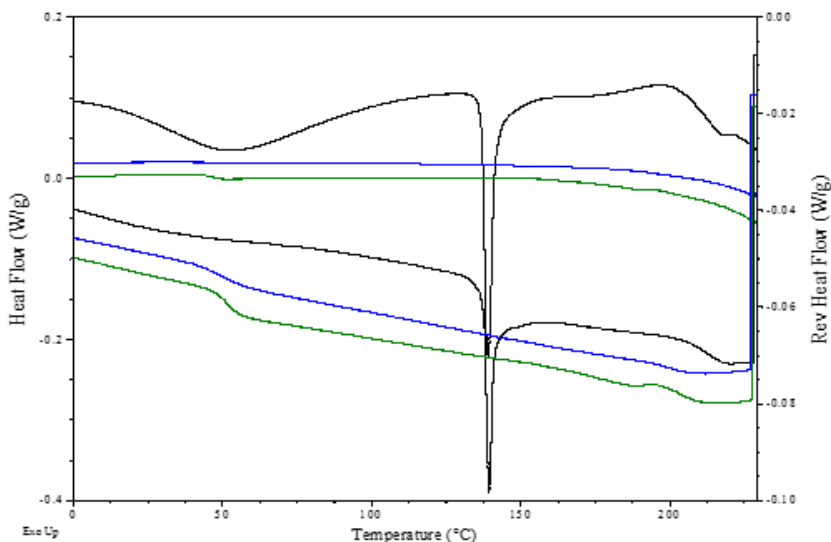
As discussed in the previous chapter, LOV presents a crystalline diffractogram with main Bragg peaks at  $2\theta$  8.05°, 9.54°, 11.03°, 15.83°, 16.86°, 17.68° and 19.07°. These data are in agreement with literature, which also reports no polymorphism for this API (YOSHIDA et al., 2011). On the other hand, EZE shows two crystalline forms, being the anhydrous (BRÜNING, ALIG and SCHMIDT, 2010) and monohydrate (RAVIKUMAR and SRIDHAR, 2005). Based on the comparison of the X-ray diffraction patterns of the polymorphic forms of EZE and the diffractogram of the raw material, especially at low angles, it is possible to affirm that the raw material used for this research corresponds to the anhydrous form. For both gelatins, amorphous halos are observed.

**Figure 15.** X-ray diffractograms of EZE, LOV and gelatin 75 and 225 raw materials



In order to check the miscibility among EZE, LOV and gelatin, a physical mixture composed of ELG75 25:25:50 was submitted to three heating cycles, following the conditions mentioned in topic 2.5 (Fig. 16). In the first heating it is possible to observe a solvent loss around 50°C followed by a melting event at 140°C. This event is a shift of EZE and LOV melting points. At 212°C the  $T_g$  of gelatin is observed. At the second and third heating cycles no melting peaks are observed indicating the amorphous state of the mixture. However, two  $T_g$  are shown in these heating cycles: 51°C and 204°C (2<sup>nd</sup> heating), 48°C and 198°C (3<sup>rd</sup> heating). The first one corresponds to the amorphous mixture between EZE and LOV and the second one is relative to pure gelatin. The shifts of the gelatin  $T_g$  indicate a possible miscibility among these components, which characterizes this system as promising.

**Figure 16.** mDSC thermograms of ELG75 25:25:50 physical mixture. Black, blue and green represent the first, second and third heating cycles, respectively. The three curves up represent the heat flow and the three curves down the reversing heat flow.



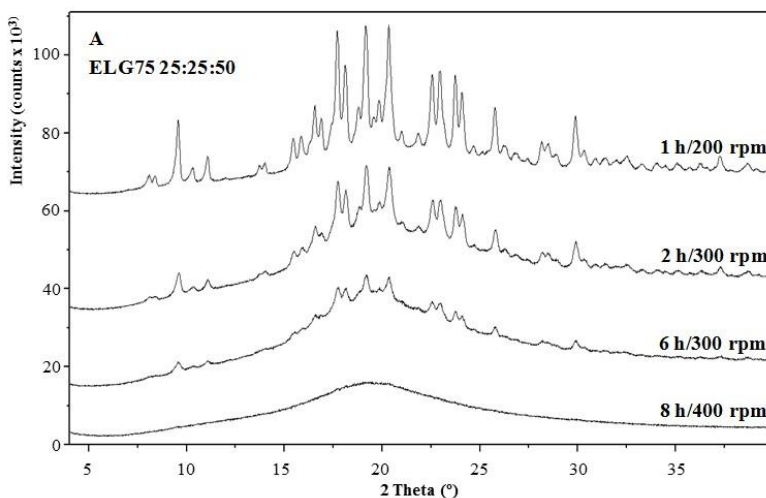
### 3.2 OPTIMIZATION OF THE MILLING PROCESS

In order to determine the optimal milling conditions, different rotation speeds, milling time, and amount of powder were tested. The samples submitted to these conditions were ELG75 25:25:50 and ELG225 25:25:50. The results are shown in Figures 17A-D.

First, a decrease in crystallinity was observed as the milling time and rotation speed increased, providing completely amorphous samples within 8 hours at 400 rpm (Figure 17A). After that, the number and combination of balls were also tested (Figures 17B,C). For the sample ELG75 25:25:50, amorphous samples were obtained with the combination of 1 ball of 5 mm with 8 balls of 3 mm. On the other hand, similar results were observed for ELG225 25:25:50 when 1 ball of 5 mm and 8 balls of 3 mm were combined with 16 balls of 1 mm. These results demonstrate that there is a difference in the impact needed

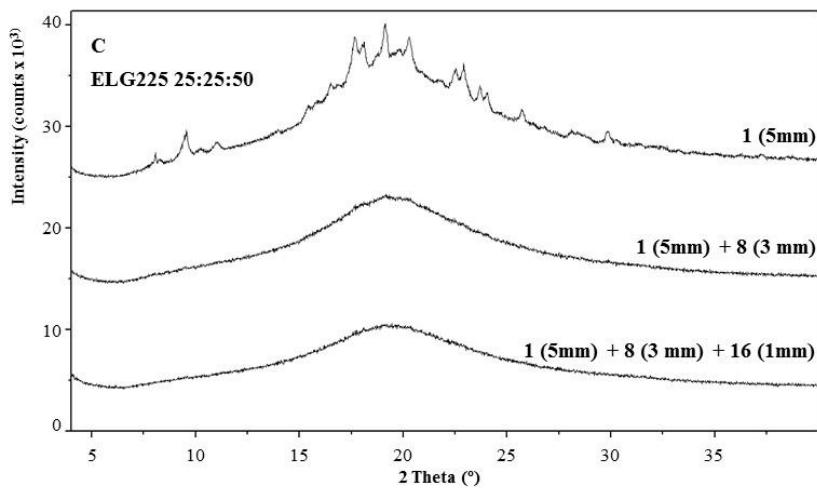
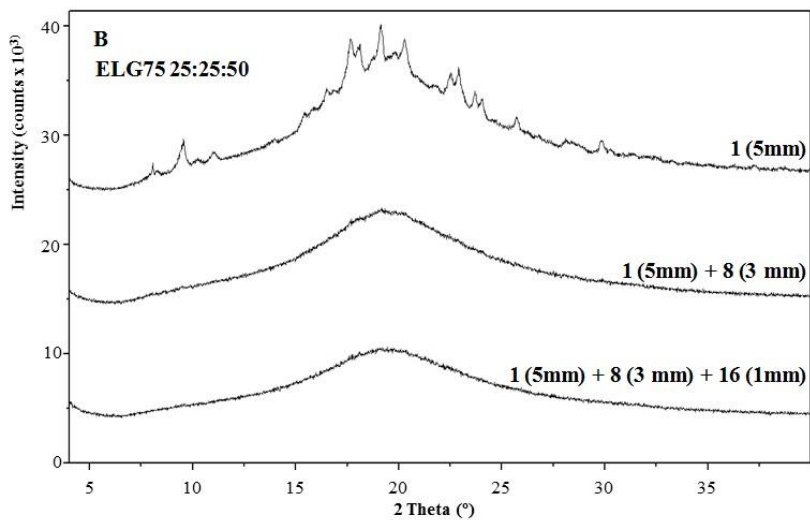
to obtain amorphous samples composed of different types of gelatin. In addition, the combination of balls was also positive, since the bigger balls were probably responsible for increasing the impact and the smaller ones reduced the amount of powder adhered to the bottom of the eppendorfs. Finally, the amount of powder was also tested and better results were observed for 30 mg instead of 50 mg, for both formulations (Fig. 17D). This is also attributed to a higher impact, due to a higher ball to powder ratio. Based on these data, the selected milling conditions were: 400 rpm rotation speed, 8 hours of milling time, 1 ball of 5 mm plus 8 balls of 3 mm plus 16 balls of 1 mm as grinding media and 30 mg of powder.

**Figure 17.** X-ray diffractograms regarding samples prepared with (A) different rotation speeds and milling times, (B, C) number and combination of balls and (D) amount of powder

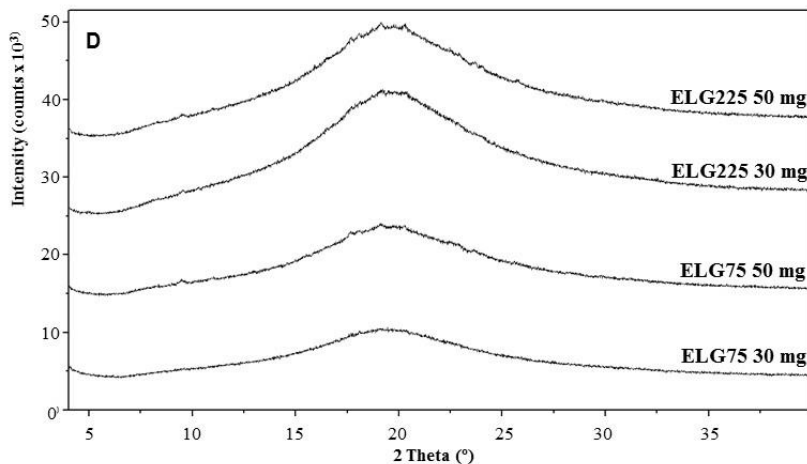


(to be continued)





(to be continued)

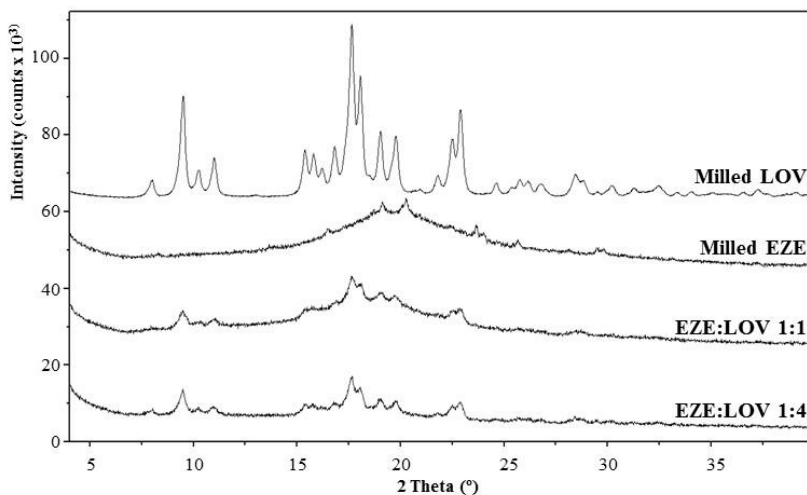


### 3.3 X-RAY POWDER DIFFRACTION OF MILLED MATERIALS

In order to verify the need of a hydrophilic carrier, pure raw materials and binary combinations of EZE:LOV in 1:1 and 1:4 were milled. The results are shown in Figure 18.

After 8 hours at 400 rpm, pure LOV presented a discrete broadening of its Bragg peaks as well as a small decrease of their intensity in comparison to the unprocessed raw material. On the other hand, pure EZE presented an amorphous halo with small Bragg peaks, which indicates a drastic change in its crystalline structure after milling, although presenting some remaining crystallinity. In addition, the peak at  $8.3^\circ$ , characteristic of the anhydrous form, is still observed for this sample, demonstrating that no phase transition occurred during milling. Interestingly, when EZE and LOV are combined in different ratios, a drastic decrease of their crystallinity is observed, which indicates the beneficial effect of this combination. It is important to note that the remaining Bragg peaks for these samples are mostly attributed to LOV. However, no amorphous samples were obtained, indicating the need for a carrier.

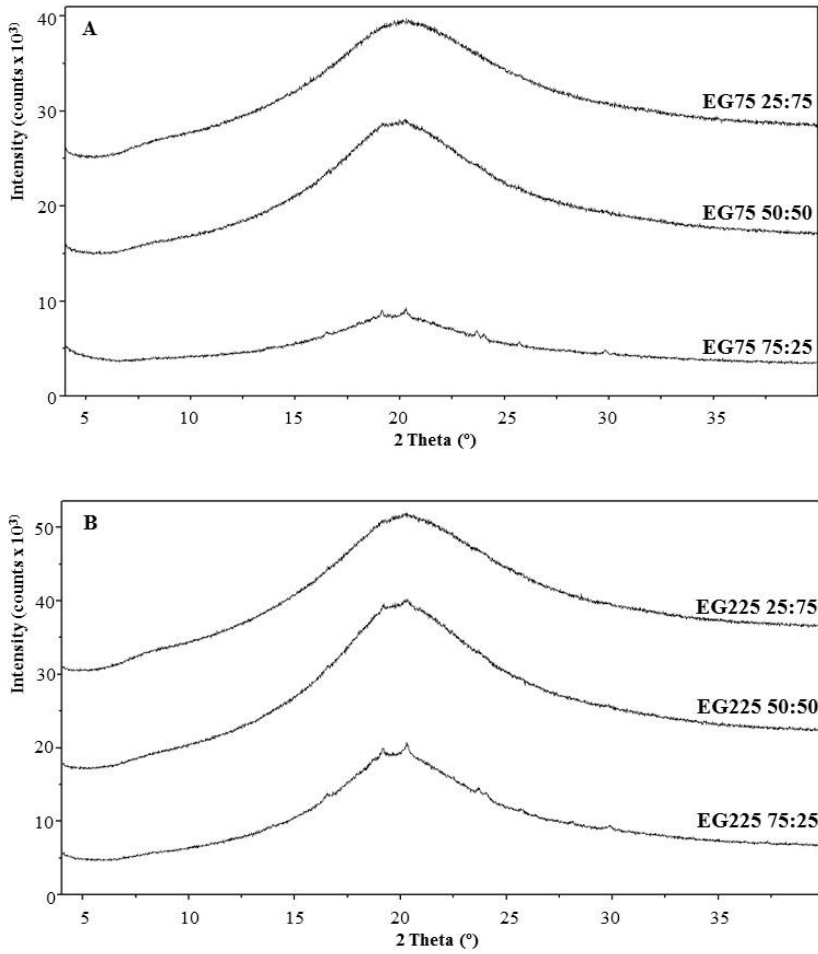
**Figure 18.** Diffractograms relative to milled pure raw materials and binary combinations at different ratios



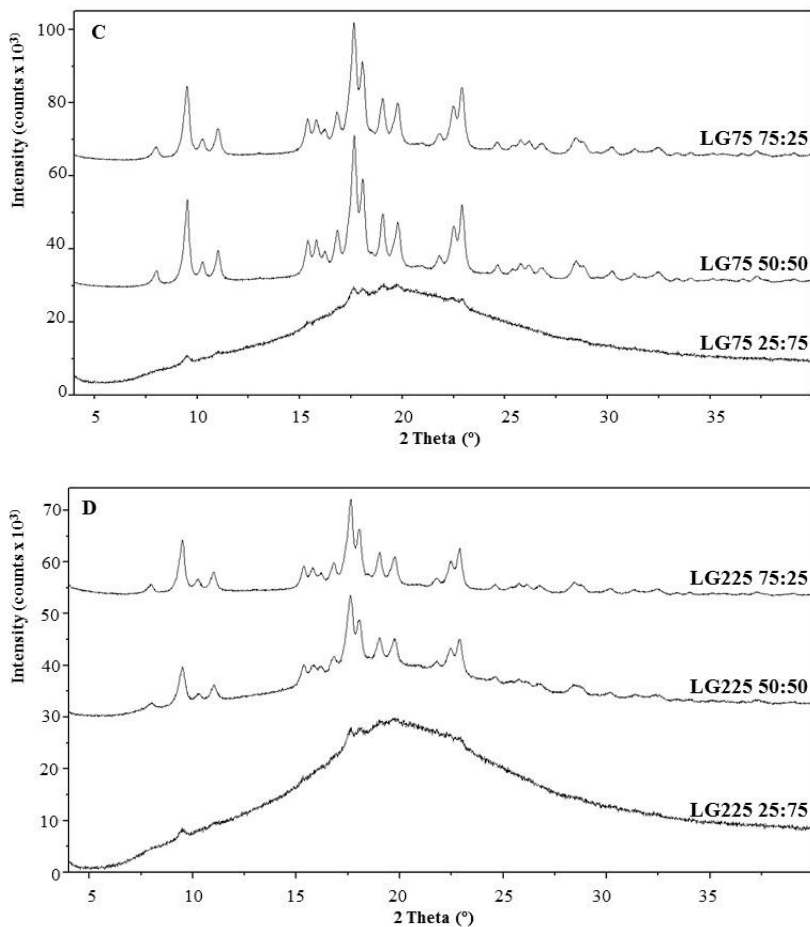
In order to check the influence of gelatin on the degree of amorphization of the pure APIs, binary systems composed of EZE:Gelatin and LOV:Gelatin were obtained in different ratios (25:75, 50:50 and 75:25, w/w) with the two types of gelatin (75 and 225) (Figures 19A-D).

Amorphous binary systems composed of EZE were prepared in presence of 75 and 50% of gelatin 75 and with 75% of gelatin 225. Small Bragg peaks overlapped to the amorphous halo are observed for the other combinations. These results demonstrate the importance of gelatin in the amorphization of EZE, since the pure API was not completely amorphous when milled as such. On the other hand, no amorphous samples were obtained for binary systems of LOV:Gelatin, although a drastic decrease of crystallinity was observed for the samples composed of 75% of gelatin.

**Figure 19.** X-ray diffractograms relative to binary systems composed of EZE:Gelatin and LOV:Gelatin in different ratios



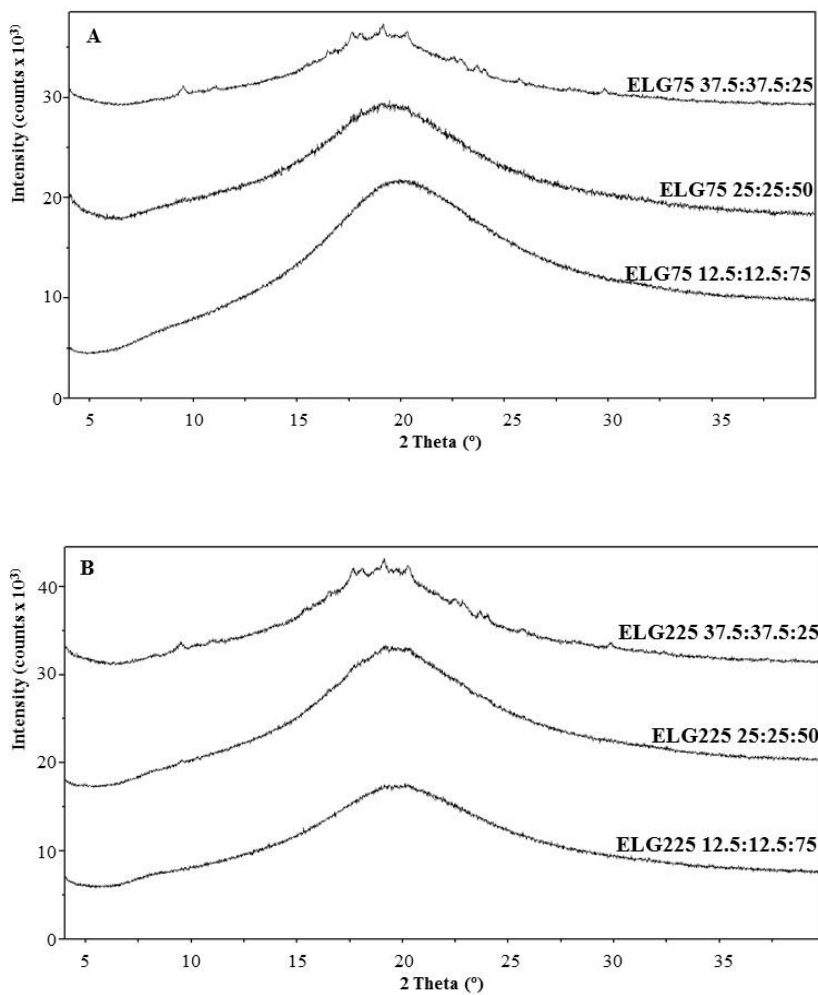
(to be continued)



The following step included the obtainment of the ternary milled systems. Initially, the ratios between the APIs was kept as 1:1 (w/w) and the amount of gelatin varied from 25 to 75% (Figures 20A-B). As it can be visualized, amorphous ternary systems were obtained with 50 and 75% of both types of gelatin. Small Bragg peaks that overlapped with the amorphous halo for ELG75/225 37.5:37.5:25 were observed. These results demonstrate the success of this combination, especially regarding LOV, which was not completely amorphous even in binary mixtures with

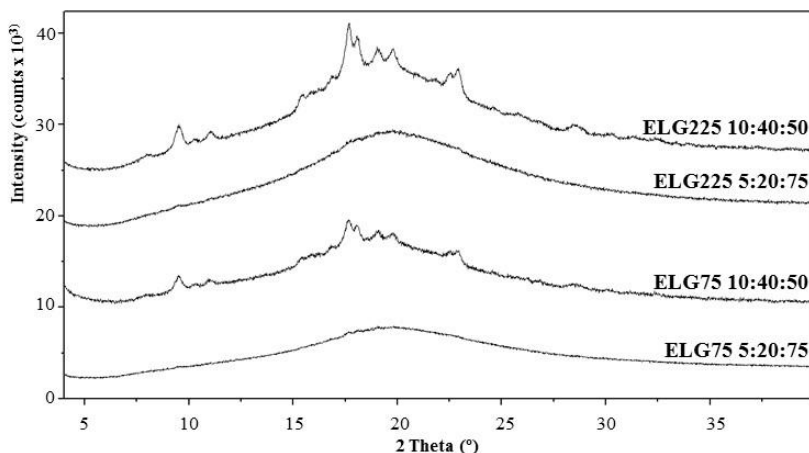
EZE or gelatin, in different ratios. No differences were observed between the two types of gelatin.

**Figure 20.** X-ray diffractograms relative to ternary systems composed of EZE:LOV:Gelatin in different ratios



In order to evaluate the influence of the ratio between the APIs, ternary systems composed of EZE:LOV in 1:4 (w/w) ratios were obtained in presence of 50 and 75% of gelatin (Figure 21). This ratio was selected since it represents the combination with the highest dose of LOV associated to EZE in clinical practice. Interestingly, as the amount of LOV increases it was not possible anymore to obtain amorphous systems with 50% of gelatin. However, when the amount of gelatin increases to 75% and the ratio between the APIs is kept as 1:4 (EZE:LOV w/w) amorphous samples are obtained. These data demonstrate the deleterious effect of high amounts of LOV, prejudicing the obtainment of amorphous systems. In addition, it is important to mention the beneficial effect of gelatin, since binary systems composed purely of EZE:LOV in 1:4 ratios were semicrystalline.

**Figure 21.** X-ray diffractograms relative to ternary systems composed of EZE:LOV in 1:4 ratios in presence of different amounts of gelatin

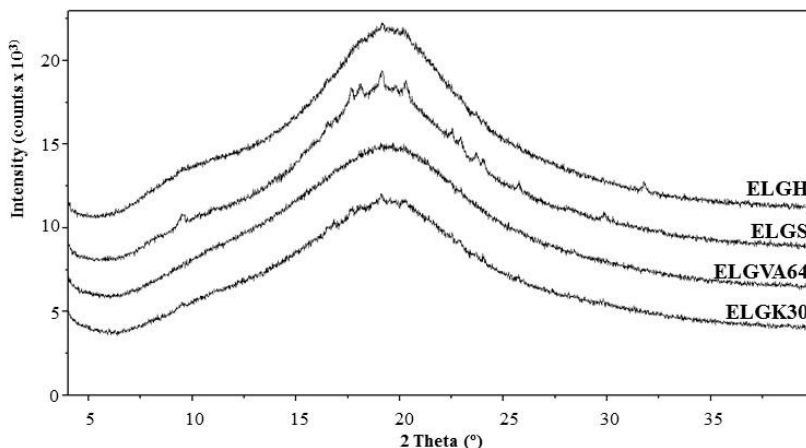


As a final step, the influence of polymers typically used in the formulation of solid dispersions was investigated (Figure 22). For this purpose, the total amount of APIs was kept at 50% (1:1 EZE:LOV ratio). This condition was selected since amorphous samples are obtained with this composition in presence of gelatin. To minimize the number of experiments, these tests were performed with gelatin 75. The polymers

tested were Soluplus®, Kollidon® 30, Kollidon® VA64 and HPMC E5. The final composition of these samples was E:L:G:Polymer 25:25:25:25.

As it can be visualized, completely amorphous samples were obtained in presence of HPMC E5 and Kollidon® VA64. However, small Bragg peaks are observed for samples composed of Soluplus® and Kollidon® 30. These data demonstrate that these polymers prejudice the amorphization of the APIs in presence of gelatin.

**Figure 22.** X-ray diffractograms regarding E:L:G:Polymer (25:25:25:25 w/w/w/w) milled samples



### 3.4 mDSC ANALYSIS

The ternary systems characterized as amorphous through XRPD were also analyzed by means of mDSC. The results regarding the samples ELG75/225 5:20:75, ELG75/225 25:25:50 and ELG75/225 12.5:12.5:75 are shown in Figures 23A-C.

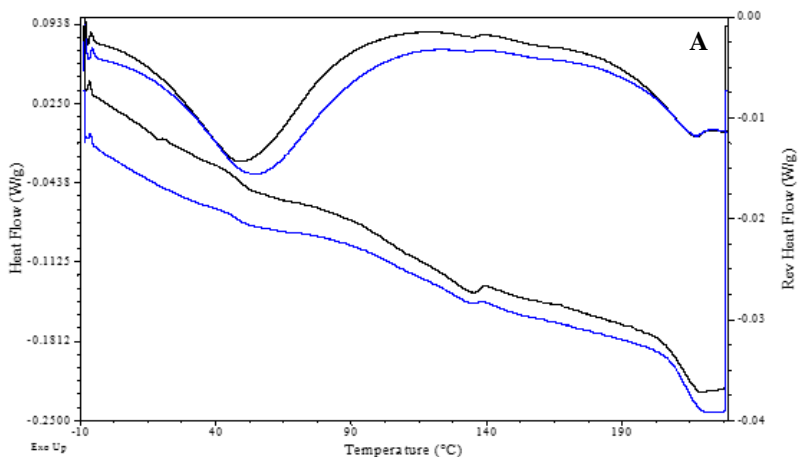
For samples ELG75/225 5:20:75 a solvent loss event is observed around 54°C that overlapped with a T<sub>g</sub> at 47°C, which corresponds to the mixture of amorphous EZE and LOV. A small shifted melting event is observed at 134°C, probably attributed to small remaining crystals not detected by XRPD. At 213°C the T<sub>g</sub> of gelatin is observed. No significant differences were observed between the two types of gelatin (Fig 23A).



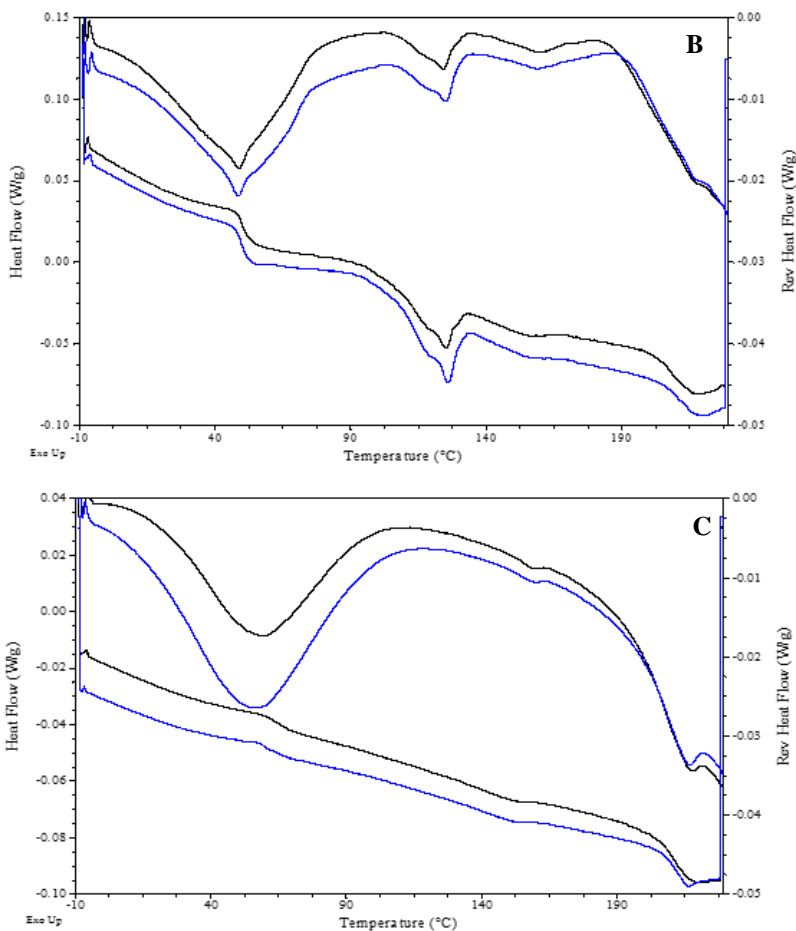
The same tendency is observed for samples composed of 50% of gelatin. A first Tg at 50°C overlapped with the solvent loss, followed by a small melting event at 123°C and the gelatin Tg at 123°C (Fig.23B). On the other hand, the samples ELG 75/225 12.5:12.5:75 presented no melting event regarding EZE and LOV. Two Tg are observed; one at 63°C and the other at 211°C respective to phases composed of the APIs and gelatin, respectively.

These results demonstrate that although amorphous halos were detected by XRPD some remaining crystallinity is still observed for some samples. In addition, all the ternary systems presented two different amorphous phases.

**Figure 23.** mDSC thermograms of (A) ELG75/225 5:20:75, (B) ELG75/225 25:25:50 and (C) ELG75/225 12.5:12.5:75. Black and blue curves represent samples prepared with gelatin 75 and 225, respectively. The two curves up represent the heat flow and the two curves down the reversing heat flow



(to be continued)



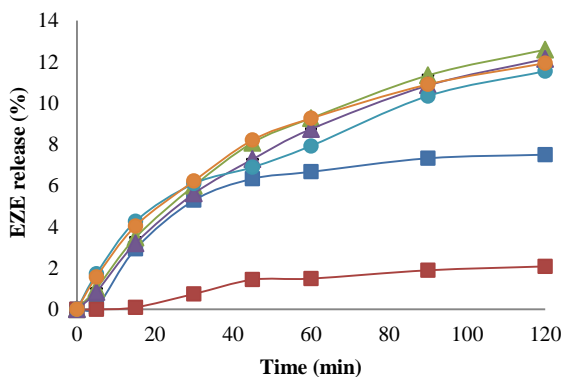
### 3.5 *IN VITRO* DISSOLUTION STUDIES

Samples submitted to dissolution studies were chosen based on their amorphous state. In this regard, samples ELG75/225 12.5:12.5:75 and ELG75/225 25:25:50 were evaluated by means of their *in vitro* performance and compared to the crystalline raw materials and coSD samples. Results are shown in Figure 24.

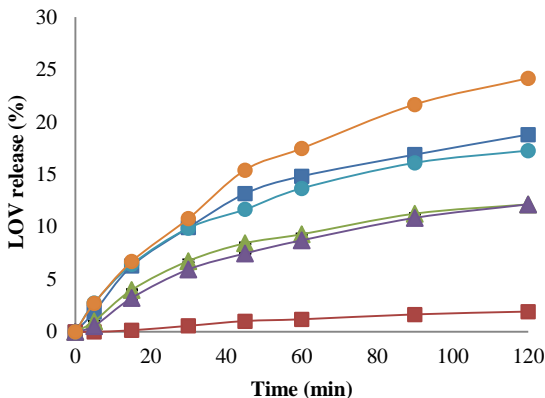
Unexpectedly, for both APIs the amorphous coSD sample presented a lower dissolution rate in comparison to the crystalline raw material, achieving a maximum of 2% release after 120 minutes. However, all the ternary milled systems presented a higher dissolution rate for EZE compared to raw material. For these samples, the type of gelatin and the composition of the samples did not play an important role in the dissolution rate since all the formulations presented similar dissolution profiles. At the end of the assay, an increase was observed in the dissolution rate of EZE in ternary samples of 1.7 and 6.0 times in comparison to the crystalline and coSD samples, respectively.

For LOV, the only ternary system able to increase the dissolution rate in comparison to the crystalline raw material was ELG225 25:25:50. This result was also unexpected, since usually an increased amount of the hydrophilic carrier tends to increase the dissolution rate of the poorly water-soluble API. The enhancement of the dissolution rate of this sample within 2 hours in comparison to the crystalline raw material and the coSD sample was of 1.3 and 12.7 times, respectively.

**Figure 24.** *In vitro* dissolution profiles of ternary ball milled systems ELG75 12.5:12.5:75 (▲), ELG225 12.5:12.5:75 (▲), ELG75 25:25:50 (●), ELG225 25:25:50 (●), compared to co-spray dried materials (■) and crystalline raw materials (■)



(to be continued)



#### 4. CONCLUSIONS

Ternary systems composed by EZE, LOV and two different types of gelatin were successfully obtained through ball milling. The milling procedure was optimized and parameters like rotation speed, milling time, number and combination of balls and amount of powder demonstrated an important role on the obtainment of amorphous ternary systems. Gelatin was necessary to provide amorphous materials, since pure drugs and binary combinations of EZE and LOV showed remaining crystallinity. In addition, mDSC analyses revealed a tendency of mixing between gelatin and the APIs in physical mixtures as observed by a shift of its glass transition temperature. However, all ternary samples were composed of two different phases. When classical polymers were added to ternary gelatin systems, two of them (Soluplus<sup>®</sup> and Kollidon<sup>®</sup> 30) were not able to generate amorphous samples. Dissolution studies demonstrated an increase in the dissolution rate of LOV only through the formulation ELG225 25:25:50, which was able to increase the dissolution rate 1.3 and 12.7 times in comparison to the crystalline raw material and co-spray dried sample, respectively. However, for EZE, all ternary systems enhanced its dissolution rate in comparison to the crystalline raw material and co-spray dried sample. These results emphasize the promising aspect of using gelatin in drug delivery systems composed of poorly water-soluble APIs.

## 5. REFERENCES

- BARZEGAR-JALALI, M.; VALIZADEH, H.; SHADBAD, M. S.; ADIBKIA, K.; MOHAMMADI, G.; FARA-HANI, A., et al. Cogrounding as an approach to enhance dissolution rate of a poorly water-soluble drug (glicazide). *Powder Technology*, v. 197, p. 150–158, 2010.
- BRÜNING, J.; ALIG, E.; SCHMIDT, M.U. Ezetimibe anhydrate, determined from laboratory powder diffraction data. **Acta Crystallographic C**, v. 66, p. o341-o344, 2010.
- CHONO, S.; TAKEDA, E.; SEKI, T.; MORIMOTO, K. Enhancement of the dissolution rate and gastrointestinal absorption of pranlukast as a model poorly water-soluble drug by grinding with gelatin. **International Journal of Pharmaceutics**, v. 347, p. 71-78, 2008.
- DUONSEILLE, A.; ASTRUC, T.; QUINTANA, N.; MEERSMAN, F.; SANTE-LHOUELLIER, V. Gelatin structure and composition linked to hard capsule dissolution: A review. **Food Hydrocolloids**, v. 43, p. 360-376, 2015.
- ELZOGHBY, A.O. Gelatin-based nanoparticles as drug and gene delivery systems: Reviewing three decades of research. **Journal of Controlled Release**, v. 172, p. 1075-1091, 2013.
- KALLINTERI, P.; ANTIMISIARIS, S.G. Solubility of drugs in presence of gelatin: effect of drug lipophilicity and degree of ionization. **International Journal of Pharmaceutics**, v. 221, p. 219-216, 2001.
- LI, D.X.; OH, Y.-K.; LIM, S.-J.; KIM, J.O.; YANG, H.J.; SUNG, J.H.; YONG, C.S.; CHOI, H.-G. Novel gelatin microcapsule with bioavailability enhancement of ibuprofen using spray-drying technique. **International Journal of Pharmaceutics**, v. 355, p. 277-284, 2008.
- RAVIKUMAR, K.; SRIDHAR, B. Ezetimibe monohydrate. **Acta Crystallographica Section E**, v. E61, p. o2907-2909, 2005.
- YOSHIDA, M.I.; OLIVEIRA, M.A.; GOMES, E.C.L.; MUSSEL, W.N.; CASTRO, W.V.; SOARES, C.D.V. Thermal characterization of lovastatin in pharmaceutical formulations. **Journal of Thermal Analysis and Calorimetry**, v. 106, p. 657-664, 2011.
- YOUSAF, A.M.; KIM, D.W.; KIM, J.K.; KIM, J.O.; YONG, C.S.; CHOI, H.-G. Novel fenofibrate-loaded gelatin microcapsules with enhanced

solubility and excellent flowability: Preparation and physicochemical characterization. **Powder Technology**, v. 275, p. 257-262, 2015.

## **CHAPTER IV**

### **DEVELOPMENT, CHARACTERIZATION AND *IN VITRO* DISSOLUTION STUDIES OF TERNARY AMORPHOUS SYSTEMS OF EZETIMIBE, LOVASTATIN AND DIFFERENT HYDROPHILIC POLYMERS PREPARED BY SPRAY DRYING**

---

## 1. INTRODUCTION

The application of solid dispersions as strategies to improve the solubility and dissolution rate of poorly water-soluble compounds was firstly introduced in 1961 by Sekiguchi and Obi (SEKIGUCHI e OBI, 1961). Since then, this type of formulation has been improved and widely investigated. Nowadays, solid dispersions can be classified according to their composition in binary and ternary systems, if composed by one lipophilic drug associated to one or two hydrophilic polymers, respectively.

Aiming to develop a formulation capable of increasing simultaneously the solubility and dissolution rate of ezetimibe (EZE) and lovastatin (LOV), co-amorphous systems were investigated as a first approach. However, as described in Chapter II, they were not able to reach the proposed goal and the obtained results proved that just the amorphous state is not enough to enhance the mentioned properties, especially for EZE.

In this way, the necessity to incorporate a third compound in the amorphous system of EZE and LOV was verified. Gelatin type 75 and 225 have also been investigated, in absence and presence of synthetic polymers (Chapter III). Although a slight increase in dissolution rate was observed, these systems have still not reached 100 % release of EZE and LOV in *in vitro* dissolution studies.

Based on that, this chapter aims to investigate the effect of the addition of different hydrophilic polymers to the amorphous system between EZE and LOV. It is also aimed here that the preparation method can decrease the particle size, in order to have a positive impact on the dissolution rate of the compounds. Spray drying consists of a continuous one-step process, especially known for the fast solvent evaporation, which usually generates small amorphous particles. Besides, the physical chemical properties of the resulting product, as particle size and shape, humidity content and powder flow properties can be controlled by this process (PAUDEL et al., 2013).

In this context, this chapter introduced for the first time the concept of ternary solid dispersions prepared by spray drying two poorly water-soluble compounds and one hydrophilic polymer. The selected polymers were polyvinyl caprolactam-polyvinyl acetate-polyethylene glycol graft copolymer (Soluplus®), poly(vinylpyrrolidone-co-vinyl



acetate) (PVP VA64), polyvinylpyrrolidone (PVP K-30) and hydroxypropylmethyl cellulose (HPMC E5). The obtainment of single amorphous phase systems with intermolecular interactions (e.g hydrogen bonding) was targeted, in order to guarantee a better physical stability of the formulation. Variables such as type of polymer, drug:drug ratio, drugs:polymer ratio and addition of surfactants were investigated to reach the formulation with the desired properties.

## 2. EXPERIMENTAL

### 2.1 MATERIALS

EZE (anhydrous, 409.41 g/mol) and LOV (404.54 g/mol) were purchased from Pharma Nostra (Rio de Janeiro, Brazil) with batch numbers FM017H13 and 130312, respectively. Polyvinyl caprolactam-polyvinyl acetate-polyethylene glycol graft copolymer (Soluplus®), poly(vinylpyrrolidone-co-vinyl acetate) (PVP VA64) and polyvinylpyrrolidone (PVP K-30) were obtained from BASF® ChemTrade GmbH (Ludwigshafen, Germany), and hydroxypropylmethyl cellulose (HPMC E5) was obtained from Federa (Rotterdam, The Netherlands). Cremophor RH40® was obtained from BASF® (Ludwigshafen Rhine, Germany), Gelucire 44/14® from Gattefossé SAS (Saint Priest, France), Tween 80® from Fagron SAS (Waregem, Belgium), Tween 20® from Applichem GmbH (Darmstadt, Germany) and Vitamine E TPGS® from ISOchem (Gennevilliers, France). In all experiments de-ionized water (Maxima Ultra Pure Water, Elga Ltd., Wycombe, England) was used and the organic solvents were of pharmaceutical grade.

### 2.2 PREPARATION OF SPRAY DRIED SAMPLES

The spray-dried powders were obtained using a Buchi mini spray-dryer B191 (Buchi, Flawil, Switzerland). Briefly, an accurate amount of drugs and polymers, in which the total solid content was kept at 10% (w/v), was dissolved in methanol (MeOH) for formulations composed of Soluplus, PVP K30 and PVP VA64, and in a mixture of methanol:dichloromethane (DCM) (1:1, v/v) for HPMC E5. The co-spray

dried sample (EZE:LOVsd), composed exclusively of EZE:LOV (1:1, w/w), was prepared from a 2% solid content solution in MeOH:DCM (1:1, v/v) mixture and the pure APIs were dissolved in MeOH (EZEsol) and MeOH:DCM (1:1, v/v) (LOVsd), comprising a solution with 5% solid content. The composition of all samples is shown in Table 3. The ratios between the APIs were chosen based on their doses of administration and the percentage of the surfactants Tween 20, Tween 80, Cremophor RH40, Gelucire 44/14 and Vitamin E TPGS (d-alpha tocopheryl polyethylene glycol 1000 succinate) (TPGS) was kept at 5%. By means of comparison, binary solid dispersions composed of one of the APIs and Soluplus were also prepared.

**Table 3.** Composition of spray dried samples

Formulation	EZE:LOV (m/m)	Polymer (%)	Surfactant (%)
EZE:LOVsd	1:1	-	-
ELPVPK30	1:1	75	-
ELPVPVA	1:1	75	-
ELHPMC	1:1	75	-
<i>Ternary solid dispersions prepared with Soluplus®</i>			
ELS 1:1 50%	1:1	50	-
ELS 1:1 75%	1:1	75	-
ELS 1:1 90%	1:1	90	-
ELS 1:2 50%	1:2	50	-
ELS 1:2 75%	1:2	75	-
ELS 1:2 90%	1:2	90	-
ELS 1:4 50%	1:4	50	-
ELS 1:4 75%	1:4	75	-
ELS 1:4 90%	1:4	90	-
ELS Tween20	1:1	75	5
ELS Tween80	1:1	75	5
ELS Cremophor	1:1	75	5
ELS Gelucire	1:1	75	5
ELS TPGS	1:1	75	5
<i>Binary solid dispersions prepared with Soluplus®</i>			
EZESol	-	75	-
LOVSol	-	75	-

The solutions were spray dried using the following operational conditions: inlet temperature 65°C or 50°C for DCM:MeOH and MeOH, respectively, drying air flow rate 28 l/min, atomizing air flow 15 l/min and 5.5 to 7 ml/min feed rate. All spray dried samples were further post-dried in a vacuum oven at room temperature for at least 3 days to remove the residual solvent prior to analysis.

## 2.3 X-RAY POWDER DIFFRACTION (XRPD)

XRD experiments were carried out at room temperature using an automated X'pert PRO diffractometer (PANalytical, Almelo, The Netherlands) with a Cu tube ( $K\alpha \lambda = 1.5418 \text{ \AA}$ ) and the generator was set at 45 kV and 40 mA. EZE and LOV raw materials were applied on spinning zero background sample holders. Measurements were performed in a continuous scan mode from 4° to 40° with 0.0167° step size and 200 s per step counting time.

Co-amorphous samples were analyzed under the same conditions but using regular sample holders. The samples were prepared and analyzed in DSC sample holders in a continuous scan mode from 4° to 35°.

## 2.4 MODULATED DIFFERENTIAL SCANNING CALORIMETRY (mDSC)

mDSC analyses were performed on a Q2000 DSC (TA instruments, Leatherhead, UK), equipped with a refrigerated cooling system (RCS90) accessory) under a dry nitrogen purge at a flow rate of 50 ml/min. Indium standard was used for routine calibration (temperature, enthalpy), sapphire disk was used for heat capacity calibration. Approximately 5 mg samples were weighed using an analytical balance into aluminium pans with aluminium lids. The samples were scanned at 2°C/min from -10°C to 190°C (isothermal for 5 min) with an amplitude of 0.636°C and a period of 40 s. DSC thermograms were acquired and analyzed using Universal Analysis software (version 4.4, TA instruments, Leatherhead, UK). All samples were analyzed in duplicate.

## 2.5 ATTENUATED TOTAL REFLECTANCE FOURIER TRANSFORM INFRARED (FTIR) SPECTROSCOPY

FTIR spectra were acquired on a Vertex 70 spectrometer (Bruker, Billerica, USA), at room temperature, from 4000 to 400  $\text{cm}^{-1}$ , with the collection of 32 scans. Samples were analyzed as such.

## 2.6 SCANNING ELECTRON MICROSCOPY (SEM)

SEM pictures were recorded using a Phillips XL30 SEM-FEG (Philips, Eindhoven, The Netherlands) equipped with a Schottky field-emission electron gun. A beam of 15 kV was used and detection was performed using a conventional Everhart-Thornley secondary electron detector. The samples were affixed onto an aluminum stub with a double-sided adhesive carbon tape, and then coated with platinum under vacuum using a sputtering device (Balzers Union, Liechtenstein) before imaging.

## 2.7 PARTICLE SIZE MEASUREMENT

The particle size distribution of the spray dried formulations was measured by laser diffraction using a Mastersizer 2000 equipment (Malvern Instruments Ltd, Malvern, UK) coupled to the dry sample dispersion unit Scirocco 2000. The dried powder samples were placed at the dispersion unit, fed to the equipment with a vibration feed rate of 35% and dispersed with an air pressure of 4 bar.

## 2.8 EQUILIBRIUM SOLUBILITY MEASUREMENTS

The equilibrium solubility of EZE, LOV, and the binary physical mixtures of EZE:LOV (1:1, w/w) were determined in acetate buffer pH  $4.5 \pm 0.025$  of sodium lauryl sulfate (SLS), as well as in pre-dissolved Soluplus solutions ( $n = 3$ ). In glass test tubes, an excessive amount of pure EZE, LOV and the binary mixtures were added into 5 ml of the above media and the samples were kept for 48 hours in a rotary mixer (L26

Labinco BV, Breda, The Netherlands). After that, 1 ml of the supernatant was filtered through a PTFE membrane with 0.45 µm pore size (Grace Davison Discovery Science, Illinois, USA).

The content of EZE and LOV dissolved in the filtrate was determined by using isocratic HPLC analysis (Merk-Hitachi LaChrom system). The experiments were conducted on a reversed-phase Chromolith® Performance C18 column (100 x 4.6 mm i.d., 5 µm pore size). The mobile phase was made up of acetonitrile:water (50:50 v/v), with a flow rate of 1.0 ml/min, at room temperature. The UV detection was performed at 235 nm. 20 µl of samples was injected and the data acquisition was performed using Merck LaChrom D-7000 System Manager software (see Appendix).

The statistical analysis of the data was conducted in GraphPad Prism 6 software through one-way ANOVA followed by Tukey test, in which significant results present a probability lower than 5% ( $p < 0.05$  with a 95% confidence interval).

## 2.9 *IN VITRO* DISSOLUTION STUDIES

Dissolution profiles were obtained under non-sink conditions using a SR8PLUS dissolution station (SpectraLab Scientific Inc., Markham, Canada). For solid dispersions, an accurate amount of spray dried sample, equivalent to 10 mg EZE and/or 10 mg LOV, was evaluated in 500 ml of acetate buffer solution pH 4.5 with 0.025% of SLS, at 37°C. The solution was stirred with paddle apparatus II at a speed of 100 rpm. Samples were taken at different time intervals, filtered using a PTFE filter (pore size 0.45 µm) and immediately replaced with the same volume of fresh dissolution medium. The obtained dissolution profiles were evaluated by means of their dissolution efficiency (DE, Equation 5). For this purpose, the area under the dissolution curve (AUC) at time  $t$  was calculated and expressed as the percentage of the rectangular area described by 100% of dissolution within the same period. The area under the curve was determined using the software Graph Pad Prism 6.

$$DE (\%) = \frac{AUC_{0-60 \text{ min}}}{AUC_{TOTAL}} \times 100 \quad \text{Equation 5}$$

The content of EZE and LOV dissolved in the filtrate was determined as described in topic 2.8.

The 'in vitro' profiles were compared applying one-way ANOVA followed by Tukey test Results were considered statistically significantly different if  $p < 0.05$ . The data were processed in Graph Pad Prism 6 software.

## 2.10 STABILITY STUDIES

The sample ELS 1:1 75% was stored in desiccators and exposed to different conditions (40°C/0% RH, 40°C/75% RH and 4°C/0% RH) during 1 year. The conditions regarding 0% and 75% RH were achieved with phosphorous pentoxide and NaCl saturated solution, respectively. The stability of the samples was evaluated by means of XRD and 'in vitro' dissolution studies.

## 3. RESULTS AND DISCUSSION

Initially, by means of comparison, both APIs were spray dried separately (EZEsd, LOVsd) and in combination (EZE:LOVsd). As it can be seen in the Figure 25A, EZEsd was completely amorphous after the spray drying process, as well as EZE:LOVsd. On the other hand, LOVsd was still highly crystalline. Dissolution testing of EZEsd, LOVsd and EZE:LOVsd were performed in acetate buffer pH 4.5 + 0.025% of SLS. Very low percentages of release were observed for EZE from EZEsd ( $1.3\% \pm 0.9$ ) and EZE:LOVsd ( $2.0\% \pm 0.2$ ) after 120 min. Similar results were observed for LOV with  $16.0\% \pm 0.5$  and  $2.4\% \pm 0.2$  of release for LOVsd and EZE:LOVsd, respectively.

Based on these poor dissolution characteristics, different hydrophilic polymers (HPMC, PVP K-30, PVP VA-64 and Soluplus) were combined to EZE and LOV, comprising the novel spray dried ternary solid dispersions. Solid-state characterization through XRD showed that all formulations were completely x-ray amorphous (Figure 25B). mDSC analysis revealed single phase systems for samples composed of PVP K-30 and PVP VA-64 with  $T_g$  values at 131.5 and 96.3 °C, respectively. Formulations prepared with Soluplus and HPMC E5

showed two amorphous phases with  $T_g$  values at 59.9/92.4°C and 91.4/150.5°C, respectively (Figure 26).

**Figure 25.** XRPD data regarding spray dried (A) raw materials isolated (EZEsd;LOVsd) and in combination (EZE:LOVsd), and (B) ternary solid dispersions with different hydrophilic polymers

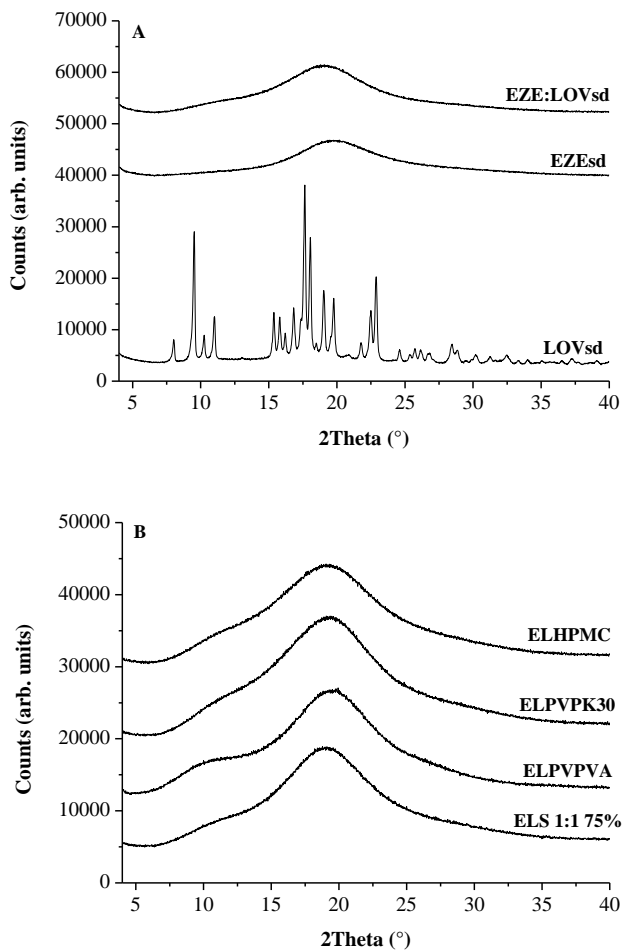
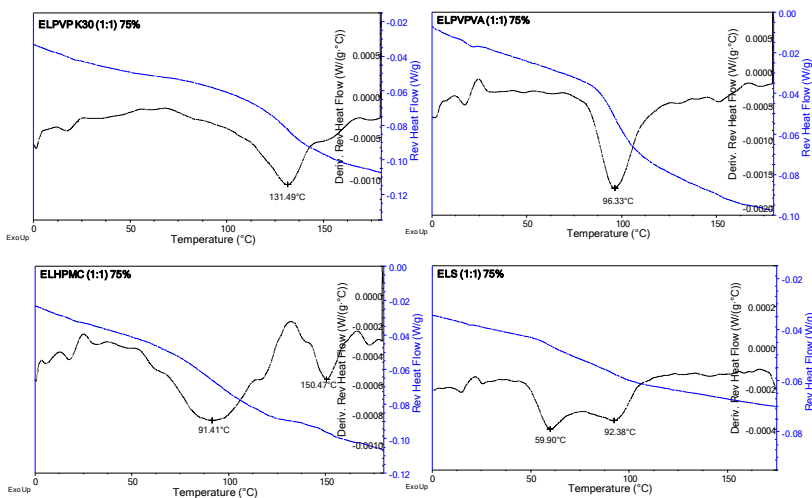


**Figure 26.** mDSC data for ternary solid dispersions composed of different hydrophilic polymers. Blue and black curves correspond to the reversing heat flow and its derivative, respectively. The peak temperatures of each glass transition event is shown in °C

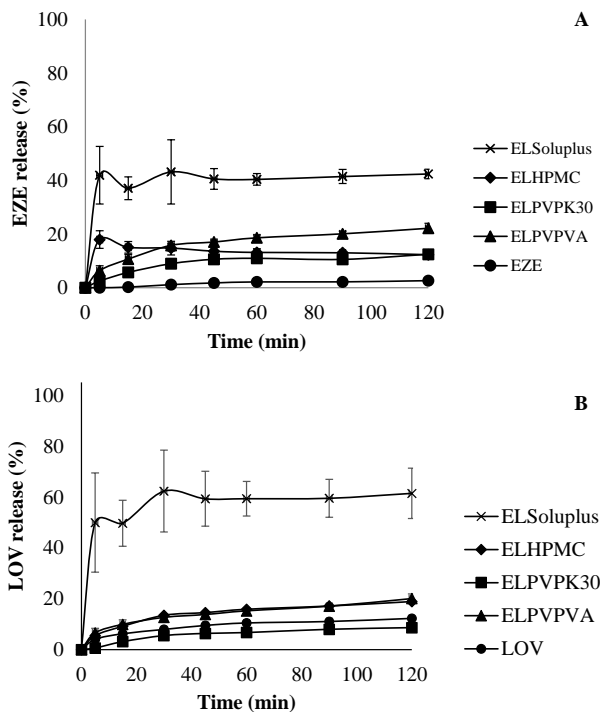


The dissolution profiles of the ternary solid dispersions were compared to those of the crystalline raw materials as depicted in Figure 27. For EZE, all the solid dispersions were able to increase the dissolution rate of the API, which dissolved to ca. 2.6% in 120 min, versus 12.5% (ELPVPK30), 12.3% (ELHPMC), 22.2% (ELPVPVA) and 42.4% (ELSoplus). On the other hand, for LOV, ELPVPK30 showed a slightly lower release (8.6%) when compared to the crystalline raw material (12.3%). Other ternary solid dispersions showed higher percentages of release of 18.9% (ELHPMC), 20.1% (ELPVPVA) and 61.4% (ELS 1:1 75%).

For both APIs, Soluplus showed the best dissolution characteristics. This polymer is known for providing solubility enhancement by its amphiphilic structure, but also offers the feasibility of forming solid solutions with poorly soluble drugs (LINN et al., 2012).



**Figure 27.** (A) EZE and (B) LOV release profiles from ternary solid dispersions compared to their respective crystalline raw materials



First of all, in order to prove the need for ternary solid dispersions, instead of a physical mixture of two binary formulations, binary solid dispersions composed of EZE or LOV with 75% of Soluplus were prepared. Firstly, the equilibrium solubility of both APIs from these formulations was determined and compared to that from the ternary systems. After 48 hours, EZE achieved  $1.6 \pm 0.1$   $\mu\text{g/ml}$  in ES 75%, whilst in the ternary formulation with the same amount of polymer (ELS 1:1 75%) the equilibrium solubility reached  $3.1 \pm 0.1$   $\mu\text{g/ml}$ . For LOV, these values were  $1.9 \pm 0.2$  and  $2.7 \pm 0.1$   $\mu\text{g/ml}$  for binary and ternary systems, respectively. Equilibrium solubility data for all the ternary solid dispersions are shown in Table 4. For EZE, the solubility tends to be higher as the amount of polymer and LOV increases. ELS 1:4 90% reaches a solubility up to  $26.1 \pm 0.9$   $\mu\text{g/ml}$ , which corresponds to an increase of more than 27 times when compared to the crystalline raw

material. On the other hand, the equilibrium solubility of LOV was not influenced by the amount of polymer.

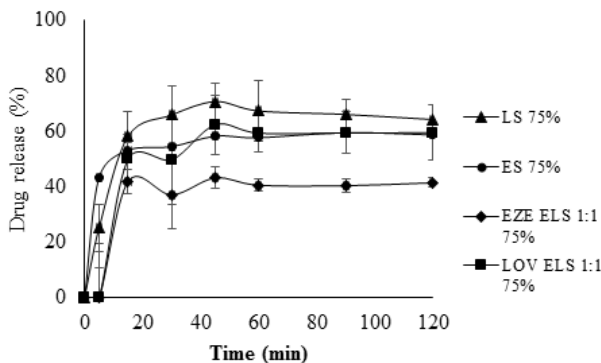
**Table 4.** Equilibrium solubility data in acetate buffer pH 4.5 + 0.025% SLS after 48 h

Sample	EZE	LOV
	$\mu\text{g/mL} \pm \text{SD}$	
ES 50%	$1.0 \pm 0.1$	-
LS 50%	-	$2.0 \pm 0.3$
ES 75%	$1.6 \pm 0.1$	-
LS 75%	-	$1.9 \pm 0.2$
ES 90%	$4.7 \pm 0.1$	-
LS 90%	-	$2.2 \pm 0.2$
ELS 1:1 50%	$1.3 \pm 0.1$	$2.4 \pm 0.2$
ELS 1:1 75%	$3.1 \pm 0.1$	$2.7 \pm 0.1$
ELS 1:1 90%	$9.7 \pm 0.1$	$3.9 \pm 0.2$
ELS 1:2 50%	$1.9 \pm 0.1$	$2.0 \pm 0.1$
ELS 1:2 75%	$3.7 \pm 0.1$	$2.2 \pm 0.1$
ELS 1:2 90%	$15.9 \pm 0.2$	$2.8 \pm 0.2$
ELS 1:4 50%	$3.0 \pm 0.1$	$1.7 \pm 0.1$
ELS 1:4 75%	$7.4 \pm 0.1$	$2.1 \pm 0.1$
ELS 1:4 90%	$26.1 \pm 0.9$	$3.3 \pm 0.2$

Dissolution studies were, in combination with equilibrium solubility, also useful to compare binary and ternary solid dispersions (Figure 28). Although the dissolution profiles of the binary solid dispersions seem to be slightly higher in comparison to the ternary one (ELS 1:1 75%), no significant difference was observed among the three formulations ( $p \leq 0.05$ ). This is another proof that the APIs do not influence their mutual dissolution rate. In addition, this can be considered advantageous for ternary systems, since the same release is achieved with a single step process, instead of a two-step process and a further powder blending step, if compared to a physical mixture of binary solid dispersions composing a FDC. These data clearly show the advantage of a ternary solid dispersion compared to a binary system. Soluplus was selected for more detailed investigation by applying different API:API ratios (1:1 to 1:4, related to the dose of EZE and LOV; 10 and 10, 20 and 40 mg, respectively), APIs:polymer ratios (from 50:50 to 10:90), and

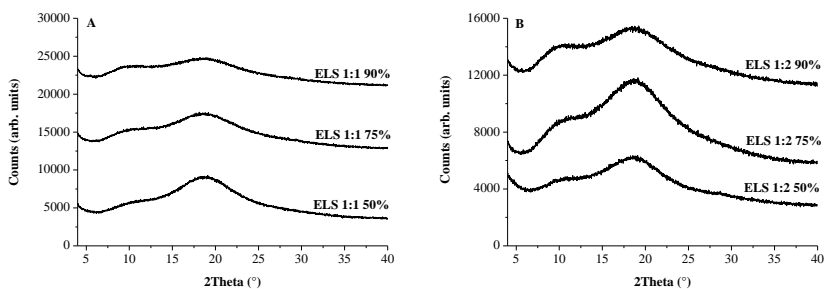
adding surfactants, in an attempt to increase the wettability and the dissolution rate of the APIs.

**Figure 28.** Dissolution profiles of binary (LS 75% and ES 75%) versus the ternary solid dispersion ELS 1:1 75%

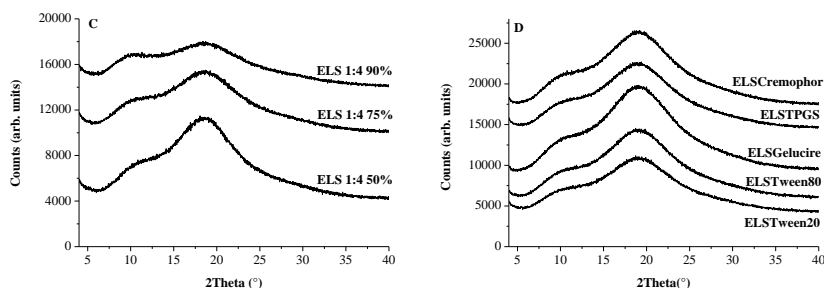


Firstly, as can be seen in Figure 29, spray drying is a successful technique to obtain x-ray amorphous ternary solid dispersions, independent on their composition.

**Figure 29.** XRD data relative to ternary solid dispersions composed of Soluplus with (A) 1:1, (B) 1:2 and (C) 1:4 EZE:LOV ratios, and (D) in presence of surfactants



(to be continued)



However, the number of amorphous phases varied among the formulations (Table 5). Single phase amorphous systems were observed with lower ratios of polymer, indicating a better miscibility among the three components. In addition, similar  $T_g$  values were observed among these samples, which ranged from 55.8 to 57.9°C. As the amount of Soluplus increases to 75 and 90%, a second  $T_g$  is observed at higher temperatures, ranging from 70.4 to 100.5°C.

**Table 5.** mDSC data of ternary solid dispersions

Sample	Melting Point	Glass Transition Temperature ( $T_g$ )			
		Number	Onset (°C)	Peak (°C)	Endset (°C)
ELS 1:1 50%	No	1	51.6	56.9	74.3
ELS 1:1 75%	No	2	50.1	59.9	64.0
			78.8	92.4	93.9
ELS 1:1 90%	No	2	55.8	62.3	70.4
			90.4	100.5	108.2
ELS 1:2 50%	No	1	51.1	57.9	73.1
ELS 1:2 75%	No	2	52.2	57.2	63.0
			83.3	84.2	91.4
ELS 1:2 90%	No	2	54.6	65.5	71.4
			86.4	89.8	99.8
ELS 1:4 50%	No	1	47.5	55.8	70.1
ELS 1:4 75%	No	2	52.6	57.5	64.7
			80.5	83.0	94.1
ELS 1:4 90%	No	2	57.3	72.0	73.6
			95.6	96.8	103.5
ELSTween20	No	2	49.6	53.6	56.2
			72.5	73.7	83.4

ELSTween80	No	2	51.8	58.0	59.0
			70.2	70.4	85.0
ELSCremophor®	No	2	51.1	58.0	59.0
			76.2	77.0	88.1
ELSGelucire®	No	1	55.1	69.6	84.3
ELSTPGS	No	2	48.6	56.0	62.2
			74.2	75.9	88.1

FTIR analysis was carried out to investigate possible intermolecular interactions between the APIs and the polymer. Table 6 summarizes the FTIR data for the ternary solid dispersions. Spectra corresponding to ternary solid dispersions with 1:1 API:API ratios are found in Figure 30.

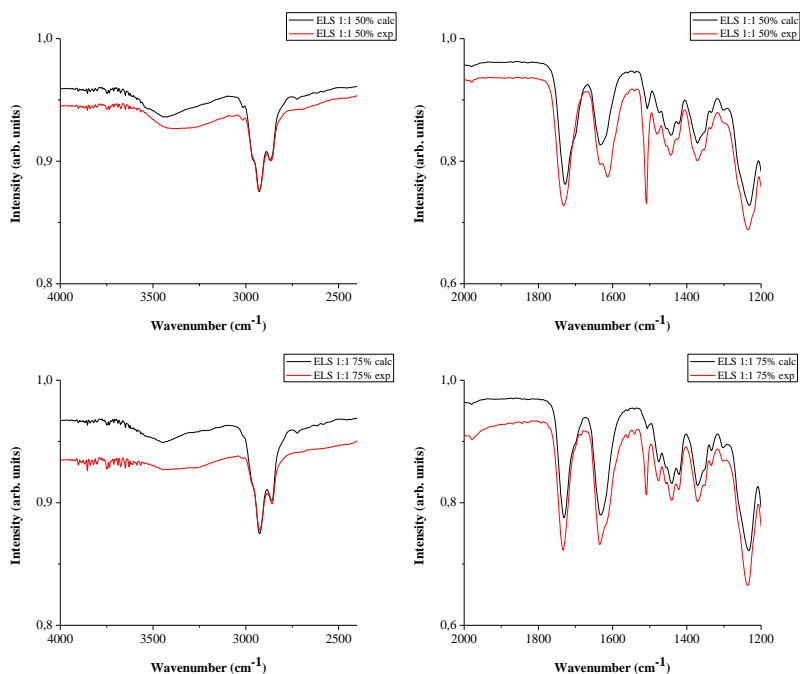
**Table 6.** Experimental and calculated FTIR data of ternary solid dispersions with Soluplus

Sample	O-H band (cm <sup>-1</sup> )		C=O band (cm <sup>-1</sup> )	
	Calculated	Experimental	Calculated	Experimental
1:1 50%	3433	3338	1727/1633	1733/1635
1:2 50%	3441	3341	1726/1630	1730/1637
1:4 50%	3446	3350	1726/1631	1728/1635
1:1 75%	3449	3356	1730/1631	1734/1634
1:2 75%	3451	3351	1729/1630	1733/1634
1:4 75%	3447	3355	1730/1631	1732/1633
1:1 90%	3450	3444	1731/1630	1733/1634
1:2 90%	3449	3441	1731/1631	1733/1633
1:4 90%	3448	3442	1730/1630	1732/1635
Cremophor	3450	3360	1729/1631	1732/1634
Gelucire	3446	3355	1729/1631	1733/1634
TPGS	3449	3345	1730/1631	1732/1633
Tween20	3447	3348	1730/1631	1732/1634
Tween80	3446	3367	1730/1631	1733/1633

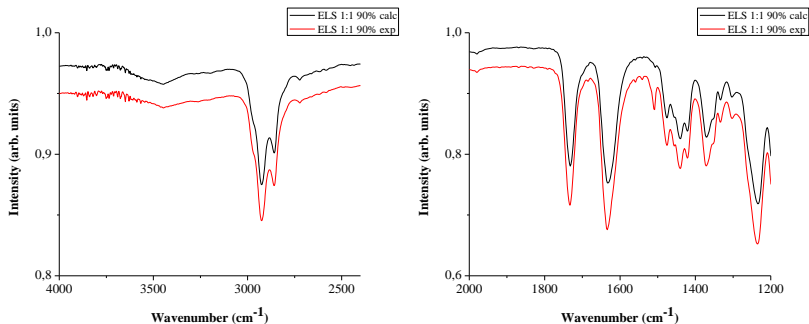
As discussed previously, EZE and LOV present potential sites for hydrogen bonding. The Soluplus spectrum shows intermolecularly hydrogen bonded O-H stretching at 3448 cm<sup>-1</sup>, vinyl acetate monomer ester stretching at 1733 cm<sup>-1</sup> and vinyl caprolactam monomer C=O

stretching at  $1633\text{ cm}^{-1}$  (data not shown), in agreement with previously reported data (LIN et al., 2015). As both bands of interest are present in the spectra of the two APIs and Soluplus, the FTIR data of the formulations were compared to the amorphous physical mixtures of the three components, in order to facilitate the data analysis (Figure 30). Bands indicative of interactions among drugs and the polymer, which include the hydrogen bonding acceptor C=O stretching and the hydrogen bond donor O–H stretching, presented significant shifts in all formulations. In addition, a broadening of the O–H band was also noted. Based on that, it can be concluded that intermolecular hydrogen bonds were established. Samples presenting different API:API ratios but the same amount of polymer showed similar FTIR spectra, as well as samples with surfactants and ELS 1:1 75%.

**Figure 30.** Experimental and calculated ATR data for ternary solid dispersions with Soluplus composed of 1:1 API:API ratio and different polymer concentrations (50, 75 and 90%)



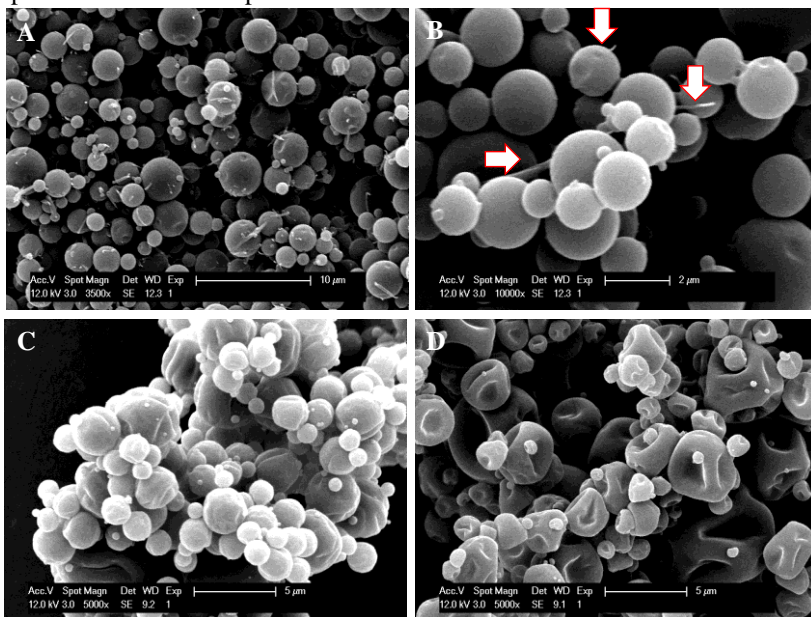
(to be continued)



SEM micrographs of the ternary solid dispersions were compared with EZE:LOVsd to evaluate the influence of the polymer on the morphology of the particles. As can be seen in Figure 31, the spray dried particles are spherical and show a heterogeneous particle size distribution. EZE:LOVsd present a smooth surface on which some needle shape-like crystals can be observed. This can most likely be associated with the low solubility of the compounds in the solvents chosen. Although both EZE and LOV are poorly water-soluble compounds, their solubility in organic solvents is distinct and finding a suitable solvent mixture combined to an adequate feed concentration was challenging. The average particle size for this sample is 3.16  $\mu\text{m}$  (D[4,3]). When in presence of polymer, the crystals disappear and the surface of the particles shows indentations which tend to increase in presence of higher amounts of Soluplus. Basically, the ternary solid dispersions showed bigger, but similar mean particle sizes which ranged from 5.4  $\mu\text{m}$  (ELS 1:4 90%) to 7.7  $\mu\text{m}$  (D[4,3]) (ELS 1:1 90%). These results can be explained by the different feed concentrations between EZE:LOVsd (2%) and the ternary solid dispersions (10%). It is well known that the feed concentration is directly proportional to the mean diameter of spray dried particles (MEEUS et al., 2015). In addition, more concentrated feed solutions tend to generate hollow particles with rough surface, higher porosity and lower bulk density (VAN GYSEGHEM et al., 2009; LITTRINGER et al., 2012). Besides, the wrinkled morphology of the ternary solid dispersions can also be attributed to the high solubility of the polymer in methanol. Further evaporation of the solvent from the core of the droplets leads to shell folding and wrinkled morphology. Also, as methanol requires low quantities of thermal energy for vaporization, due to its low boiling point, the solidification point will be reached faster, resulting in an increase in void volume and porosity (POKHARKAR et al., 2006; RIZI et al., 2011).

Formulations prepared with surfactants led to bigger mean particle sizes ranging from 9.47  $\mu\text{m}$  (ELSTween80) to 17.43  $\mu\text{m}$  (D[4,3]) (ELSCremophor).

**Figure 31.** SEM micrographs of (A) EZE:LOVsd (3500x), (B) EZE:LOVsd (10000x), (C) ELS 1:2 50% (5000x) and (D) ELS 1:2 90% (5000x). The arrows in B indicate the presence of crystalline needles on the surface of the spherical EZE:LOVsd particles



‘In vitro’ dissolution studies demonstrate that for the first time reported a spray dried ternary solid dispersion is able to increase the dissolution rate of two poorly water-soluble APIs simultaneously. Ternary solid dispersions composed of Soluplus demonstrated enhanced dissolution properties as the amount of polymer increased (Table 7). Very low release profiles were observed in presence of 50% of polymer for both APIs. As the amount of Soluplus increased to 75%, ELS 1:4 75% for example, achieved  $88.7\% \pm 2.0$  and  $70.0\% \pm 5.2$  for EZE and LOV, respectively, at 120 min. The fastest dissolution rate for both APIs was observed for ELS (1:1) 90%, in which  $92.5\% \pm 6.2$  of EZE and  $83.7\% \pm 7.6$  of LOV were released in 5 min (Figure 32). This formulation presented an increase in the dissolution efficiency of almost 18 and 6 times for EZE and LOV, respectively, when compared to the crystalline



raw materials. Although 90% can be considered a high amount of polymer, the low doses of both compounds still make the development of a formulation feasible. In addition, this ternary solid dispersion is advantageous compared to the ones with 1:2 and 1:4 EZE:LOV (w/w) ratios. In this case, the dose of the statin can be decreased, which is ideal concerning its side effects and influence on the development of type 2 diabetes in hypercholesterolemic patients (CEDERBERG et al., 2015). Importantly, Soluplus was able to maintain the supersaturation of both APIs during the dissolution test for all formulations. The ratios between the APIs did not have a clear influence on the release profiles. For the samples composed of surfactants, no significant increase in the dissolution rate of EZE and LOV was observed when they were compared to ELS (1:1) 75% (Figure 33). A similar finding was reported for solid dispersions of EZE, hydroxypropylcellulose and Tween 80. The polymer had an important influence of the solubility and dissolution rate of the API, while no significant difference was observed with the addition of the surfactant (RASHID et al., 2015).

**Table 7.** Percentage of dissolution (% D) at 120 min and dissolution efficiency (DE) data

Sample	EZE	LOV		
	%D $\pm$ SD	DE (%)	%D $\pm$ SD	DE (%)
Raw material	2.6 $\pm$ 0.2	5.5	12.3 $\pm$ 0.6	14.5
ELS 1:1 50%	18.4 $\pm$ 5.7	16.4	28.3 $\pm$ 5.8	22.3
ELS 1:1 75%	42.4 $\pm$ 1.8	40.2	61.4 $\pm$ 6.8	57.2
ELS 1:1 90%	97.5 $\pm$ 0.6	98.9	85.2 $\pm$ 2.7	84.9
ELS 1:2 50%	15.3 $\pm$ 3.8	10.7	15.3 $\pm$ 3.2	11.3
ELS 1:2 75%	44.5 $\pm$ 1.5	46.8	45.7 $\pm$ 1.9	39.8
ELS 1:2 90%	98.6 $\pm$ 5.0	90.7	59.4 $\pm$ 2.7	56.3
ELS 1:4 50%	17.1 $\pm$ 1.3	12.2	13.3 $\pm$ 2.6	10.0
ELS 1:4 75%	88.7 $\pm$ 2.0	82.3	70.0 $\pm$ 5.2	69.0
ELS 1:4 90%	103.8 $\pm$ 0.9	101.0	73.2 $\pm$ 1.8	71.4
ELS Tween 20	36.5 $\pm$ 0.4	43.9	55.6 $\pm$ 3.6	53.6
ELS Tween 80	37.0 $\pm$ 0.4	42.3	59.4 $\pm$ 1.6	58.8
ELSCremophor®	54.7 $\pm$ 4.0	47.0	67.1 $\pm$ 3.8	64.1
ELSGelucire®	41.5 $\pm$ 5.0	39.8	57.1 $\pm$ 4.4	53.0
ELS TPGS	41.5 $\pm$ 0.3	40.6	64.2 $\pm$ 0.9	62.9

**Figure 32.** Dissolution profiles of EZE and LOV in the ternary solid dispersion ELS 1:1 90% compared to their respective crystalline raw materials

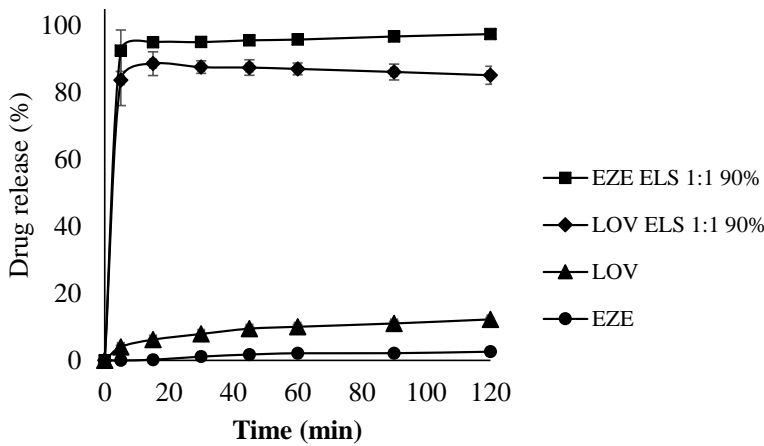
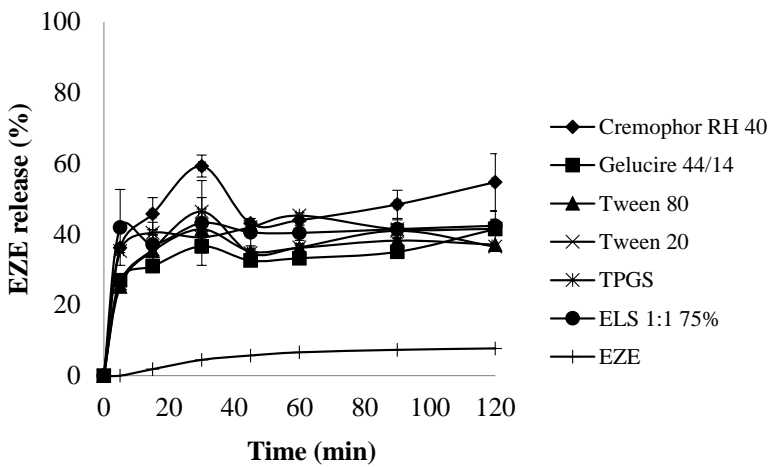
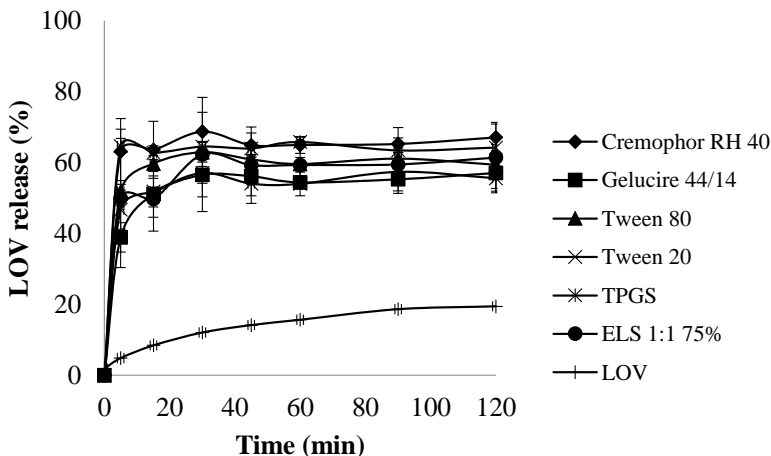


**Figure 33.** ‘In vitro’ dissolution data for (A) EZE and (B) LOV regarding ternary solid dispersions composed of surfactants



(to be continued)



Stability assays conducted during 1 year in different storage conditions were studied through XRD and ‘in vitro’ dissolution analyses (Figures 34 and 35). ELS 1:1 75% was selected for stability investigation due to its intermediate dissolution performance. Hence, changes (positive or negative) during the study could be more easily visualized. After 6 months, it was noted that temperature did not have an influence on the stability of samples in dry conditions. Samples kept at these conditions remained amorphous. On the other hand, at high relative humidity (75%), a drastic decrease in the dissolution performance was found for EZE and LOV, although this sample remained x-ray amorphous. In this case, a possible phase demixing between the APIs and the polymer could have happened, jeopardizing drug release.

After 1 year storage, EZE and LOV could not be detected in dissolution studies at 40°C/75% RH. In addition, within the same timeframe, a significant decrease in dissolution percentage was also observed for samples kept at 40°C/0% RH. These results demonstrate that for these samples drastic temperature conditions must be avoided. On the other hand, samples kept at 4°C/0% RH remained amorphous and showed no statistical difference regarding their dissolution profile compared to time zero.

**Figure 34.** XRD data for ELS 1:1 75% at time zero (T0) and after 1 year exposed to different stability conditions

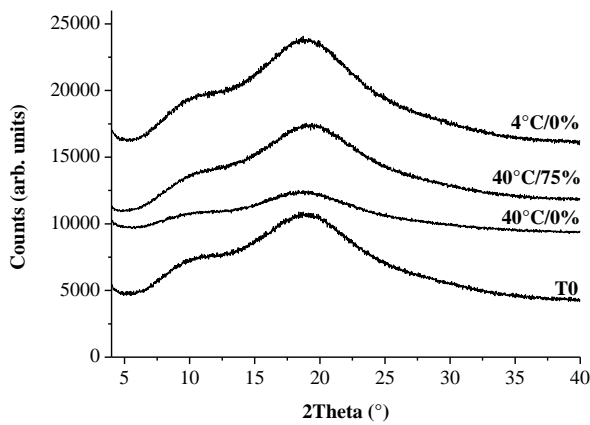
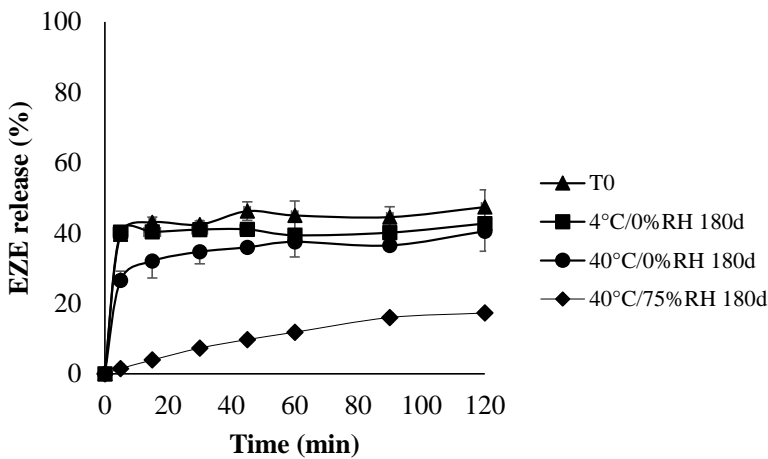
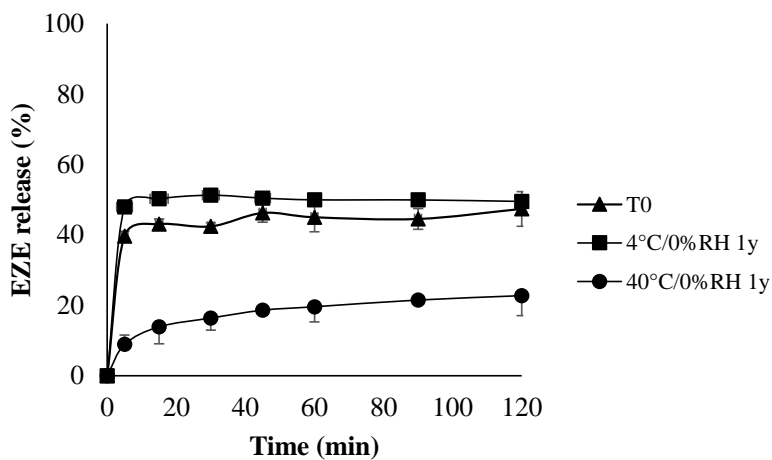
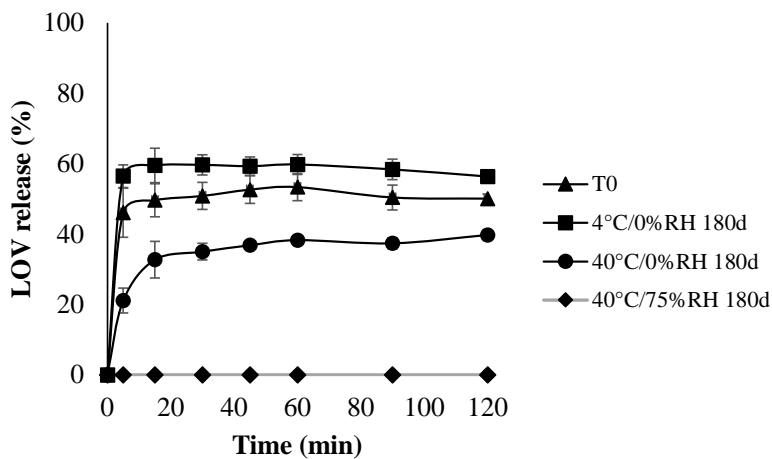


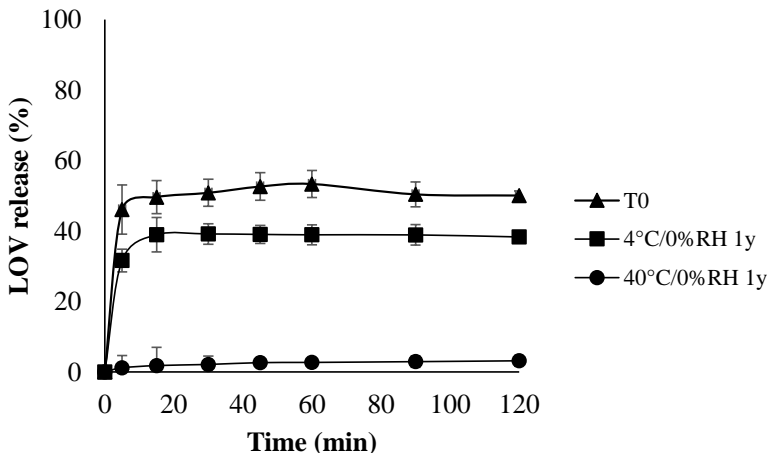
**Figure 35.** ‘In vitro’ dissolution profiles of ELS 1:1 75% at time zero (T0), after 180 days (180d) and after 1 year (1y) exposed to different stability conditions



(to be continued)



(to be continued)



Lower dissolution rates observed for samples kept at 40°C/75% RH were also observed for solid dispersions composed of cinarizine and Soluplus. Samples under stress conditions showed a reduced dissolution and a crystallization of the drug with an increased crystallinity in the order of 40°C/75% RH, >60°C/0% RH, >25°C/94% RH, >40°C/0% RH, >25°C/75% RH. In addition, although still amorphous, samples stored at 25°C showed a decrease in their dissolution rate. According to the authors, the change in  $T_g$  values could be pointed as a possible explanation for this behavior (TIAN et al., 2014). Decreased dissolution during stability studies at high temperature and humidity were also described for solid dispersions of piroxicam and Soluplus. The samples remained amorphous under dry conditions (0% RH/6°C and 0% RH/25°C) and crystallization was observed at 40% RH/25°C and 75% RH/25°C. A decrease in the dissolution profile was noted already after the first week for the sample at 75% RH/25°C and increased over time up to 6 months (LUST et al., 2015).

#### 4. CONCLUSIONS

This chapter describes for the first time enhanced dissolution characteristics of two poorly water-soluble compounds from a single spray dried ternary solid dispersion. Due to their physical chemical properties and therapeutically relevant association, EZE and LOV were selected as model compounds in a fixed dose combination. Equilibrium

solubility data proved the feasibility of this combination, since the APIs did not influence their mutual solubility. Based on the failure of co-amorphous systems and gelatin to improve the dissolution rate of EZE and LOV, different hydrophilic polymers were investigated to compose the novel ternary solid dispersions. Among them, Soluplus showed the best performance and all the spray dried ternary solid dispersions prepared with this polymer enhanced the dissolution rate of the APIs. The advantages of these formulations were also proved versus binary solid dispersions composed of the same amount of Soluplus. All the formulations were X-ray amorphous and hydrogen bonding interactions between the compounds were detected by FTIR analysis. An increase of 18 (EZE) and 6 (LOV) times regarding the dissolution efficiency was observed for ELS 1:1 90%, when compared to the crystalline raw materials. This formulation was able to release ca. 92 and 83% of EZE and LOV, respectively, in 5 min. Stability studies conducted at 40°C/75% RH demonstrated a decrease in the dissolution rate for both APIs, although the samples remained X-ray amorphous. However, in dry storage conditions and low temperature, the ternary solid dispersion showed a similar dissolution profile compared to the sample at time zero and unaltered physical stability. These promising data open new perspectives regarding the development of fixed dose combinations composed of poorly water-soluble APIs.

## 5. REFERENCES

- CEDERBERG, H.; STANCÁKOVÁ, A.; YALURI, N.; MODI, S.; KUUSISTO, J.; LAAKSO, M. Increased risk of diabetes with statin treatment is associated with impaired insulin sensitivity and insulin secretion: a 6 year follow-up study of the METSIM cohort. **Diabetologia**, v. 58, p. 1109-1117, 2015.
- LIN S-Y.; LIN H-L.; CHI Y-T.; HUANG Y-T.; KAO C-Y.; HSIEH W-H. Thermoanalytical and Fourier transform infrared spectral curve-fitting techniques used to investigate the amorphous indomethacin formation and its physical stability in Indomethacin-Soluplus® solid dispersions. **International Journal of Pharmaceutics**, v. 496, p. 457-465, 2015.
- LINN, M.; COLLNOT, E.M.; DJURIC, D.; HEMPEL, K.; FABIAN, E.; KOLTER, K.; LEHR, C.M. Soluplus® as an effective absorption

enhancer of poorly soluble drugs in vitro and in vivo. **European Journal of Pharmaceutical Sciences**, v. 45, p. 336-343, 2012.

LITTRINGER, E.M.; MESCHER, A.; ECKHARD, S.; SCHRÖTTNER, H.; LANGES, C.; FRIES, M.; GRIESSER, U.; WALZEL, P.; URBANETZ, N.A. Spray Drying of Mannitol as a Drug Carrier—The Impact of Process Parameters on Product Properties. **Drying Technology**, v. 30, p. 114-124, 2012.

LUST, A.; STRACHAN, C.J.; VESKI, P.; AALTONEN, J.; HEINÄMÄKI, J.; YLIRUUSI, J.; KOGERMANN, K. Amorphous solid dispersions of piroxicam and Soluplus®: Qualitative and quantitative analysis of piroxicam recrystallization during storage. **International Journal of Pharmaceutics**, v. 486, p. 306-314, 2015.

MEEUS J.; LENAERTS M.; SCURR D.J.; AMSSOMS K.; DAVIES M.C.; ROBERTS C.J.; VAN DEN MOOTER G. The influence of spray-drying parameters on phase behavior, drug distribution, and in vitro release of injectable microspheres for sustained release. **Journal of Pharmaceutical Sciences**, v. 104, p. 1451-1460, 2015.

PAUDEL, A.; WORKU, Z.A.; MEEUS, J.; GUNS, S.; VAN DEN MOOTER, G. Manufacturing of solid dispersions of poorly water soluble drugs by spray drying: formulation and process considerations. **International Journal of Pharmaceutics**, v. 453, p. 253-284, 2013.

POKHARKAR V.B.; MANDPE L.P.; PADAMWAR M.N.; AMBIKE A.A.; MAHADIK K.R.; PARADKAR A. Development, characterization and stabilization of amorphous form of a low T<sub>g</sub> drug. **Powder Technology**, v. 167, p. 20-25, 2006.

RASHID, R.; KIM, D.W.; DIN, F.U.; MUSTAPHA, O.; YOUSAF, A.M.; PARK, J.H.; KIM, J.O.; YONG, C.S.; CHOI, H.G. Effect of hydroxypropylcellulose and Tween 80 on physicochemical properties and bioavailability of ezetimibe-loaded solid dispersion. **Carbohydrate Polymers**, v. 130, p. 26-31, 2015.

RIZI, K.; GREEN, R.J.; DONALDSON, M.; WILLIAMS, A.C. Production of pH-responsive microparticles by spray drying: investigation of experimental parameter effects on morphological and release properties. **Journal of Pharmaceutical Sciences**, v. 100, p. 566-579, 2011.

SEKIGUCHI, K.; OBI, N. Studies on absorption of eutectic mixture. A comparison of the behavior of eutectic mixture of sulfathiazole and that



of ordinary sulfathiazole in man. **Chemical and Pharmaceutical Bulletin**, v. 9, p. 866-872, 1961.

TIAN, B.; ZHANG, L.; PAN, Z.; GOU, J.; ZHANG, Y.; TANG, X. A comparison of the effect of temperature and moisture on the solid dispersions: aging and crystallization. **International Journal of Pharmaceutics**, v. 475, p. 385-392, 2014.

VAN GYSEGHEM, E.; STOKBROEKX, S.; DE ARMAS, H.N.; DICKENS, J.; VANSTOCKEM, M.; BAERT, L.; ROSIER, J.; SCHUELLER, L.; VAN DEN MOOTER, G. Solid state characterization of the anti-HIV drug TMC114: interconversion of amorphous TMC114, TMC114 ethanolate and hydrate. **European Journal of Pharmaceutical Sciences**, v. 38, p. 489-497, 2009.



## **CHAPTER V**

### **DEVELOPMENT, CHARACTERIZATION AND *IN VITRO* DISSOLUTION STUDIES OF AN ENTERIC-COATED FIXED- DOSE COMBINATION COMPOSED OF TERNARY SOLID DISPERSIONS OF EZETIMIBE AND LOVASTATIN**

---

## 1. INTRODUCTION

Fixed-dose combinations (FDCs), defined as a combination of two or more active pharmaceutical ingredients (APIs) in a fixed ratio of doses, are becoming increasingly important from a public health perspective. Nowadays, FDCs have been commonly used for a wide range of conditions, including cardiovascular, metabolic and hormonal-related pathologies, infections, allergies and pain, and have been designed for different routes of administration (EMA, 2015; WHO, 2005).

Regarding the use of FDCs for hypercholesterolemia, recent studies have proven that the combination of statins, the so-called first choice lipid lowering agents, with other drugs, such as ezetimibe (EZE), is highly recommended. Besides the frequent and severe side effects, such as myopathy, which can result in rhabdomyolysis leading to renal failure, the use of statins has also been associated with an increase of 46% in the development of diabetes type 2 (CEDERBERG et al., 2015).

The successful development of a ternary solid dispersion with Soluplus® (polyvinyl caprolactam-polyvinyl acetate-polyethylene glycol graft copolymer) by spray drying was demonstrated in the previous chapter. The dissolution enhancement of both compounds was directly proportional to the amount of polymer, reaching its best performance with the formulation composed of EZE:LOV:Soluplus®, in a mass ratio of 5:5:90 (ELS 1:1 90%) (RIEKES et al., 2016). However, dissolution studies performed in simulated gastric fluid (0.1 M HCl) provoked the hydrolysis of LOV (data not shown), causing the premature formation of its hydroxyacid derivative (LOVh). Importantly, as both LOV and LOVh have the liver as their site of action, their concentration in this organ should be maximized as much as possible. Studies in animals have demonstrated that LOV shows a better hepatic sequestration than LOVh, which in turn minimizes the systemic side effects (DUGGAN et al., 1988). As the author states that this provides a rational basis for the lactone to be the preferred API for the dosage form, the hydrolytic formation of the active metabolite in gastric conditions should be avoided. For this purpose, the development of an enteric-coated formulation is ideal, to safely prevent the premature formation of LOVh.

Fluid bed coating is one of the most used coating processes. Despite of the different configurations of fluid bed coaters, the bottom spray mode with a Würster insert is especially interesting to coat small particles, as pellets, since it diminishes the risk of agglomeration, typical

of the standard bottom spray mode (DIXIT and PUTHLI, 2009). Preparation of multiparticulate systems, such as pellets, granules and mini-tablets, instead of the conventional single unit dosage forms, offers the advantage of presenting a more predictable gastric transit time, better distribution and absorption, facilitated disintegration, less frequent dose dumping issues and reduced risks of systemic toxicity and local irritation (ASGHAR and CHANDRAN, 2006). In theory, multiparticulate systems can also be an interesting choice to compose a FDC, since they allow the combination of more than one API, obtaining various release profiles from a single dosage form. However, more scientific investigation is necessary to understand it more deeply and optimize the critical manufacturing parameters. In the case of EZE and LOV, as the coating process involves the obtainment of a two-layered formulation, the manufacturing becomes more complex. The developed formulation should be able to protect especially LOV from the gastric environment, avoiding the formation of LOVh, and later rapidly release both APIs in the upper intestine.

In this context, this chapter aims to investigate the preparation of enteric-coated FDC solid dispersions composed of EZE and LOV, manufactured by fluid bed coating. Formulation and process parameters were tested and the obtained formulations were characterized by solid-state techniques and *in vitro* dissolution studies.

## **2. EXPERIMENTAL**

### **2.1 MATERIALS**

EZE and LOV were purchased from Pharma Nostra® (Rio de Janeiro, Brazil) with batch numbers FM017H13 and 130312, respectively. LOVh was prepared according to Bogman and coworkers (2001), by hydrolyzing LOV in 0.05 M NaOH, resulting in a theoretical concentration of 1 mg/ml. The solution was stirred at room temperature during 30 min, followed by pH adjustment to 7.4 with 0.2 M HCl. The solution was stored at 4°C prior to use (BOGMAN et al., 2001).

Soluplus® was obtained from BASF® ChemTrade GmbH (Ludwigshafen, Germany), while Eudragit L100® (poly(methacrylic acid-co-methyl methacrylate) 1:1) and Eudragit L100-55® (poly(methacrylic acid-co-ethyl acrylate) 1:1) were kindly donated by Evonik Industries AG® (Darmstadt, Germany). Sucrose beads (mean diameter of 300-415 µm and 710-850 µm) were provided by Hanns G. Werner GmbH (Tornesch, Germany).

## 2.2 PREPARATION OF THE FLUID BED COATED BEADS

Based on the previous chapter, a system composed of EZE:LOV:Soluplus® (5:5:90, w/w/w) was selected to make up the glass solution layer. For this purpose, EZE, LOV and Soluplus®, dissolved in 2.5 l of a 10% (w/v) ethanolic solution, were coated onto 500 g of sucrose beads, using a bottom-spray fluid bed system with a Würster insert (Aeromatic MP 1 Multiprocessor, GEA Pharma System AG, Bubendorf, Switzerland). Prior to coating, the beads were pre-heated for 30 min in the coating chamber. The operational conditions were: drying air volume of 1566.3 l/min, inlet temperature of 50°C, atomizing air pressure of 1.5 bar and feed rate of 12 ml/min for beads of 710-850 µm mean diameter. For the smaller ones (300-415 µm), the parameters were kept the same, except the atomizing air pressure and the feed rate, changed to 1 bar and 9 ml/min, respectively.

The enteric coating process was started immediately after the glass solution layer was applied. In this step, 1 l of a 10% (w/v) ethanolic solution containing either Eudragit L100® or Eudragit L100-55®, and 20 g of triethyl citrate (TEC) was sprayed onto the sucrose beads coated with the ternary solid dispersion layer. Regarding the beads of 710-850 µm mean diameter, the operational conditions used for the glass solution remained the same for Eudragit L100®, whilst for Eudragit L100-55® the feed rate was lowered to 6 ml/min, due to the higher viscosity of this solution, leading to aggregation of the beads. The smaller beads (300-415 µm) adopted the same experimental parameters described for Eudragit L100-55®, except that in this case the solid content of the enteric coating solution was decreased to 5% (w/v), to avoid agglomeration of the pellets.

In all cases, during the enteric coating step, approximately 5 g of samples were withdrawn periodically until the end of the process, to

verify the effect of coating time and the thickness of the enteric layer on drug release.

The coated beads were unloaded, weighed and kept in a desiccator, at 0% RH (using phosphorous pentoxide), at room temperature. Stability of the formulations was investigated by X-ray powder diffraction (XRPD) and drug release studies (section 2.3 and 2.6, respectively) after 6 months of storage under the mentioned conditions.

## 2.3 X-RAY POWDER DIFFRACTION (XRPD)

XRPD experiments were carried out using an automated X'pert PRO diffractometer (PANalytical, Almelo, The Netherlands) with a Cu tube ( $K\alpha$   $\lambda = 1.5418$  Å), and a generator set at 45 kV and 40 mA. The measurements were performed at room temperature on whole beads, in transmission mode. The selected experimental settings included a continuous scan mode from  $4^\circ$  to  $40^\circ$   $2\theta$  with  $0.0167^\circ$  step size and 200 s per step counting time.

## 2.4 SCANNING ELECTRON MICROSCOPY (SEM)

SEM pictures were recorded using a Phillips XL30 SEM-FEG (Philips, Eindhoven, The Netherlands) equipped with a Schottky field-emission electron gun. A beam of 15 kV was used and detection was performed using a conventional Everhart-Thornley secondary electron detector. Cross-sectioned and entire beads were affixed onto an aluminum stub with a double-sided adhesive carbon tape, and then coated with platinum under vacuum using a sputtering device (Balzers Union, Liechtenstein) before imaging.

## 2.5 PARTICLE SIZE MEASUREMENT

The mean particle size distribution of the coated beads was measured by laser diffraction using a Mastersizer 2000 equipment (Malvern Instruments Ltd, Malvern, UK) coupled to the dry sample

dispersion unit Scirocco 2000. The samples were placed in the dispersion unit, fed to the equipment with a vibration feed rate of 30% and dispersed with an air pressure of 2 bar. All samples were measured in triplicate.

## 2.6 *IN VITRO* RELEASE STUDIES

Release profiles were obtained under non-sink conditions using a SR8PLUS dissolution station (SpectraLab Scientific Inc., Markham, Canada). An accurate amount of beads, equivalent to 10 mg of EZE and 10 mg of LOV, was evaluated in 900 ml of 0.1 M HCl containing 0.025 % (m/v) of sodium lauryl sulfate (SLS) and in 900 ml of 10 mM phosphate buffer pH 6.8 + 0.01% (m/v) SLS, at 37°C, in order to mimic the gastric and intestinal conditions, respectively. The solution was stirred with paddle apparatus II at a speed of 120 rpm, in order to avoid the agglomeration of the beads at the bottom of the dissolution vessels. Samples were taken at different time intervals, filtered using a PTFE filter (pore size 0.45 µm) and immediately replaced with the same volume of fresh dissolution medium. Dissolution profiles were compared by means of one-way ANOVA followed by Tukey's test. Results were considered to be statistically significantly different if  $p < 0.05$ . The statistical analysis was performed by the GraphPad Prism 6 software.

The amount of EZE and LOV dissolved was determined using an isocratic HPLC method (see Appendix). The experiments were conducted on a reversed-phase Thermo® BDS Hypersil C18 column (250 x 4.6 mm i.d., 5 µm pore size). The mobile phase was composed of acetonitrile:water (60:40 v/v), and used at a flow rate of 1.0 ml/min, at room temperature. The UV detection was performed at 235 nm. 20 µl of samples was injected and the data acquisition was performed using Merck LaChrom D-7000 System Manager software.

## 3. RESULTS AND DISCUSSION

### 3.1 PREPARATION AND CHARACTERIZATION OF THE ENTERIC-COATED FDC

In order to achieve efficient drug delivery, pharmaceutical formulations must be able to deliver a sufficient concentration of



unchanged API at its intended site of action. The development of ternary solid dispersions with EZE, LOV and Soluplus® by our group provided enhanced dissolution rate of both APIs in acetate buffer pH 4.5, but also showed the formation of the active metabolite, LOVh, in gastric environment (see Appendix, Figure 45). In this case, the undesired and premature formation of LOVh in the stomach jeopardizes the efficiency of the dosage form, since the parent drug presents a higher hepatic sequestration than LOVh. The high pre-hepatic concentration of the metabolite increases the systemic burden, instead of maximizing the concentration of LOV in the liver, its site of action (DUGGAN, et al., 1988).

Based on these findings, the development of an enteric-coated formulation was considered. For this purpose, fluid bed coating was selected. Consisting of a one-step process, it does not require separate drying steps, addition of excipients and further manufacturing stages, such as milling or compression, which can induce phase separation or crystallization (SINGH et al., 2016; AYENEW et al., 2012). However, although this technique has been successfully applied to the development of solid dispersions (YAN et al., 2016; DEREYMAKER and VAN DEN MOOTER, 2015; LI et al., 2012; SUN et al., 2008), the preparation of more complex formulations still remains relatively unexplored.

We investigated the influence of bead size, type of enteric polymer and coating time (which is related to the coating thickness), on the release performance of the two APIs. The other processing parameters were selected based on a previous study (DEREYMAKER and VAN DEN MOOTER, 2015) and were optimized for each formulation. The inlet temperature (50°C) was selected since it provides adequate solvent evaporation and it is below the glass transition temperature of Soluplus® (ca. 70°C) (BASF, 2010). An atomizing air pressure of 1.5 bar was ideal to fluidize the beads without inducing particle entrainment.

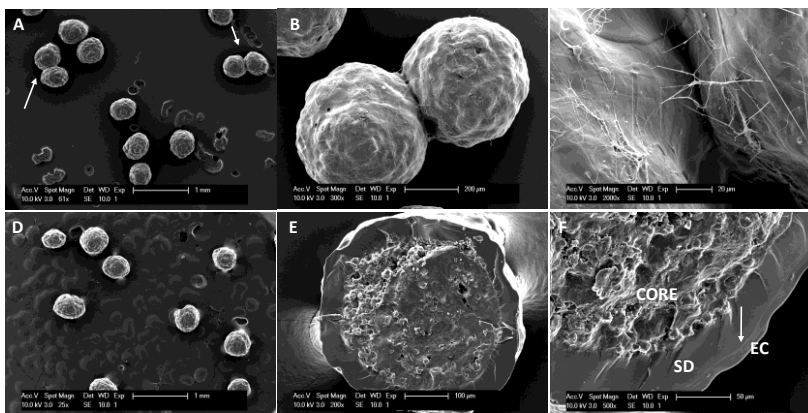
### 3.2 IMPACT OF BEAD SIZE

The size of inert sucrose beads is an important parameter, which should be taken into consideration in fluid bed coating. Especially in this type of processing, particles must present adequate cohesive and density properties, in order to allow fluidization and avoid agglomeration. Moreover, the change in bead size can have a direct impact on the

thickness of the coating layer, interfering with the in vitro drug release (WESDYK et al., 1990).

For this reason, inert sucrose beads with mean diameters ranging from 300 to 415  $\mu\text{m}$  and 710 to 850  $\mu\text{m}$  have been tested and their impact has been analyzed through in vitro studies in acidic conditions. This criterion was selected based on the importance of the coating layer to avoid the premature formation of LOVh in the stomach. At this stage of investigation, the type of enteric polymer remained constant and Eudragit L100-55<sup>®</sup> was selected.

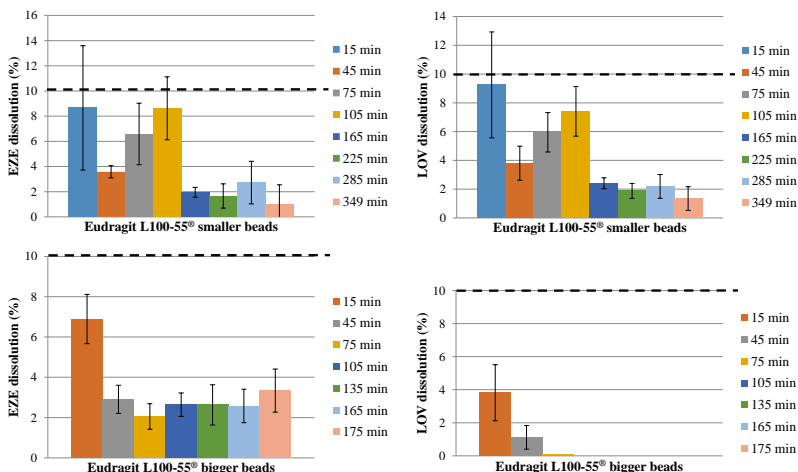
**Figure 36.** SEM micrographs of enteric-coated smaller beads (300-415  $\mu\text{m}$ ) before (A-C) and after (D-F) process optimization. Agglomeration is indicated in A by the arrows. Polymeric nets are shown in B and C after enteric coating. The coating layers relative to the solid dispersion (SD) and enteric coating (EC) are shown in F and their borders are indicated by the arrow



Different bead sizes required distinct processing parameters. Particle agglomeration was a common problem faced by the smaller beads, mainly during the enteric coating step, and lowering the feeding rate at this stage from 12 to 6 ml/min was necessary. A similar approach was attempted with the glass solution layer; 9 ml/min feeding rate was adopted instead of 12 ml/min. In addition, the solid content of the enteric solution was decreased by half (5% w/v), increasing the total coating volume. Based on SEM images (Figure 36), it was possible to observe

that the adhesion between the beads was attributed to the presence of polymeric nets, probably formed by inadequate solvent evaporation of the highly viscous solution. After process optimization, coating layers were clearly formed and agglomeration was less frequently observed. However, as an important disadvantage, the enteric coating process took much longer with the smaller beads (349 min), compared to the bigger ones (175 min).

**Figure 37.** Influence of coating time on in vitro dissolution of EZE and LOV in acidic conditions (presented as % release), from small (300–415  $\mu\text{m}$ ) and large (710–850  $\mu\text{m}$ ) beads



When compared by in vitro dissolution studies in acidic conditions, beads with distinct size ranges yielded different results (Figure 37). According to official compendia, less than 10% release in HCl 0.1 M meets the criteria of gastro protection for enteric-coated formulations. Both EZE and LOV showed less than 10% drug release for all coating times in case of the larger beads, as well as more consistent data and lower drug release as the coating time increased, especially for LOV. On the other hand, large variability was observed for drug release from the smaller beads, which reached values higher than 10% in some cases (up to  $8.7 \pm 4.5\%$  for EZE and  $9.2 \pm 3.7\%$  for LOV). In addition,

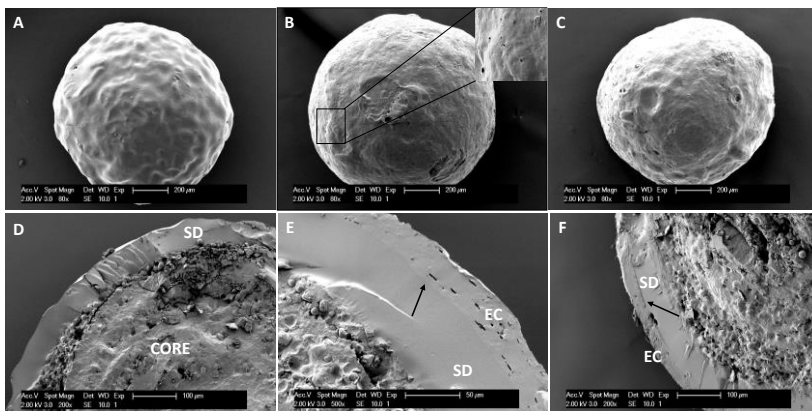
there was no logical trend with respect to the coating time. This data demonstrates that the coating of these samples was probably not homogeneous, suggesting the occurrence of agglomeration, even after the process optimization. In this case, the use of small inert beads, with sizes ranging from 300 to 415  $\mu\text{m}$  is not ideal. Based on these data, further tests (varying the type of enteric polymer and coating time) have been performed with inert beads ranging from 710 to 850  $\mu\text{m}$ .

### 3.3 IMPACT OF POLYMER TYPE AND COATING TIME

Enteric coating layers composed of Eudragit L100® and Eudragit L100-55® were tested with inert sucrose beads (particle size 710-850  $\mu\text{m}$ ), in order to verify the impact of the type of polymer. Although more viscous solutions were obtained with Eudragit L100-55®, thus requiring the optimization of process parameters, both formulations have been successfully obtained. The yield was 93.8% and 88.4% for the final formulations composed of Eudragit L100® and Eudragit L100-55®, respectively.

SEM micrographs (Figure 38) show spherical particles with different morphological aspects regarding the coating process and the polymer used. The surface of the pellets is rough with indentations after coating with the first layer (solid dispersion). However, after coating with the enteric polymers, the surface becomes smoother with homogeneous distribution of the enteric layer. Concave pores, which were probably generated during the volatilization of the spray solution from the surface of the pellets, are observed on the surface of the formulations composed of Eudragit L100®. These apertures are more scarce in samples composed of Eudragit L100-55®. The spherical morphology remains after the enteric coating process, indicating adequate drying and rigidity of the particles. The cross-section views indicate that the inner core has a rough structure, tightly coated by the solid dispersion layer, which is compact and smooth. A delimited border can be easily distinguished between this layer and the enteric coating layers. The concave pores observed on the surface of the formulations composed of Eudragit L100-55® remain in the inner enteric layer. Their presence on the surface increases the pellet surface area and facilitates water penetration and eventual release of the drugs.

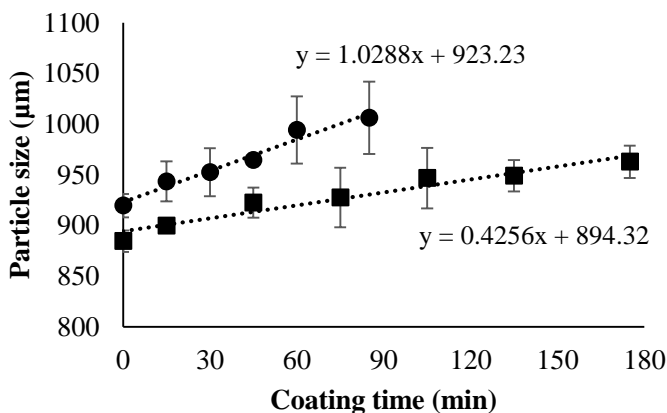
**Figure 38.** SEM micrographs of pellets coated with the solid dispersion layer (A and D) and enteric-coated with Eudragit L100® (B and E) and Eudragit L100-55® (C and F). Panel B shows an enlarged surface view to provide a better visualization of the pores. The cross-sectioned pellets (D-F) show the core, the solid dispersion (SD) and the enteric coating (EC) layers. Arrows indicate the borders between the SD and the EC layers



Particle size measurements by laser diffraction were performed to follow the coating thickness along the processing. Application of the solid dispersion coating layer increased the mean particle size to  $919.7 \pm 11.6 \mu\text{m}$ , and a coating ratio of  $0.48 \mu\text{m}/\text{min}$  was determined based on the coating time (208 min). The mean particle size reached  $1006.4 \pm 35.6 \mu\text{m}$  and  $963.1 \pm 15.9 \mu\text{m}$  at the end of the enteric coating process, for samples composed of Eudragit L100® and Eudragit L100-55®, respectively. Both formulations displayed a linear relation between the enteric coating time and the increase of their particle size (Figure 39). The coating rate could be determined by the slope of their linear equation as  $1.03 \mu\text{m}/\text{min}$  and  $0.43 \mu\text{m}/\text{min}$  for beads with Eudragit L-100® and Eudragit L100-55®, respectively. The concern about monitoring the film thickness during the coating process is of high importance due to its relation to the release profile and drug stability. Too thick coating layers can prejudice the release of immediate release dosage forms, resulting in delayed release. On the other hand, if too thin, the coating layer can expose the dosage form to premature release and provoke degradation or crystallization (KNOP and KLEINEBUDDE, 2013). Although continuous and in-line monitoring methods are more appropriate, e.g. visual imaging (KADUNC et al., 2014), and spectroscopic methods like near infrared (NIR) and Raman

spectroscopy (KNOP and KLEINEBUDDE, 2013), the off-line monitoring by particle size measurement is also feasible, since it generates simple, fast and reliable measurements to determine the end point of coating. For this purpose, they need to be related to the dissolution performance of the withdrawn samples.

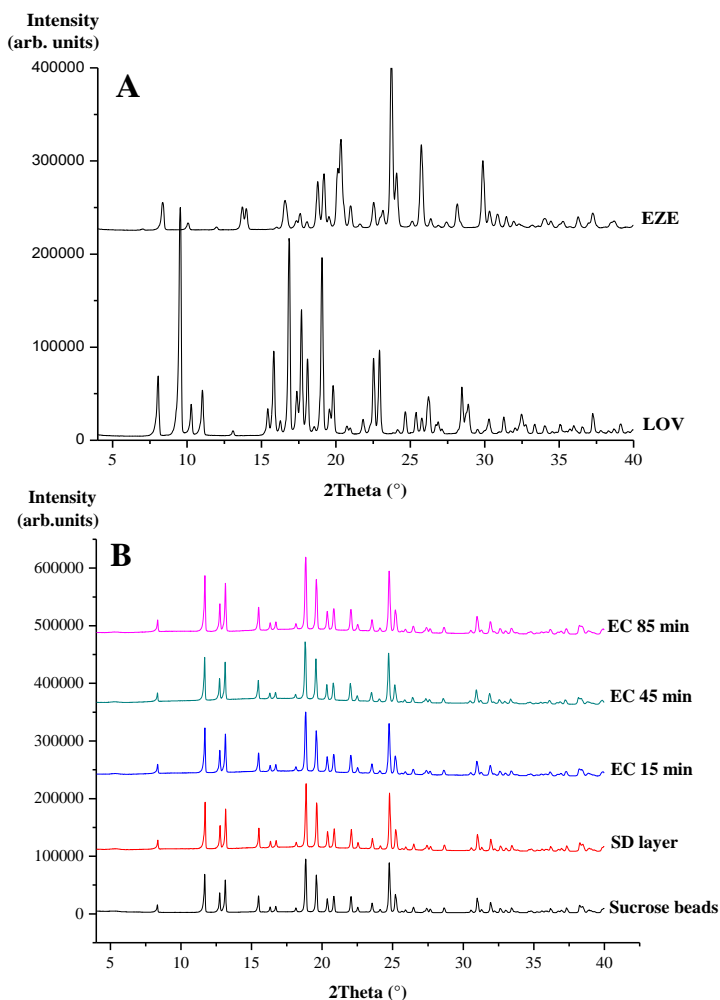
**Figure 39.** Linear relation between the particle size, in  $\mu\text{m}$ , and the coating time of the enteric coating layers composed of Eudragit L100® (●) and Eudragit L100-55® (■)



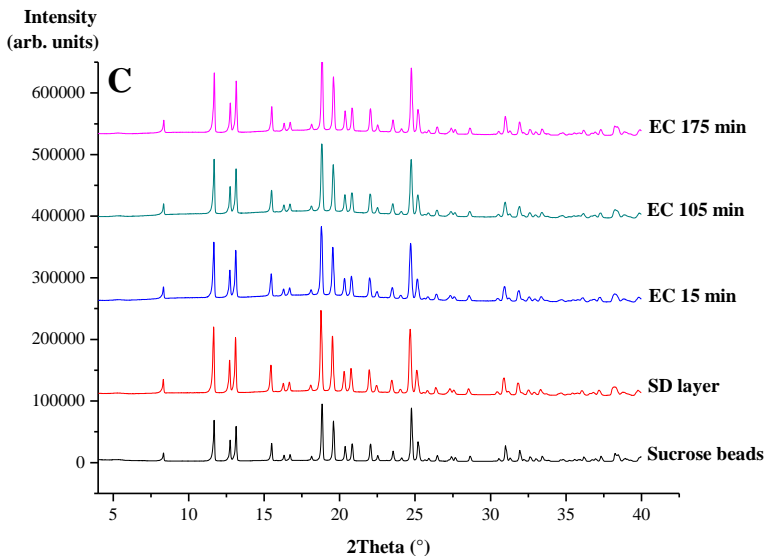
As the degree of crystallinity of LOV and EZE is an important parameter related to drug release, the samples were analyzed with XRD. The diffractograms shown in Figure 6 demonstrate that the starting raw materials are crystalline. LOV has main Bragg peaks at  $2\theta$   $8.05^\circ$ ,  $9.54^\circ$ ,  $11.03^\circ$ ,  $15.83^\circ$ ,  $16.86^\circ$ ,  $17.68^\circ$  and  $19.07^\circ$ , in agreement with previous reports (YOSHIDA et al., 2011). EZE can be found in anhydrate or monohydrate forms, which are differentiated at low  $2\theta$  angles in XRD data; the peaks at  $7.02$ ,  $8.36$  and  $10.04^\circ$  belong exclusively to the anhydrate, while the ones found at  $7.98$ ,  $9.84$  and  $13.23^\circ$  correspond to the monohydrate (BRÜNING et al., 2010; RAVIKUMAR and SRIDHAR, 2005). The raw material used in this study has main crystalline peaks at  $7.01$ ,  $8.34$ ,  $10.04$ ,  $16.54$ ,  $20.30$ ,  $23.71$  and  $25.73^\circ$ , indicating that it corresponds to the anhydrate form. However, after the coating process, from both solid dispersion and enteric layers, all formulations only show Bragg peaks characteristic of the sucrose beads, indicating amorphization of the APIs (Figure 40). These results indicate

that the coating process did not lead to a deleterious effect to the formulation, since the spray dried formulation ELS 1:1 90% (composed of EZE, LOV and Soluplus® in 5:5:90 mass ratio, respectively) was completely amorphous (RIEKES et al., 2016).

**Figure 40.** Diffractograms of (A) crystalline raw materials, (B) formulations with Eudragit L100® and (C) formulations with Eudragit L100-55®, compared to the inert sucrose beads



(to be continued)



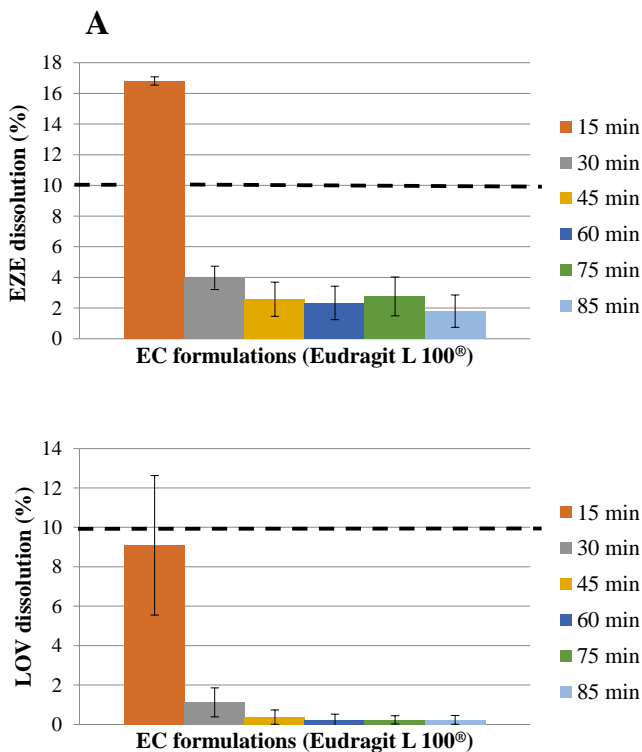
In order to investigate the impact of the different enteric polymers on the dissolution performance of the enteric-coated formulations, the pellets were evaluated in gastric conditions (in order to assess its gastro resistance) and in phosphate buffer pH 6.8, aiming to verify if a fast release of both APIs could be achieved in this condition.

Figure 41 shows the percentage release of EZE and LOV in gastric conditions (HCl 0.1 M + 0.025% (m/v) of SLS). If the desired release in this condition is considered (less than 10% release in HCl 0.1 M), it can be observed that only the formulation coated for 15 min with Eudragit L100® does not comply with this rule. This formulation released  $16.8 \pm 0.3\%$  of EZE and  $9.1 \pm 3.5\%$  of LOV. If this data is associated to the thickness of the enteric coating layer, it is possible to conclude that for this polymer, at least  $30.9 \mu\text{m}$  is necessary to sufficiently reduce drug release in acidic condition. On the other hand, for Eudragit L100-55®, acceptable release was already obtained after 15 min of coating ( $6.9 \pm 1.2\%$  for EZE and  $3.8 \pm 1.7\%$  for LOV), although the coating thickness of this layer is much thinner ( $6.45 \mu\text{m}$ ) than the one obtained with Eudragit L100®. This indicates that Eudragit L100-55® provides a more efficient gastro protection. In addition, it is important to mention that even after 15 min, the presence of LOVh was negligible. The different release

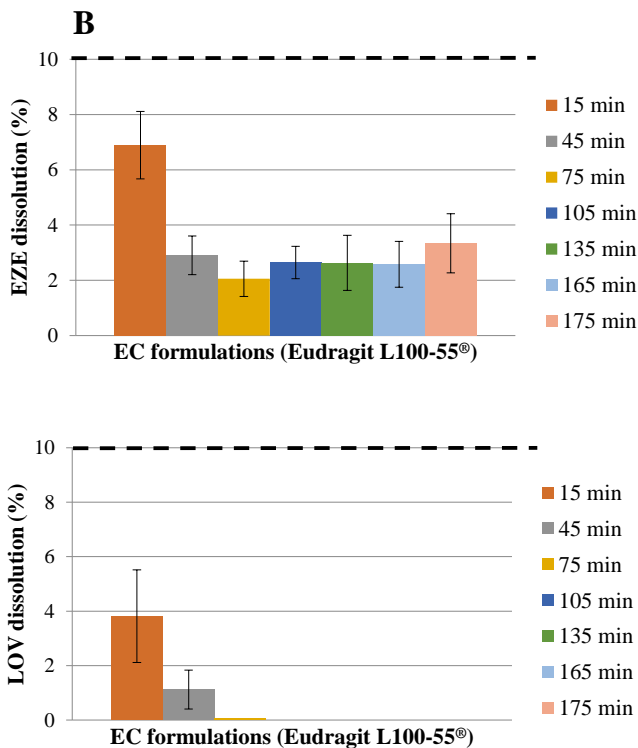


behavior between the two polymers can be at least partially explained by the morphological aspects observed by SEM analysis. Samples composed of Eudragit L100® showed concave pores on the surface, which could ease water penetration and drug release. For both polymers, almost no release of LOV was observed after 45 min of coating regarding the systems with Eudragit L100® and after 75 min for the samples composed of Eudragit L100-55®. This can be translated into 46.4  $\mu\text{m}$  (Eudragit L100®) and 32.3  $\mu\text{m}$  (Eudragit L100-55®) of enteric layer thickness.

**Figure 41.** Percentage release of EZE and LOV from formulations prepared with (A) Eudragit L100® and (B) Eudragit L100-55®, after 90 min of dissolution studies in HCl 0.1 M + 0.025% of SLS



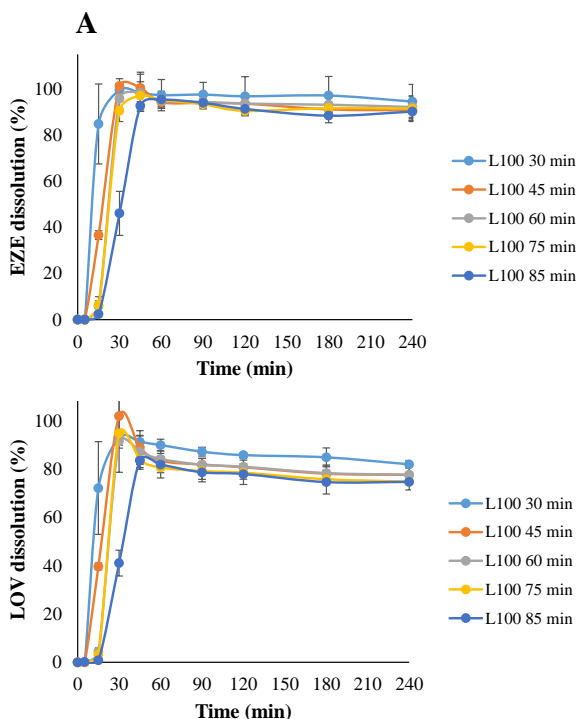
(to be continued)



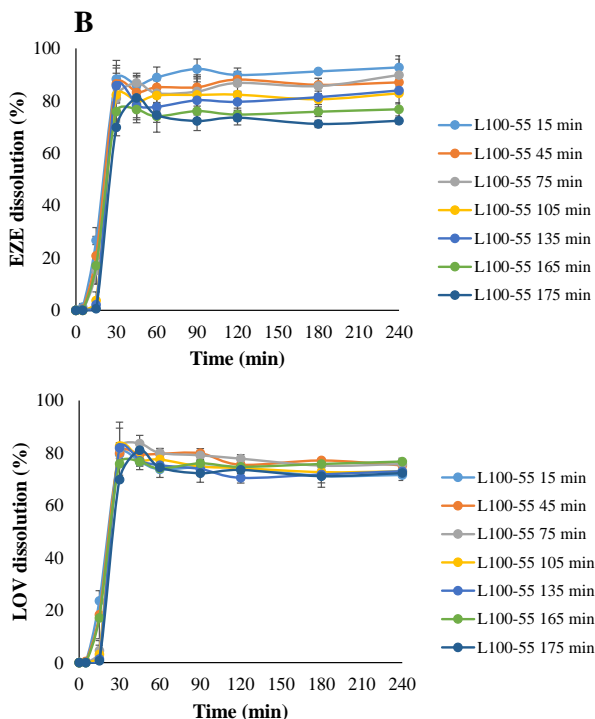
After the gastric stage, samples were submitted to release studies in phosphate buffer pH 6.8, as shown in Figure 42. As the sample coated for 15 min with Eudragit L100® did not meet the acceptance criteria in gastric environment, it was not selected for further studies. Results show a fast release for all formulations, which were considered statistically similar, despite of the different coating times. Approximately 100% of release was achieved after 30 min for EZE with samples composed of Eudragit L100®, while formulations with Eudragit L100-55® released approximately 92%. LOV, on the other hand, showed lower dissolution percentages in general, as compared to EZE, releasing approximately 80%. This trend was also observed with the ternary solid dispersions of EZE, LOV and Soluplus® previously reported (RIEKES et al., 2016), indicating that the coating process did not provoke deleterious effects on the release profiles of the APIs. In addition, both systems were able to

enhance the dissolution rate of the two compounds compared to the respective crystalline raw materials, which released  $5.9 \pm 0.5\%$  (EZE) and  $4.6 \pm 0.1\%$  (LOV) within the same timeframe. Based on the *in vitro* dissolution studies, it is possible to conclude that both polymers were successful. However, Eudragit L100-55<sup>®</sup> was more efficient, requiring less coating time and consequently, thinner coating layer, to provide lower drug release and conversion to LOVh. In addition, a short coating time, 15 min, was considered adequate for this polymer, since gastro protection and fast release in pH 6.8 was observed. In case of Eudragit L100<sup>®</sup>-based formulations, 30 min were necessary to obtain the gastro protective effect.

**Figure 42.** *In vitro* dissolution profiles of enteric-coated formulations composed of (A) Eudragit L100<sup>®</sup> and (B) Eudragit L100-55<sup>®</sup>, in phosphate buffer pH 6.8 containing 0.01% of SLS



(to be continued)

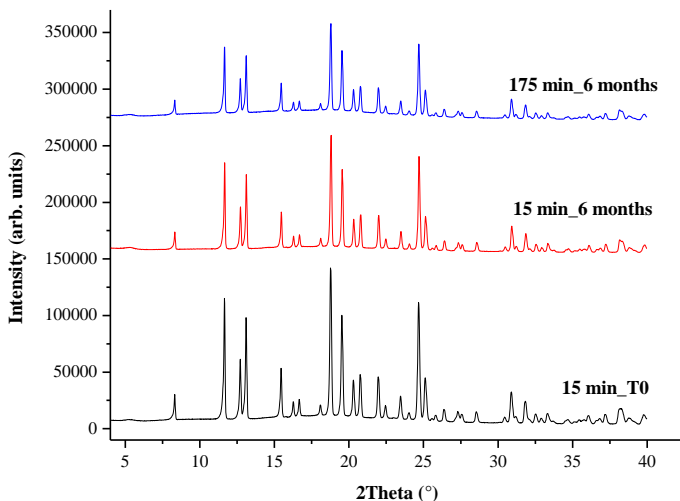


### 3.4 STABILITY STUDIES

As Eudragit L100-55®-based formulations prepared with large sucrose beads (710-850  $\mu\text{m}$  particle size) were considered the most appropriate ones for enteric-coated EZE/LOV pellets, the stability of these samples was verified.

Stability studies were conducted after 6 months storage at 0% RH and room temperature. The XRD data (Figure 43) show the diffractograms at the start and end of the coating process, in comparison with a fresh sample. No additional Bragg peaks are observed, besides those from the sucrose beads, indicating that the samples remain stable and the APIs amorphous, during storage.

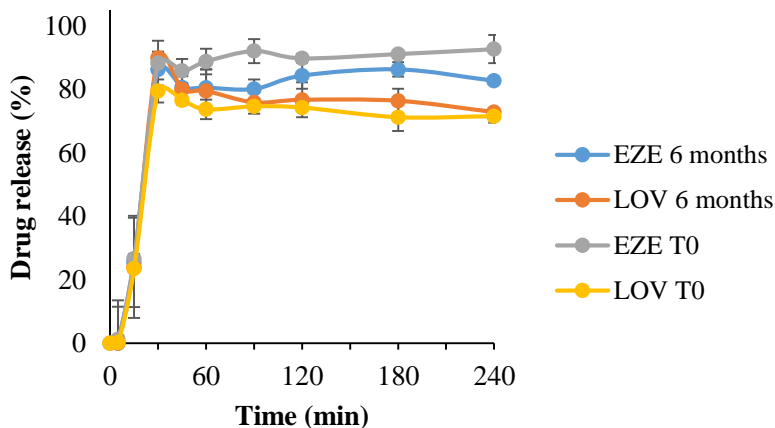
**Figure 43.** Diffractograms relative to formulations with Eudragit L100-55®, at time zero (T0) and after 6 months of storage



For the *in vitro* dissolution studies, samples were selected from the initial stages of the coating process since they are more prone to crystallization and surface defects. Data obtained in acidic condition demonstrate similar percentage release for both APIs from both enteric-coated formulations, reflecting the integrity of the coating layer. EZE release in acidic medium was  $6.89 \pm 1.22\%$  from a freshly prepared sample, compared to  $6.92 \pm 1.04\%$  after 6 months storage. For LOV,  $3.81 \pm 1.69\%$  and  $4.16 \pm 2.17\%$  were released from samples at T0 and 6 months storage, respectively. Dissolution data were considered statistically similar for EZE and LOV ( $p > 0.05$ ).

Similar trends were observed regarding the dissolution profiles obtained in phosphate buffer pH 6.8 (Figure 44). Although a slight decrease in EZE's release was observed, formulations from T0 and stored after for 6 months were statistically similar ( $p > 0.05$ ).

**Figure 44.** Dissolution profiles of EZE and LOV from Eudragit L100-55®-based formulation, with 15 min of enteric coating time, at time zero (T0) and after 6 months



#### 4. CONCLUSIONS

In order to avoid the premature formation of LOVh in gastric environment, enteric-coated FDCs of EZE and LOV were developed. We demonstrate for the first time the feasibility of an enteric-coated FDC based on ternary solid dispersions, prepared by fluid bed coating. In order to develop an adequate formulation, process parameters such as inert bead size, type of enteric polymer and coating time have been investigated. Inert sucrose beads were firstly coated with a glass solution layer composed of EZE, LOV and Soluplus®, in a 5:5:90 mass ratio, according to previous results reported by our group. The use of smaller beads (300-415  $\mu\text{m}$  mean diameter) revealed difficulties with processing, leading to frequent pellet agglomeration. This in turn, reflected on highly variable drug release in acidic conditions, even after process optimization. In addition, the lower feeding rate (6 ml/min) and solid content of the enteric polymer solution (5% w/v) implied in a longer time processing, compared to the beads with larger mean diameter. When Eudragit L100® and Eudragit L100-55®-based formulations were compared, different morphological features were noticed. Microscopy analysis revealed spherical particles with concave pores on the surface of pellets coated with Eudragit L100®, which possibly contributed to a higher drug release from this polymer, despite of presenting a thicker coating layer. Absence

of crystals in SEM micrographs suggested the amorphicity of the compounds, which was confirmed by XRD for Eudragit L100® and Eudragit L100-55®-based formulations. Importantly, laser diffraction analysis allowed the off-line particle size measurements providing fast and reliable values of coating thickness. From these data, it was possible to determine the minimum coating thickness to assess an adequate release in gastric and intestinal conditions. Values of 30.9 µm and 6.5 µm were obtained for samples coated with Eudragit L100® and Eudragit L100-55®, respectively, demonstrating better performance of the latter. Regarding the coating time, although faster and higher percentages of release were observed with shorter coating times, samples selected at the beginning and end of the coating process were considered similar. Finally, after 6 months of storage, samples showed unaltered physical properties and dissolution behavior. Based on these findings, these formulations comprise an interesting alternative to administer EZE and LOV in a FDC.

## 5. REFERENCES

ASGHAR, L.F.A. and CHANDRAN, S. Multiparticulate formulation approach to colon specific drug delivery: Current perspectives. **Journal of Pharmaceutical Sciences**, v. 9, p. 327-338, 2006.

AYENNEW, Z.; PAUDEL, A.; VAN DEN MOOTER, G. Can compression induce demixing in amorphous solid dispersions? A case study of naproxen-PVP K25. **European Journal of Pharmaceutics and Biopharmaceutics**, v. 81, p. 207-213, 2012.

BASF, 2010. Soluplus®: Technical Information. Available at: <https://industries.basf.com/en/Drug-Formulation/Soluplus.html> (accessed 11.07.2016).

BOGMAN, K.; PEYER, A-K.; TÖRÖK, M.; KÜSTERS, E.; DREWE, J. HMG-CoA reductase inhibitors and P-glycoprotein modulation. **British Journal of Pharmacology**, v. 132, p. 1183-1192, 2001.

BRÜNING, J.; ALIG, E.; SCHMIDT, M.U. Ezetimibe anhydrate, determined from laboratory powder diffraction data. **Acta Crystallographic C**, v. 66, p. o341-o344, 2010.

CEDERBERG, H.; STANCÁKOVÁ, A.; YALURI, N.; MODI, S.; KUUSISTO, J.; LAAKSO, M. Increased risk of diabetes with statin treatment is associated with impaired insulin sensitivity and insulin

secretion: a 6 year follow-up study of the METSIM cohort. **Diabetologia**, v. 58, p. 1109-1117, 2015.

DEREYMAKER, A. and VAN DEN MOOTER, G. The peculiar behavior of the glass transition temperature of amorphous drug-polymer films coated on inert sugar spheres. **Journal of Pharmaceutical Sciences**, v. 104, p. 1759-1766, 2015.

DIXIT, R. and PUTHLI, S. Fluidization technologies: Aerodynamic principles and process engineering. **Journal of Pharmaceutical Sciences**, v. 98, p. 3933-3960, 2009.

DUGGAN, D.E.; CHEN, I.W.; BAYNE, W.F.; HALPIN, R.A.; DUNCAN, C.A.; SCHWARTZ, M.S.; STUBBS, R.J.; VICKERS, S. The physiological disposition of lovastatin. **Drug Metabolism and Disposition**, v. 17, p. 166-173, 1988.

European Medicines Agency (EMA), 2015. Guideline on clinical development of fixed combination medicinal products. Available at: [http://www.ema.europa.eu/docs/en\\_GB/document\\_library/Scientific\\_guideline/2015/05/WC500186840.pdf](http://www.ema.europa.eu/docs/en_GB/document_library/Scientific_guideline/2015/05/WC500186840.pdf) (accessed 11.07.2016).

KADUNC, N.O.; SIBANC, R.; DREU, R.; LIKAR, B.; TOMAZEVIC, D. In-line monitoring of pellet coating thickness growth by means of visual imaging. **International Journal of Pharmaceutics**, v. 470, p. 8-14, 2014.

KNOP, K. and KLEINEBUDDE, P. PAT-tools for process control in pharmaceutical film coating applications. **International Journal of Pharmaceutics**, v. 457, p. 527-536, 2013.

LI, J.; LIU, P.; LIU, J.-P.; ZHANG, W.-L.; YANG, J.-K.; FAN, Y.-Q. Novel Tanshione II A ternary solid dispersion pellets prepared by a single-step technique: In vitro and in vivo evaluation. **European Journal of Pharmaceutics and Biopharmaceutics**, v. 80, p. 426-432, 2012.

RAVIKUMAR, K. and SRIDHAR, B. Ezetimibe monohydrate. **Acta Crystallography E**, v. 61, p. o2907-2909, 2005.

RIEKES, M.K.; ENGELEN, A.; APPELTANS, B.; ROMBAUT, P.; STULZER, H.K.; VAN DEN MOOTER, G. New perspectives for fixed dose combinations of poorly water-soluble compounds: a case study with ezetimibe and lovastatin. **Pharmaceutical Research**, v. 33, p. 1259-1275, 2016.



SINGH, A.; BHARATI, A.; FREDERIKS, P.; VERKINDEREN, O.; GODERIS, B.; CARDINAELS, R.; MOLDENAERS, P.; VAN HUMBEECK, J.; VAN DEN MOOTER, G. Effect of compression on the molecular arrangements of itraconazole-soluplus solid dispersions: induction of liquid crystals or exacerbation of phase separation? **Molecular Pharmaceutics**, v 13, p. 1879-1893, 2016.

SUN, N.; ZHANG, X.; LU, Y.; WU, W. In vitro evaluation and pharmacokinetics in dogs of solid dispersion pellets containing *Silybum marianum* extract prepared by fluid-bed coating. **Planta Medica**, v. 74, p. 126-132, 2008.

WESDYK, R.; JOSHI, Y.M.; JAIN, N.B.; MORRIS, K.; NEWMAN, A. The effect of size and mass on the film thickness of beads coated in fluidized bed equipment. **International Journal of Pharmaceutics**, v. 65, p. 69-76, 1990.

WORLD HEALTH ORGANIZATION (WHO). Annex 5: Guidelines for registration of fixed-dose combination medicinal products, 2005. Available at: <http://apps.who.int/medicinedocs/documents/s19979en/s19979en.pdf> (access 11.07.2016).

YAN, H.-X.; ZHANG, S.-S.; HE, J.-H.; LIU, J.-P. Application of ethyl cellulose, microcrystalline cellulose and octadecanol for wax based floating solid dispersion pellets. **Carbohydrate Polymers**, v. 148, p. 143-152, 2016.

YOSHIDA, M.I.; OLIVEIRA, M.A.; GOMES, E.C.L.; MUSSEL, W.N.; CASTRO, W.V.; SOARES, C.D.V. Thermal characterization of lovastatin in pharmaceutical formulations. **Journal of Thermal Analysis and Calorimetry**, v. 106, p. 657-664, 2011.



## **APPENDIX**

### **DEVELOPMENT AND VALIDATION OF A HIGH PERFORMANCE LIQUID CHROMATOGRAPHY METHOD FOR SIMULTANEOUS DETECTION OF EZETIMIBE AND LOVASTATIN**

---

## 1. INTRODUCTION

The analysis of drugs is required both during the development and quality control of dosage forms. In this way, it is necessary that the methods applied to detect and quantify the drugs be adequate and compliant to the analytical requirements. To assure that, analytical methods should be validated according to international regulations and the parameters usually evaluated are linearity and range, limits of detection and quantification, specificity, precision, accuracy and robustness (ICH, 2005; USP 30, 2007).

Regarding dosage forms composed of fixed dose combinations, the development of an analytical method capable of detecting simultaneously all drugs can be complex, especially if the compounds present very distinct physico chemical properties.

The combination of ezetimibe (EZE) and lovastatin (LOV) in clinical practice aiming to treat hypercholesterolemic patients is considered safe and efficient (KERZNER et al., 2003), especially if the severe side effects associated to the monotherapy with LOV are taken into account (e.g. myopathy and rhabdomyolysis). Besides, recent report has demonstrated that statins are responsible for an increase of 50% of the risk of developing type II diabetes in patients with hypercholesterolemia (CEDERBERG et al., 2015).

In this sense, the coadministration with EZE is advised to promote a dose reduction of statins. However, no commercial fixed dose combination of EZE and LOV is currently available.

In this context, as this thesis comprehend the development of a fixed dose combination dosage form of EZE and LOV, the existence of an analytical method to simultaneously detect both compounds is mandatory. Literature presents two reports of high performance liquid chromatography (HPLC) methods for EZE and LOV. Nevertheless, both require the use of buffer solutions or pH adjustment of the mobile phase (KHAN et al., 2010; RAJ et al., 2013), making the method less attractive to the quality control routine.

Based on that, this section aims for the development and validation of a robust, simple and fast analytical HPLC method, capable to detect simultaneously EZE and LOV.

## 2. EXPERIMENTAL

### 2.1 MATERIALS

EZE and LOV were purchased from Pharma Nostra (batches FM017H13 – India and 130312 – China, respectively). HPLC-grade acetonitrile was obtained from JT Baker (Phillipsburg, NJ, EUA). All other chemicals used were pharmaceutical-grade. During the analysis, ultrapure water was obtained using a Milli-Q Gradient System (Millipore, Bedford, MA).

### 2.2 METHODS

#### 2.2.1 Instrumentation and chromatographic conditions

The isocratic LC analysis was performed on a Merck-Hitachi LaChrom system using a reversed-phase Chromolith® Performance C18 column (100 x 4.6 mm i.d., 5 µm). The mobile phase was made up from acetonitrile:water (50:50 v/v), with a flow rate of 1.0 mL.min<sup>-1</sup>, at 25.0 °C. Detection was performed at 235 nm. Samples were filtered through a 0.45 µm membrane filter and a volume of 20 µL was injected. Data acquisition was performed using Merck LaChrom D-7000 System Manager software to measure the detected peaks.

#### 2.2.2 Preparation of standard solutions

An amount of 10.0 mg of EZE and 10.0 mg of LOV were accurately weighed and transferred to an individual 20.0 mL volumetric flask, then diluted to volume with acetonitrile to obtain a concentration of 500.0 µg.mL<sup>-1</sup>. The stock solutions (n=3) were stored at room temperature and protected from light. Working standard solutions were prepared daily by diluting the stock solution to a concentration of 20 µg.mL<sup>-1</sup> with acetonitrile:water (50:50 v/v). The solution was filtered through a 0.45 µm PTFE filter prior to injection.

## 2.2.3 Method validation

Validation was based on the requirements of the ICH guideline for validation of analytical procedures (ICH, 2005). The parameters analyzed were specificity, linearity, range, limits of quantification and detection, accuracy, precision and robustness.

### 2.2.3.1 Specificity

In order to determine the specificity of the method, both compounds (10 mg each) were added to 500 mL of 0.01 M HCl pH 1.2 and kept at 100 rpm during 90 min. At the end of the assay, 5 mL-aliquot was withdrawn, filtered with a 0.45  $\mu\text{m}$  PTFE membrane filter and injected in triplicate.

This condition was selected to mimick the acidic stage of an *in vitro* dissolution test. It is known that a hydrolytic conversion of LOV to its active metabolite lovastatin hydroxyacid (LOVh) occurs in acidic conditions and should be avoided. For this reason, an enteric-coated formulation is recommended for this compound.

### 2.2.3.2 Linearity, limits of detection (LOD) and quantification (LOQ)

The calibration curves were obtained from seven concentration levels ranging from 0.4 to 50.0  $\mu\text{g.mL}^{-1}$ . Analyses were performed in triplicate and the regression lines were calculated by the method of the least square of peak area versus drug concentrations.

The limits of detection (LOD) and quantification (LOQ) were estimated based on the standard deviation of the y-intercepts of regression analysis ( $\sigma$ ) and the slope (S), by the Equation 1 and Equation 2. The values of concentration obtained were further evaluated experimentally.

$$\text{LQ} = (10 \sigma) / S \quad \text{Equation 1}$$

$$\text{LD} = (3,3 \sigma) / S \quad \text{Equation 2}$$

#### 2.2.3.3 Accuracy

The accuracy was determined by comparison of the drug content results obtained with the proposed method with that of a second well-characterized analytical procedure (KHAN et al., 2010). A concentration of 10.0  $\mu\text{g.mL}^{-1}$ , which corresponds to 100.0 % of the label claim, was analyzed, in triplicate, through both HPLC methods. The statistical analysis of the data was carried out through Student's t-test, where significant results present a probability lower than 5% ( $p \leq 0.05$  with a 95% confidence interval) by MS Excel<sup>®</sup> software.

#### 2.2.3.4 Precision

The precision of the method was determined by repeatability (intra-day) and intermediate precision (inter-day). The repeatability was evaluated by assaying six samples of the 100.0 % standard concentration (50.0  $\mu\text{g.mL}^{-1}$ ) during the same day and under the same experimental conditions. The intermediate precision was evaluated by assaying solutions on three different days. The analyses were performed in triplicate and expressed as % RSD.

#### 2.2.3.5 Robustness

The robustness of the method was evaluated against variations in wavelength (234, 235 and 236 nm), flow rate (0.9, 1.0 and 1.1 mL/min) and ratio of the mobile phase constituents (ACN:H<sub>2</sub>O 48:52, 50:50 and 52:48 v/v). Samples in these conditions were analyzed in triplicate and results were expressed as % RSD.

#### 2.2.3.6 Statistical analysis

The statistical analysis of the data was carried out through one way analysis of variance (ANOVA) where significant results present a probability lower than 5% ( $p \leq 0.05$  with a 95% confidence interval). The

statistical evaluation of the results was performed in MS Excel® software.

For the accuracy parameter, statistical analysis was performed through Student's t-test, following the same specifications as described above.

### 3. RESULTS

#### 3.1 DEVELOPMENT OF THE ANALYTICAL METHOD BY HPLC

Aiming to achieve a fast method with good resolution between the peaks of EZE and LOV, as well as with LOVh, different mobile phase ratios and compositions, flow rate and oven temperatures were tested and adjusted. Besides, the need to develop a simple method that could be easily applied to the quality control routine of a lab was also taken into account, since the reported methods require the use of buffer solutions or pH adjustment (KHAN et al., 2010; RAJ et al., 2013).

In this way, mobile phase compositions were evaluated, varying the ratios of methanol, acetonitrile and water. Acetonitrile decreased the retention time and enhanced the peak shape and symmetry, however, a good resolution of peaks was only achieved when water was added, especially at 50:50 v/v ratio. 1.0 mL/min flow rate was chosen to allow an adequate separation of the peaks, besides being the usual flow rate adopted for most methods. To select the proper wavelength, 50 µg/mL solution of EZE and LOV was scanned in UV spectrophotometer (Varian UV/Vis CARY) from 200 to 400 nm. High absorption was detected at 235 nm for both compounds. The oven temperature was kept at 25.0 °C, since changes in this parameter did not seem to have an impact on the resolution between peaks.

At the end, a simple and fast method was developed, with retention times of 3.09 nm and 8.11 min for EZE and LOV, respectively, with total run time of 11 min.

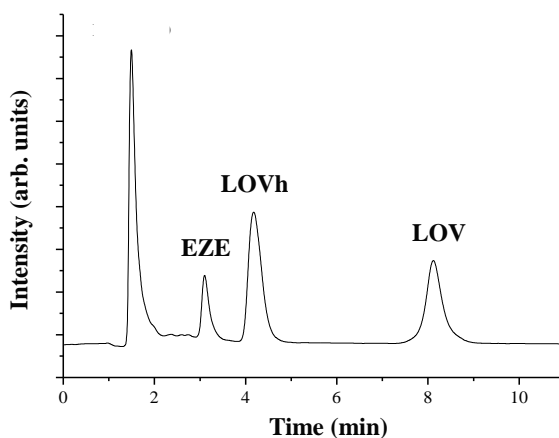
#### 3.2 ANALYTICAL VALIDATION

##### 3.2.1 Specificity



Figure 45 depicts the chromatogram containing peaks related to EZE, LOV and LOVh. The peak at approximately 1.7 min refers to 0.01 M HCl and mobile phase. As it is possible to observe, the method is capable of eluting all compounds with adequate resolution, without overlapping, verifying the specificity of the developed method.

**Figure 45.** Representative chromatogram obtained with the following conditions: ACN:H<sub>2</sub>O (50:50, v/v), 1 mL/min, 25°C, 235 nm, showing peaks of EZE (3.1 min), LOVh (4.2 min) and LOV (8.1 min)



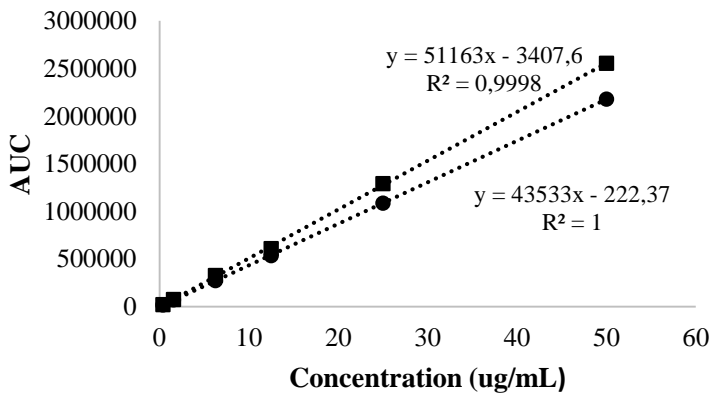
### 3.2.2 Linearity

The evaluation of the linearity demonstrates that EZE and LOV showed a linear correlation in the range of 0.4 to 50.0  $\mu\text{g}\cdot\text{mL}^{-1}$ , with a determination coefficient ( $R^2$ ) of  $> 0,999$ , for both compounds (Figure 46). The representative linear equation for EZE was  $y = 43533x - 222.37$ , and  $y = 51163x - 3407.6$  for LOV, where  $x$  is concentration in  $\mu\text{g}\cdot\text{mL}^{-1}$  and  $y$  is the peak area. The data were validated by means of the analysis of variance (ANOVA), which demonstrated linearity significant linear regression ( $p < 0.05$ ) and no significant deviation from linearity ( $p > 0.05$ ).

LOQ and LOD values were 60.0 ng/mL and 20.0 ng/mL, respectively, for both compounds. As these values are lower than the

lowest concentration of the calibration curve, it is possible to affirm that the method is sensitive.

**Figure 46.** Mean calibration curves of EZE (●) and LOV (■), obtained as a function of the peak areas *versus* concentration, in µg/mL. Their respective linear equations and determination coefficients are also depicted



3.2.3 Accuracy

Results related to accuracy (Table 8) are expressed as percentage of recovery of EZE and LOV from both methods. Significant differences ( $p > 0,05$ ) between the results obtained by the preposed method and the one reported in literature (KHAN et al., 2010) were not observed. Besides, RSD values are within the acceptable range ( $100 \pm 2 \%$ ).

**Table 8.** Data referring to the accuracy of the method

Proposed method			Comparison method	
	Concentration (%)	RSD (%)	Concentration (%)	RSD (%)
EZE	95.8	0.4	100.1	1.9
LOV	94.6	0.2	94.4	0.5

3.2.4 Precision

Data referring to the precision of the method, expressed as RSD (%) comply with the acceptance criterium of 5% (ICH, 2005). Results of 0.4 e 1.3 % for intra and inter-day analyses, respectively for EZE, and 0.7 and 1.1 % for intra and inter-day analyses, respectively for LOV, have been found. Samples quantified in three different days were considered statistically similar ( $p > 0,05$ ), for both EZE and LOV.

### 3.2.5 Robustness

**Table 9.** Data referring to the robustness of the method, compared to the parameters of the developed method (ACN:H<sub>2</sub>O (50:50, v/v), 1 mL/min, 25°C, 235 nm)

Parameter evaluated	EZE (%)	LOV (%)
234 nm	97.3	101.6
236 nm	97.0	101.9
0.9 mL/min	<b>113.2</b>	107.8
1.1 mL/min	93.2	<b>86.4</b>
ACN:H <sub>2</sub> O 48:52 (v/v)	102.9	94.4
ACN:H <sub>2</sub> O 52:48 (v/v)	102.3	93.3

As can be observed in Table 9, robust quantification against changes related to the wavelength and mobile phase ratio was obtained. However, for EZE and LOV, variations of flow rate show significant differences in their quantification, and their content varied from 86.4 to 113.2%.

Based on these data, it is possible to affirm that the method is robust against slight and deliberated changes regarding the wavelength and mobile phase ratios, however, the flow rate must remain unaltered for both compounds.

## 4. CONCLUSIONS

The HPLC method developed demonstrated to be adequate for the simultaneous detection and resolution of EZE, LOV and LOV active metabolite, LOVh, obtained through hydrolytic conditions. This method was validated in accordance to the regulatory agencies and was

considered specific, sensitive, linear, accurate, precise and robust against variations of wavelength and mobile phase ratios.

In this way, it becomes an important tool to simultaneously detect EZE and LOV in fixed dose combination dosage forms, as well as dissolution and stability studies.

## 5. REFERENCES

CEDERBERG, H.; STANCÁKOVÁ, A.; YALURI, N.; MODI, S.; KUUSISTO, J.; LAAKSO, M. Increased risk of diabetes with statin treatment is associated with impaired insulin sensitivity and insulin secretion: a 6 year follow-up study of the METSIM cohort. **Diabetologia**, v. 58, p. 1109-1117, 2015.

ICH - International Conference On Harmonisation Of Technical Requirements For Registration Of Pharmaceuticals For Human Use, Validation Of Analytical Procedures: Text And Methodology Q2(R1), 2005.

KERZNER, B.; CORBELLI, J.; SHARP, S.; LIPKA, L.J.; MELANI, L.; LEBEAUT, A.; SURESH, R.; MUKHOPADHYAY,P.; VELTRI, E.P. Efficacy and safety of ezetimibe coadministered with lovastatin in primary hypercholesterolemia. **American Journal of Cardiology**, v. 91, p. 418-424, 2003.

KHAN, I.U.; KAUSAR, T.; ASHFAQ, M.; SHARIF, S. Development and validation of liquid chromatographic method for the simultaneous estimation of ezetimibe and lovastatin in human plasma. **Journal of the Chilean Chemical Society**, v. 55, p.461-464, 2010.

RAJ, H.A.; RAJPUT, S.J.; AHIR, D.J.; CHAUDHARI,T.D. Development of stability indicating reverse phase high performance liquid chromatography for the estimation of ezetimibe, simvastatin and lovastatin. **Universal Journal of Pharmacy**, v. 2, p.71-77, 2013.

UNITED STATES PHARMACOPEIA, The (USP) 30 ed. Rockville, United States Convention, 2007.

## **FINAL DISCUSSION**

---

FDCs have proven to be an adequate choice to treat patients suffering from multiple pathologies, and lately, regulatory agencies such as FDA, have estimated the registration of new formulations. However, the development of a FDC can be challenging, since the formulation steps require a deep understanding of particular characteristics of more than one compound. In addition, if the drugs present inadequate physicochemical properties, such as poor solubility, the formulation should be able to overcome this limitation.

Nevertheless, although much effort has been put on developing more efficient formulations based on a single poorly water-soluble compound, by solid dispersions, salt formation, cocrystallization, lipid-based formulations, complexation with cyclodextrins, and other approaches, for example, a different perspective is seen for FDCs. Scarce innovation in this field is urging for the investigation and development of more modern tools.

Due to the synergistic hypolipidemic properties of EZE and LOV, with proven safe and efficient combination in clinical practice, besides their limiting physicochemical properties, these compounds have been chosen as model drugs to develop novel FDCs based on amorphous systems.

In this context, a relatively recent technological approach has been developed known as co-amorphous systems. Proposed to overcome the deficiencies inherent to solid dispersions, these systems comprise a binary, and more recently also ternary amorphous combinations, composed only of the APIs and/or small active molecules, such as aminoacids. Most of the reports regarding this topic have shown promising data, which show enhanced solubility and dissolution rate of the involved compounds, besides improving their amorphous physical stability.

As a quite classic and well-known excipient used in a great number of pharmaceutical formulations, besides its use in other fields, gelatin has also shown its potential when combined to a drug molecule to either influence its immediate or modified release. As a safe and vastly explored molecule, the generation of FDCs based on gelatin formulations could also be an interesting approach. However, although presenting important benefits, such as being water-soluble, biocompatible, biodegradable, cheap and readily available, it has never been explored as a possible carrier for FDCs composed of poorly soluble compounds.

Solid dispersions are widely known, explored and investigated, composing nowadays a few number of commercialized formulations. Focused on enhancing the solubility and dissolution rate of poorly soluble compounds, they have not been explored, by now, as a possible approach for FDCs.

In this context, this research project aimed to develop a FDC based on two poorly water-soluble compounds, EZE and LOV. Amorphous formulations were developed and investigated, being comprised by the three strategies mentioned previously. Co-amorphous systems, gelatin-based formulations and ternary solid dispersions were selected since their principles and basic knowledge have already been target of many investigations, facilitating their understanding in a more complex system. Besides, they present scarcely explored potential to compose a FDC.

Importantly, developing a single formulation composed of both compounds in amorphous state present some important advantages compared to physical mixtures of binary amorphous systems comprised by each API and its carrier. To be mentioned, the time and cost savings of a single step process, instead of a two-step process and a powder blending step, required for the preparation of two binary solid dispersions, is an interesting example.

A case of approach in this sense was reported by Taupitz and coworkers in 2013 (TAUPITZ, DRESSMAN and KLEIN, 2013). These authors focused on verifying the potential of cyclodextrins and solid dispersions to improve the dissolution rate of ezetimibe/simvastatin and pioglitazone/glimepiride in FDCs. Although the results were promising, especially concerning the ternary complex consisting of hydroxypropyl- $\beta$ -cyclodextrin (HP- $\beta$ -CD) and Soluplus®, in this research, each compound was formulated separately. This basically means that besides the formulation steps required for each compound, generating a two-step process, an additional blending step of physical mixtures would be further required. Furthermore, the total bulk volume of the final formulation could hamper the development of the dosage form. For this reason, we focused on developing a co-formulation with an adequate balance between number of processing steps and performance.

However, although much more interesting, especially concerning the scale-up perspective, co-formulating a FDC is not always a straight forward process. An example of this was reported by our group, testing the behavior of ritonavir and darunavir, both poorly water-soluble

compounds, in a FDC in the form of dispersible powders. Ternary spray dried systems composed either by HPMC, PVP K-30, and PVP/VA 64 and the two drugs were investigated. Basically, the authors verified that the presence of darunavir always decreased the supersaturation level of ritonavir and vice versa no matter which polymers were used. Moreover, the performance of the ternary systems was always inferior to the respective binary ones. Also, in this case, in order to restrict the mutual negative influence between darunavir and ritonavir, a complex of both ritonavir and darunavir with HP- $\beta$ -CD was prepared and improved the dissolution rate of both compounds (NGUYEN and VAN DEN MOOTER, 2014).

The investigation of the supersaturation behavior of one drug in presence of another in a FDC was also target of research by Trasi and Taylor (2015). These authors used ritonavir, lopinavir, paclitaxel, felodipine, and diclofenac as poorly water-soluble model compounds and verified that the amorphous solubility of each component in aqueous solution drops significantly by the second component, as long as the two drugs are miscible in the amorphous state. This data reinforces previous results reported by Nguyen and Van den Mooter (2014), demonstrating the difficulty in co-formulating with two poorly water-soluble compounds.

More recently, a novel FDC was developed by Liu and coworkers (2015). These authors prepared a novel FDC composed by salmeterol xinafoate and mometasone furoate in a composite particle formulation as brittle matrix powder and investigated its suitability as an inhaled combination product. FDCs with and without stabilizers, such as lactose, mannitol, glycine and trehalose, were investigated and the authors observed that the formulations exhibited improved aerodynamic properties when delivered by dry powder inhalation as compared to the micronized blends of the same substances. In addition, the proposed FDC resulted in delivered dose uniformity, which corroborated to a significantly higher lung concentration of drugs than for the crystalline physical blend. Although the results are promising for this type of formulation, the manufacturing process is relatively unexplored by the pharmaceutical industry.

Therefore, aiming to develop an easy and single-step processing formulation, composed of EZE and LOV, in a FDC with enhanced physicochemical properties of both compounds, co-amorphous systems prepared by quench cooling from the melt were investigated. Although



single amorphous systems were obtained, the dissolution rate of both compounds was not enhanced. Interestingly, in this case, the dissolution rate of amorphous EZE was not increased in comparison to its crystalline counterpart. Although contact angle measurements were performed to investigate the possible causes (data not shown), the explanation for this matter remains unclear. Similar reports have been found for other compounds, such as darunavir ethanolate (VAN GYSEGHEM et al., 2009) and carvedilol (POKHARKAR et al., 2006). Certainly, this behavior had a negative impact on the combined systems, since all formulations with LOV had a low dissolution rate, for both compounds. Co-amorphous systems of EZE and indapamide are described in literature, but the paper does not investigate the dissolution properties of both compounds. The focus of their research is molecular dynamics and physical stability of the co-amorphous systems and the authors conclude that the presence of indapamide reduces the molecular mobility of EZE, providing long term stability to the formulation (KNAPIK et al., 2015).

Successful reports of co-amorphous systems available in literature usually combine one poorly water-soluble compound, with a hydrophilic one, which facilitates the wettability of the system. When EZE and LOV were combined, the amorphous state of both was apparently not sufficient to improve their solubility and dissolution rate. A similar report was found in literature for a co-amorphous system composed by two poorly water-soluble compounds, simvastatin and glipizide. Also in this case, the amorphous state of both APIs was not sufficient to improve their solubility simultaneously. Although enhanced dissolution rate was noticed for glipizide in ball milled co-amorphous systems, no improvement was achieved for simvastatin (LÖBMANN et al., 2012). However, when in presence of small hydrophilic molecules, such as aminoacids, the dissolution rate of simvastatin was substantially improved (CRAYE et al., 2015; HEIKKINEN et al., 2015). This data reinforces the fact that for highly lipophilic substances, the amorphization in some cases needs to be combined to other parameters, such as improved wettability and particle size reduction, for example, to overcome the limiting solubility.

In this context, the disappointing results with the co-amorphous systems of EZE and LOV also led to the conclusion that the addition of a highly water-soluble compound was necessary to improve the solubility of EZE and LOV in a FDC.

As a second attempt, the incorporation of gelatin to the system, through an environmentally friendly process, the high energy milling, was exhaustively explored. Different API:API and APIs:gelatin ratios, as well as milling time, number of balls, rotation speed and addition of hydrophilic polymers were tested. However, although gelatin seemed to have an influence on the dissolution rate of the compounds, its impact was not sufficiently expressive, even in presence of high content of the biopolymer. Although a report in literature states that there is a tendency for larger gelatin-induced increases in solubility as drug lipophilicity increases (KALLINTERI and ANTIMISIARIS, 2001), and improved dissolution rates were observed for pranlukast (CHONO et al., 2008), ibuprofen (LI et al., 2008) and fenofibrate (YOUSAF et al., 2015) in gelatin-based systems, this fact could not be exactly transposed to EZE and LOV, based on the not too expressive enhancement on their dissolution rate in presence of the biopolymer.

It is known that gelatin can be quite unstable when exposed to humidity, heat and light, resulting in the formation of a swollen, very thin, tough, rubbery, water-insoluble membrane, known as pellicle. This membrane can act like a barrier during dissolution and restrict the release of drugs from this type of systems. This could be a possible explanation for the not so significant release profiles of EZE and LOV in gelatin-based systems. Besides, although hydrophilic polymers could be combined to gelatin to overcome this problem, the total bulk volume would increase and limit the compounding step.

Thus, the next step comprised the investigation of highly hydrophilic and synthetic polymers to compose the unexplored ternary solid dispersion concept. Until to date, the potential of solid dispersions to prepare a FDC has been scarcely explored. Nowadays, Kaletra® is the only marketed FDC based on a ternary solid dispersion system (VAN DEN MOOTER, 2011). Composed by the polymer PVP/VA, this formulation is prepared by hot melt extrusion and opens many possibilities for other novel amorphous FDCs.

The ternary solid dispersion system developed in this research investigates for the first time the use of spray drying as the manufacturing process of this type of ternary system. Extremely efficient on amorphization of compounds, spray drying is one of the most used and explored processing techniques in the pharmaceutical industry, which eases its scale up and represents a major advantage towards other manufacturing processes.

Preliminary studies were conducted with four different polymers (HPMC, PVP K-30, PVP/VA -64 and Soluplus®), which were chosen based on their common and successful use in binary solid dispersions. From all the options, Soluplus® provided significant solubility and dissolution rate enhancement, demonstrating to be an adequate choice to comprise the system. The formulation containing 90% of this polymer was able to reach around 90% release of both compounds within 15 minutes, showing a significant dissolution efficiency enhancement compared to the respective pure crystalline compounds. These data demonstrate that the addition of the hydrophilic polymer, combined to a processing technique able to promote significant particle reduction, was the solution to the limited dissolution rate of both compounds. The amorphization by itself was not enough to reach the desired release properties of EZE and LOV.

Prepared in a single step process, both compounds remained in amorphous state with adequate dissolution performance for 1 year, in low temperature and humidity conditions. In comparison to other formulations found in literature, this one does not require a blending step, and the chemical interactions between the compounds, which would not exist in a physical mixture of two binary systems, auxiliary on maintaining the physical stability of the formulation.

However, due to the instability of LOV in acidic conditions, which leads to the premature formation of its active metabolite, lovastatin hydroxyl acid, an enteric coated formulation was a necessary requisite to proceed with the development of a dosage form. In order to prepare a final formulation, the spray dried ternary solid dispersion with the best 'in vitro' performance (ELS 1:1 90%) was selected. But, due to the need for an enteric coating layer, the spray drying process was transformed up to a fluid bed coater.

The coating process is an important and complex step which demands the investigation of different formulation and process parameters. It is well known that the coating time, the polymer type, the type of equipment, the size of the coated particles, the composition of the coating solution, the drying and curing steps, besides the operational parameters, such as air flow, drying temperature, atomization air and flow rate of the coating solution play an important role on the preparation of successful formulations (DEREYMAKER and VAN DEN MOOTER, 2017; KNOP and KLEINEBUDDE, 2013; WESDYK et al, 1990).

For this reason, the type of polymer, the composition of the coating layer, the size of the inert sucrose beads and the coating time were tested and optimized to develop the desired final dosage form based on a FDC.

Fluid bed coating has already been applied to prepare binary solid dispersions, as described by Yan and coworkers (2016), in wax-based floating solid dispersion pellets, by Sun and coworkers (2008), who could enhance the dissolution rate of *Silybum marianum* extract in solid dispersion pellets, and by Li and coworkers (2012), showing improved dissolution rate of a novel compound Tanshione II, which composed a ternary solid dispersion with PVP K-30 and Poloxamer 188®. More recently, fluid bed coated solid dispersions have also shown its importance on controlling the release of indomethacin from glass solutions layered with a rate controlling membrane (DEREYMAKER and VAN DEN MOOTER, 2017; 2017a). However, to the best of our knowledge, this type of processing has never been applied before on preparing FDCs based on ternary solid dispersions.

In comparison to other manufacturing techniques, fluid bed coating shows the advantage of consisting of a one-step process, which does not require separate drying steps, addition of excipients and further manufacturing stages, such as milling or compression, which can induce phase separation or crystallization. In addition, multiparticulate systems such as pellets, can also be an interesting choice to compose a FDC, since they allow the combination of more than one API, obtaining flexible release profiles from a single dosage form. From a pharmacokinetic point of view, multiparticulate systems offer the advantage of presenting a more predictable gastric transit time, better distribution and absorption, facilitated disintegration, less frequent dose dumping issues and reduced risks of systemic toxicity and local irritation (ASGHAR and CHANDRAN, 2006)

Based on this background, fluid bed coating of the ternary solid dispersions of EZE and LOV was processed by fluid bed coating, varying the processing and formulation parameters. In comparison to Eudragit L-100, the system with Eudragit L100-55® proved to be more indicated, since it did not require a long coating time and presented a homogeneous layer which avoided the release in acidic conditions. In addition, in neutral conditions, which mimicks the intestinal environment, the APIs were fastly released. Regarding the size of the coated particles, bigger beads were better, avoiding particle agglomeration and showing a more homogeneous coating layer. Similar findings were reported by Wesdyk

and coworkers (1990), for another fluid bed coated system. Importantly, from the off-line measurement of the coating layer thickness by laser diffraction, it was possible to determine the minimum coating thickness to assess an adequate release in gastric and intestinal conditions. Values of 30.9  $\mu\text{m}$  and 6.5  $\mu\text{m}$  were obtained for samples coated with Eudragit L-100<sup>®</sup> and Eudragit L100-55<sup>®</sup>, respectively, demonstrating better performance of the latter. The results and the investigation performed in this thesis have shown that it is possible to obtain a FDC made up of two poorly water-soluble compounds, prepared by quite simple approaches. From all the options tested, the ternary solid dispersions, coated by Eudragit L100-55<sup>®</sup> through fluid bed coating, showed the most adequate performance. This represents an interesting disclosure, since, both the process and the formulation steps (*e.g.* solid dispersion preparation and enteric coating) are widely used and relatively easy to scale up.

Although promising, this formulation still has to comply with some important steps in order to be a possible candidate for marketing. Clinical studies present different stages, starting from the pre-clinical tests, performed in animals, by means of bioavailability studies. This important step comprises the future perspective of this research. In order to perform a reliable study, the first step should comprise the development of a bioanalytical method, which detects the main compounds and their metabolites in blood. Although contemplated in the initial plan of this thesis, bioavailability studies in Beagle dogs was not possible to be carried out due to lack of operational conditions at the main institution of this thesis. As a complementary study, pharmacodynamic tests verifying the lipid lowering capacity of the developed FDC in hyperlipidemic rats could also be an interesting investigation.

To conclude, it is important to highlight that although this research was carried out with EZE and LOV, the knowledge obtained with these compounds can be extended to other poorly water-soluble APIs. FDCs are very beneficial to patients, and the hope is that in the near future, more modern formulations, like the one developed in this thesis, could be applied to marketable dosage forms and reach different therapeutical targets.

## RELEVANT REFERENCES

ASGHAR, L.F.A. and CHANDRAN, S. Multiparticulate formulation approach to colon specific drug delivery: Current perspectives. **Journal of Pharmaceutical Sciences**, v. 9, p. 327-338, 2006.

CHONO, S.; TAKEDA, E.; SEKI, T.; MORIMOTO, K. Enhancement of the dissolution rate and gastrointestinal absorption of pranlukast as a model poorly water-soluble drug by grinding with gelatin. **International Journal of Pharmaceutics**, v. 347, p. 71-78, 2008.

CRAYE, G.; LÖBMANN K.; GROHGANZ, H.; RADES, T.; LAITINEN, R. Characterization of amorphous and co-amorphous simvastatin formulations prepared by spray drying. **Molecules**, V. 20, P. 21532-21548, 2015.

DEREYMAKER, A.; SCURR, D.J.; STEER, E.D.; ROBERTS, C.J.; VAN DEN MOOTER, G. Controlling the release of indomethacin from glass solutions layered with a rate controlling membrane using fluid bed processing. Part 1: Surface and cross-sectional chemical analysis. **Molecular Pharmaceutics**, v. 14, p. 959-973, 2017.

DEREYMAKER, A.; PELGRIMS, J.; ENGELN, F.; ADRIAENSENS, P.; VAN DEN MOOTER, G. Controlling the release of indomethacin from glass solutions layered with a rate controlling membrane using fluid-bed processing. Part 2: The influence of formulation parameters on drug release. **Molecular Pharmaceutics**, v. 14, p. 974-983, 2017a.

HEIKKINEN, A.T.; DECLERCK, L.; LÖBMANN, K.; GROHGANZ, H.; RADES, T. LAITINEN, R. Dissolution properties of co-amorphous drug-amino acid formulations in buffer and biorelevant media. **Pharmazie**, V. 70, P. 452-457, 2015.

KALLINTERI, P.; ANTIMISIARIS, S.G. Solubility of drugs in presence of gelatin: effect of drug lipophilicity and degree of ionization. **International Journal of Pharmaceutics**, v. 221, p. 219-216, 2001.

KNAPI, J.; WOJNAROWSKA, Z.; GRZYBOWSKA, K.; JURKIEWICZ, K.; TAJBER, L.; PALUCH, M. Molecular dynamic and physical stability of coamorphous ezetimib and indapamide mixtures. **Molecular Pharmaceutics**, v. 12, p. 3610-3619, 2015.

KNOP, K. and KLEINEBUDDE, P. PAT-tools for process control in pharmaceutical film coating applications. **International Journal of Pharmaceutics**, v. 457, p. 527-536, 2013.

LI, D.X.; OH, Y.-K.; LIM, S.-J.; KIM, J.O.; YANG, H.J.; SUNG, J.H.; YONG, C.S.; CHOI, H.-G. Novel gelatin microcapsule with bioavailability enhancement of ibuprofen using spray-drying technique. **International Journal of Pharmaceutics**, v. 355, p. 277-284, 2008.

LIU, S.; WATTS, A.B.; DU, J.; BUI, A.; HENGSAWAS, S.; PETERS, J.I.; WILLIAMS, R.O. Formulation of a novel fixed dose combination of salmeterol xinafoate and mometasone furoate for inhaled drug delivery. **European Journal of Pharmaceutics and Biopharmaceutics**, v. 96, p. 132-142, 2015.

LÖBMANN, K.; STRACHAN, C.; GROHGANZ, H.; RADES, T.; KORHONEN, O.; LAITINEN, R. Co-amorphous simvastatin and glipizide combinations show improved physical stability without evidence of intermolecular interactions. **European Journal of Pharmaceutics and Biopharmaceutics**, v. 81, p. 159-169, 2012.

NGUYEN D.N. and VAN DEN MOOTER G. The fate of ritonavir in the presence of darunavir. **International Journal of Pharmaceutics**, v. 475, p. 214-226, 2014.

POKHARKAR, V.B.; MANDPE, L.P.; PADAMWAR, M.N.; AMBIKE, A.A.; MAHADIK, K.R.; PARADKAR, A. Development, characterization and stabilization of amorphous form of a low Tg drug. **Powder Technology**, v. 167, p. 20-25, 2006.

SUN, N.; ZHANG, X.; LU, Y.; WU, W. In vitro evaluation and pharmacokinetics in dogs of solid dispersion pellets containing Silybum marianum extract prepared by fluid-bed coating. **Planta Medica**, v. 74, p. 126-132, 2008.

TAUPITZ, T.; DRESSMAN, J.B.; KLEIN, S. New formulation approaches to improve solubility and drug release from fixed dose combinations: case examples pioglitazone/glimepiride and ezetimibe/simvastatin. **European Journal of Pharmaceutics and Biopharmaceutics**, v. 84, p. 208-218, 2013.

TRASI, N.S. and TAYLOR, L.S. Thermodynamics of highly supersaturated aqueous solutions of poorly water-soluble drugs – Impact of a second drug on the solution phase behavior and implications for combined products. **Journal of Pharmaceutical Sciences**, v. 104, p. 2583-2593, 2015.

VAN DEN MOOTER, G. The use of amorphous solid dispersions: A formulation strategy to overcome poor solubility and dissolution rate. **Drug Discovery Today: Technologies**, v. 9, p. e79-e85, 2011.

VAN GYSEGHEM, E.; STOKBROEKX, S.; DE ARMAS, H.N.; DICKENS, J.; VANSTOCKEM, M.; BAERT, L.; ROSIER, J.; SCHUELLER, L.; VAN DEN MOOTER, G. Solid state characterization of the anti-HIV drug TMC114: interconversion of amorphous TMC114, TMC114 ethanolate and hydrate. **European Journal of Pharmaceutical Sciences**, v. 38, p. 489-497, 2009.

WESDYK, R.; JOSHI, Y.M.; JAIN, N.B.; MORRIS, K.; NEWMAN, A. The effect of size and mass on the film thickness of beads coated in fluidized bed equipment. **International Journal of Pharmaceutics**, v. 65, p. 69-76, 1990.

YAN, H.-X.; ZHANG, S.-S.; HE, J.-H.; LIU, J.-P. Application of ethyl cellulose, microcrystalline cellulose and octadecanol for wax based floating solid dispersion pellets. **Carbohydrate Polymers**, v. 148, p. 143-152, 2016.

YOUSAF, A.M.; KIM, D.W.; KIM, J.K.; KIM, J.O.; YONG, C.S.; CHOI, H.-G. Novel fenofibrate-loaded gelatin microcapsules with enhanced solubility and excellent flowability: Preparation and physicochemical characterization. **Powder Technology**, v. 275, p. 257-262, 2015.